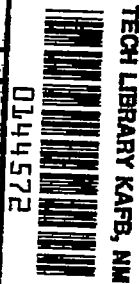


NACA TM 1421

1767



# NATIONAL ADVISORY COMMITTEE FOR AERONAUTICS

TECHNICAL MEMORANDUM 1421

A THEORETICAL INVESTIGATION OF THE DRAG OF GENERALIZED  
AIRCRAFT CONFIGURATIONS IN SUPERSONIC FLOW

By E. W. Graham, P. A. Lagerstrom, R. M. Licher,  
and B. J. Beane

Douglas Aircraft Company, Inc.



Washington

January 1957

AFMDC  
TECHNICAL LIBRARY  
AFL 2811



TABLE OF CONTENTS

I.	SUMMARY . . . . .	1
II.	INTRODUCTION . . . . .	2
III.	SINGULARITIES USED IN THE "LINEARIZED" DESCRIPTION OF THE FLOW ABOUT AIRCRAFT . . . . .	3
	A. BASIC SINGULARITIES . . . . .	3
	B. SOME EQUIVALENT SINGULARITY DISTRIBUTIONS . . . . .	12
IV.	THE EVALUATION OF DRAG . . . . .	25
	A. THE "CLOSE" AND THE "DISTANT" VIEWPOINTS . . . . .	25
	B. GENERAL MOMENTUM THEOREM FOR THE EVALUATION OF DRAG . . . . .	26
	C. HAYES' METHOD FOR DRAG EVALUATION . . . . .	35
	D. LEADING EDGE SUCTION . . . . .	49
	E. DISCONTINUITIES IN LOADINGS . . . . .	50
	F. THE USE OF SLENDER BODY THEORY WITH THE DISTANT VIEWPOINT . . . . .	52
	G. THE DEPENDENCE OF DRAG COEFFICIENT ON MACH NUMBER . . . . .	55
	H. SUPERPOSITION PROCEDURES AND INTERFERENCE DRAG . . . . .	55
	I. ORTHOGONAL DISTRIBUTIONS AND DRAG REDUCTION PROCEDURES . . . . .	56
	J. THE PHYSICAL SIGNIFICANCE OF INTERFERENCE DRAG . . . . .	56
	K. INTERFERENCE AMONG LIFT, THICKNESS AND SIDEFORCE DISTRIBUTIONS . . . . .	57
	L. REDUCTION OF DRAG DUE TO LIFT BY ADDITION OF A THICKNESS DISTRIBUTION . . . . .	59

V.	THE CRITERIA FOR DETERMINING OPTIMUM DISTRIBUTIONS OF LIFT OR VOLUME ELEMENTS ALONE . . . . .	60
	A. COMBINED FLOW FIELD CONCEPT . . . . .	60
	B. COMBINED FLOW FIELD CRITERION FOR IDENTIFYING OPTIMUM LIFT DISTRIBUTIONS . . . . .	60
	C. COMBINED FLOW FIELD CRITERION FOR IDENTIFYING OPTIMUM VOLUME DISTRIBUTIONS . . . . .	61
	D. UNIFORM DOWNWASH CRITERION FOR MINIMUM VORTEX DRAG . . . . .	61
	E. ELLIPTICAL LOADING CRITERION FOR MINIMUM WAVE DRAG DUE TO LIFT . . . . .	61
	F. "ELLIPTICAL LOADING CUBED" CRITERION FOR MINIMUM WAVE DRAG DUE TO A FIXED TOTAL VOLUME . . . . .	62
	G. COMPATIBILITY OF MINIMUM WAVE PLUS VORTEX DRAG WITH MINIMUM WAVE OR MINIMUM VORTEX DRAG . . . . .	62
	H. ORTHOGONAL LOADING CRITERIA . . . . .	63
	APPENDIX V. DISTRIBUTION OF LIFT IN A TRANSVERSE PLANE FOR MINIMUM VORTEX DRAG . . . . .	64
VI.	THE OPTIMUM DISTRIBUTION OF LIFTING ELEMENTS ALONE . . . . .	68
	A. THE OPTIMUM DISTRIBUTION OF LIFT THROUGH A SPHERICAL SPACE . . . . .	68
	B. THE OPTIMUM DISTRIBUTION OF LIFT THROUGH AN ELLIPSOIDAL SPACE . . . . .	70
	C. THE OPTIMUM DISTRIBUTION OF LIFT THROUGH A DOUBLE MACH CONE SPACE . . . . .	72
	APPENDIX VI. DERIVATION OF OPTIMUM DISTRIBUTION OF LIFT THROUGH A SPHERICAL SPACE . . . . .	75
VII.	THE OPTIMUM DISTRIBUTION OF VOLUME ELEMENTS ALONE . . . . .	78
	A. THE SINGULARITY REPRESENTING AN ELEMENT OF VOLUME . . . . .	78
	B. THE DISTRIBUTION OF VOLUME ELEMENTS . . . . .	79

C.	THE DRAG OF VOLUME DISTRIBUTIONS ON A STREAMWISE LINE AND THE SEARS-HAACK BODY . . . . .	80
D.	THE SEARS-HAACK BODY AS AN OPTIMUM VOLUME DISTRIBUTION IN SPACE . . . . .	81
E.	RING WING AND CENTRAL BODY OF REVOLUTION COMBINATION HAVING THE SAME DRAG AS A SEARS-HAACK BODY . . . . .	83
F.	OPTIMUM THICKNESS DISTRIBUTION FOR A PLANAR WING OF ELLIPTICAL PLANFORM . . . . .	84
VIII.	UNIQUENESS PROBLEMS FOR OPTIMUM DISTRIBUTIONS IN SPACE . .	89
A.	THE NON-UNIQUENESS OF OPTIMUM DISTRIBUTIONS IN SPACE - "ZERO LOADINGS" . . . . .	89
B.	UNIQUENESS OF THE DISTANT FLOW FIELD PRODUCED BY AN OPTIMUM FAMILY . . . . .	90
C.	UNIQUENESS OF THE ENTIRE "EXTERNAL" FLOW FIELD PRODUCED BY AN OPTIMUM FAMILY . . . . .	91
D.	EXISTENCE OF SYMMETRICAL OPTIMUM DISTRIBUTIONS IN SYMMETRICAL SPACES . . . . .	92
IX.	INVESTIGATION OF SEPARABILITY OF LIFT, THICKNESS, AND SIDEFORCE PROBLEMS . . . . .	94
A.	THE SEPARABILITY OF OPTIMUM DISTRIBUTIONS PROVIDING LIFT AND VOLUME . . . . .	94
B.	THE NON-INTERFERENCE OF SOURCES WITH OPTIMUM DISTRIBUTIONS OF LIFTING ELEMENTS IN A SPHERICAL SPACE . . . . .	97
C.	THE NON-INTERFERENCE OF SIDEFORCE ELEMENTS WITH OPTIMUM DISTRIBUTIONS OF LIFTING ELEMENTS IN A SPHERICAL SPACE . . . . .	98
D.	INTERFERENCE PROBLEMS IN CERTAIN SPACES BOUNDED BY MACH ENVELOPES . . . . .	101

E.	THE INTERFERENCE BETWEEN LIFT AND SIDEFORCE ELEMENTS AND AN OPTIMUM DISTRIBUTION OF VOLUME ELEMENTS . . . . .	102
F.	THE RING WING AND CENTRAL BODY OF REVOLUTION HAVING ZERO DRAG . . . . .	103
X.	RESULTS AND CONCLUSIONS . . . . .	106
XI.	REFERENCES . . . . .	107

NATIONAL ADVISORY COMMITTEE FOR AERONAUTICS

TECHNICAL MEMORANDUM 1421

A THEORETICAL INVESTIGATION OF THE DRAG OF GENERALIZED  
AIRCRAFT CONFIGURATIONS IN SUPERSONIC FLOW\*

By E. W. Graham, P. A. Lagerstrom, R. M. Licher,  
and B. J. Beane

CHAPTER I. SUMMARY

It seems possible that, in supersonic flight, unconventional arrangements of wings and bodies may offer advantages in the form of drag reduction. It is the purpose of this report to consider the methods for determining the pressure drag for such unconventional configurations, and to consider a few of the possibilities for drag reduction in highly idealized aircraft.

The idealized aircraft are defined by distributions of lift and volume in three-dimensional space, and Hayes' method of drag evaluation, which is well adapted to such problems, is the fundamental tool employed. Other methods of drag evaluation are considered also wherever they appear to offer simplifications.

The basic singularities such as sources, dipoles, lifting elements and volume elements are discussed, and some of the useful inter-relations between these elements are presented. Hayes' method of drag evaluation is derived in detail starting with the general momentum theorem.

In going from planar systems to spatial systems certain new problems arise. For example, interference between lift and thickness distributions generally appears, and such effects are used to explain the difference between the non-zero wave drag of Sears-Haack bodies and the zero wave drag of Ferrari's ring wing plus central body.

Another new feature of the spatial systems is that optimum configurations generally are not unique, there being an infinite family of lift or thickness distributions producing the same minimum drag. However it is shown that all members of an optimum family produce the same flow field in a certain region external to the singularity distribution.

Other results of this study indicate that certain spatial distributions may produce materially less wave drag and vortex drag than comparable planar systems. It is not at all certain that such advantages can be realized in practical aircraft designs, but further investigation seems to be warranted.

---

\* Unedited by the NACA (the Committee takes no responsibility for the correctness of the author's statements).

## CHAPTER II. INTRODUCTION

The primary purpose of this report is to consider the problems involved in exploring a broader class of aircraft configurations than is ordinarily studied for supersonic flight. It is necessary to determine whether any unconventional arrangements of wings and bodies offer sufficient aerodynamic advantages in the form of drag reduction to merit more detailed study. As a first step in this direction attention is directed to optimum configurations, even though they are highly idealized in form and do not necessarily represent practical aircraft.

In the preliminary exploration of such configurations it is not necessary to know their detailed shapes. It is sufficient to define the aircraft as a distribution of lift and volume in space, without knowing the camber and twist of the wing surfaces supporting the lift distribution, and knowing only approximately the shapes of the bodies containing the volume.

Hayes' method of drag evaluation is well adapted to this type of analysis and is one of the primary tools used. However other methods and points of view are employed wherever they appear to offer further understanding of the problems.

The properties of sources, dipoles, etc., are reviewed, and a singularity corresponding to an element of volume is introduced. Some useful relations between three-dimensional distributions of different types of singularities are developed and later applied. Also Hayes' method for drag evaluation is developed in detail.

Since this report is exploratory in nature the investigations made are frequently incomplete and somewhat isolated from each other. Some of the material of Ref. 2 and most of the material of Ref. 3 are included in this report for convenience. The latter has also been published in The Aeronautical Quarterly, May 1955, under the title, "The Drag of Non-Planar Thickness Distributions in Supersonic Flow." Permission to reproduce this material has been granted by The Royal Aeronautical Society.

CHAPTER III. SINGULARITIES UTILIZED IN THE "LINEARIZED"  
DESCRIPTION OF THE FLOW ABOUT AIRCRAFT

A. BASIC SINGULARITIES

The Source

For incompressible, non-viscous fluids the equation governing the flow is the Laplace equation,

$$\frac{\partial^2 \phi}{\partial x^2} + \frac{\partial^2 \phi}{\partial y^2} + \frac{\partial^2 \phi}{\partial z^2} = 0 \quad (3a-1)$$

where  $\phi$  is the perturbation velocity potential. A basic solution, which exhibits spherical symmetry, is the source,

$$\phi_{S_I} = \frac{-1}{4\pi \sqrt{(x - \xi)^2 + (y - \eta)^2 + (z - \zeta)^2}} \quad (3a-2)$$

This solution can be interpreted as representing the emanation of unit volume of fluid per unit of time from the point  $\xi, \eta, \zeta$ . Because of the linearity of Eq. (3a-1), other solutions of it can be built up by a superposition of sources through the use of certain limiting procedures; such resulting solutions are the horseshoe vortex, doublet, line vortex, etc. Much is known about these solutions and with them the flow over wings and bodies can be described mathematically.

In supersonic flow the governing differential equation is the linearized potential equation,

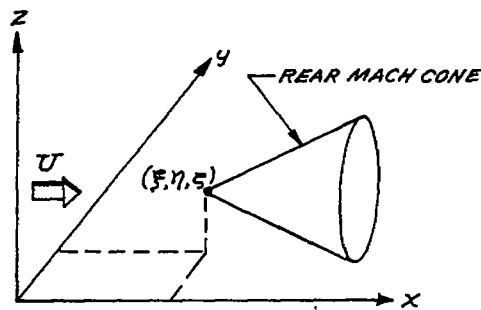
$$-\beta^2 \frac{\partial^2 \phi}{\partial x^2} + \frac{\partial^2 \phi}{\partial y^2} + \frac{\partial^2 \phi}{\partial z^2} = 0 \quad (3a-3)$$

where  $x$  is the coordinate in the stream direction and  $\beta = \sqrt{M^2 - 1}$ . Equation (3a-3) can also be considered as the two-dimensional wave equation where the  $x$  coordinate is thought of as the "time" variable.

If the  $y$  and  $z$  coordinates in the Laplace equation (Eq. 3a-1) are multiplied by  $i\beta$ , then that equation is transformed into the wave equation; a similar transformation of the source potential from Eq. (3a-2) results in

$$\phi_S \sim \frac{1}{\sqrt{(x - \xi)^2 - \beta^2 [(y - \eta)^2 + (z - \zeta)^2]}} \quad (3a-4)$$

which can easily be shown to be a solution of Eq. (3a-3). Equation (3a-4) is real inside the forward and rear Mach cones,  $(x - \xi)^2 > \beta^2 [(y - \eta)^2 + (z - \zeta)^2]$ , and imaginary elsewhere; however, due to the nature of supersonic flow only the solution in the rear Mach cone is used to represent a source. Since half of the real solution is discarded, the constant



REGION OF INFLUENCE OF SUPERSONIC SOURCE

associated with the incompressible  $\phi$  must be doubled to represent a unit supersonic source. Thus the supersonic source at  $\xi, \eta, \zeta$  has the potential

$$\phi_S = \begin{cases} \frac{-1}{2\pi \sqrt{(x - \xi)^2 - \beta^2 [(y - \eta)^2 + (z - \zeta)^2]}} & x - \xi \geq \beta \sqrt{(y - \eta)^2 + (z - \zeta)^2} \\ 0 & \text{Elsewhere} \end{cases} \quad (3a-5)$$

where the x axis is in the free stream direction. It can be shown that Eq. (3a-5) represents unit volume flow from the point  $\xi, \eta, \zeta$ ; however, care must be taken in the proof because of the singularities on the Mach cone (cf. Ref. 4). In the proof given by Robinson<sup>(4)</sup> he made use of the concept of the finite part of an infinite integral, an idea originally

introduced by Hadamard<sup>(5)</sup>. As in incompressible flow, other solutions of Eq. (3a-3) can be built up by superposition of the basic source solutions; some of the solutions can also be obtained, as was the source, by analogy with the incompressible solutions.

Before going on to other solutions let us examine the supersonic source in more detail. Since the velocities are infinite on the Mach cone from a finite source, care must be taken in using such sources to describe real flows. It is instructive to examine the isolated source in terms of the limit of a finite line of sources in the free stream direction as the length tends to zero while the total strength remains constant. Under the assumptions of slender body theory, if the line of sources extends from  $x = 0$  to  $x = x_0$  with strength  $Kx$ , it represents a cone of semi-vertex angle  $K/2U$  with a semi-infinite cylindrical after-body (Fig. 3a-1a). The velocities are constant along conical surfaces

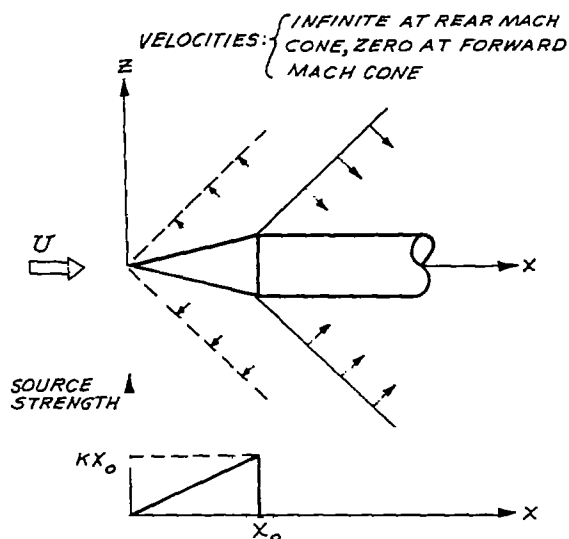


Fig. 3a-1a: Cone-cylinder and source distribution representing it

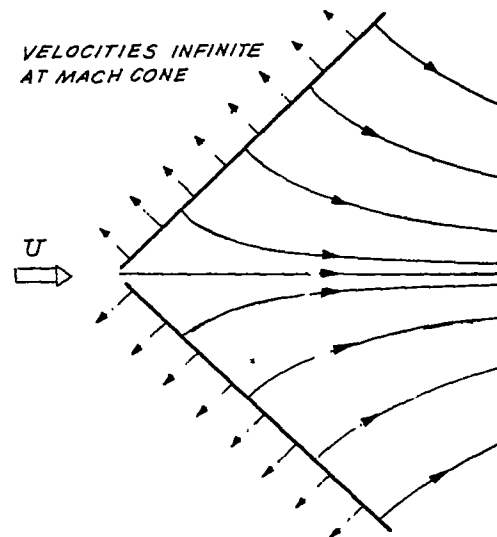


Fig. 3a-1b: Perturbation flow lines in  $x$ - $z$  plane for supersonic source,  $M = \sqrt{2}$

from the origin; but on the Mach cone from  $x = x_0$  the velocities become infinite due to the discontinuity in source strength. The total integrated source strength  $C$  is equal to  $1/2 Kx_0^2$ . If  $x_0$  is allowed to approach zero while  $C$  remains constant then in the limit a concentrated source of strength  $C$  is obtained. The flow pattern in the  $xz$  plane for the source at  $M = \sqrt{2}$  is shown in Fig. 3a-1b. (See also Ref. 6.) For a source of finite strength the velocities are infinite on the Mach cone.

#### The Three-Dimensional Doublet

The three-dimensional doublet (or dipole) is a second basic solution of the wave equation; it is obtained by allowing a source and sink of equal strength to approach one another while the product of source strength and distance between source and sink remains constant (and equal to unity for a unit doublet). The axis of the doublet is defined here as the vector extending from the center of the sink to the center of the source; positive values are taken to be those along the positive directions of the coordinate system. For a doublet with its axis vertical, the above method of derivation is equivalent to taking the negative partial derivative of the source potential in the  $z$  direction; that is,

$$\phi_D = - \frac{\partial \phi_S}{\partial z} = \frac{\beta^2 z}{2\pi(x^2 - \beta^2 r^2)^{3/2}} \quad x \geq \beta r \quad (3a-6)$$

where  $r^2 = y^2 + z^2$ . Equation (3a-6) represents a positive doublet at the origin, i.e., one with the source above the sink.

#### The Horseshoe Vortex

In supersonic theory, as well as in subsonic, the flow around a wing of finite span can be described by certain solutions of the wave equation called horseshoe vortices. In the subsonic case this singularity is derived by integrating in the streamwise direction a semi-infinite line of negative doublets with axes vertical. The supersonic horseshoe vortex can be derived in the same way as the subsonic one if only the finite part of the integral, as defined by Hadamard<sup>(5)</sup>, is taken as the solution. This solution can also be obtained without the use of the Hadamard finite part if a streamwise line of sources is differentiated in the vertical direction; thus,

$$\phi_{HSV} = \text{Finite part} \left\{ \int_0^{x-\beta r} \phi_D d\xi \right\} = \frac{\partial}{\partial z} \int_0^{x-\beta r} \phi_S d\xi$$

$$= \frac{xz}{2\pi r^2 \sqrt{x^2 - \beta^2 r^2}} \quad x \geq \beta r \quad (3a-7)$$

The flow pattern for a horseshoe vortex in planes normal to the free stream axis is shown in Fig. 3a-2. Far behind the bound vortex,

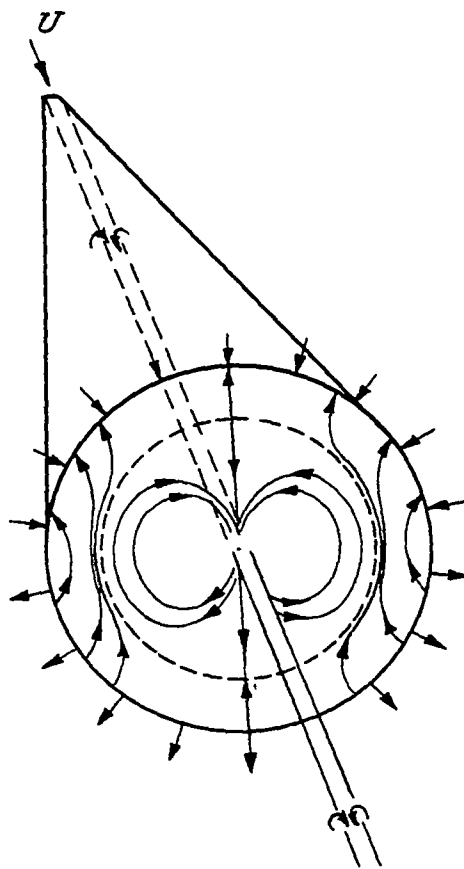


Fig. 3a-2: Flow pattern for supersonic horseshoe vortex

the flow near the x axis is similar to the flow far downstream around a subsonic horseshoe vortex and it is this part which gives rise to the "vortex" drag. The drag associated with the flow near the Mach cone is called "wave" drag. Equation (3a-7) represents a supersonic horseshoe vortex of unit strength, i.e., unit circulation around the bound vortex. Since a force  $\rho U r$  is associated with a bound vortex of strength  $\Gamma$ , we shall, for convenience, discuss unit lifting elements which have as their velocity potentials

$$\phi_l = \frac{xz}{2\pi\rho U r^2 \sqrt{x^2 - \beta^2 r^2}} \quad x \geq \beta r \quad (3a-8)$$

Similarly, the potential for a unit side force element is

$$\phi_{SF} = \frac{1}{\rho U} \frac{\partial}{\partial y} \int_0^{x-\beta r} \phi_S d\xi = \frac{xy}{2\pi\rho U r^2 \sqrt{x^2 - \beta^2 r^2}} \quad x \geq \beta r \quad (3a-9)$$

The force associated with Eq. (3a-9) is directed in the positive y direction; a force in any direction normal to the flow direction may be represented by a combination of lift and side force elements.

In the light of the discussion of the horseshoe vortex, the three-dimensional doublet (Eq. 3a-6) may be given added significance as a lift transfer element or element of moment. That is, the doublet potential can be formed by subtracting the potential for a horseshoe vortex at  $x = \Delta x$  from one at  $x = 0$  (Fig. 3a-3) and applying the proper limiting processes (equivalent to differentiating the horseshoe vortex potential); in this process the trailing vortices from the negative or rear element are canceled out by those from the positive one, and the remaining part forms the doublet or lift transfer element.

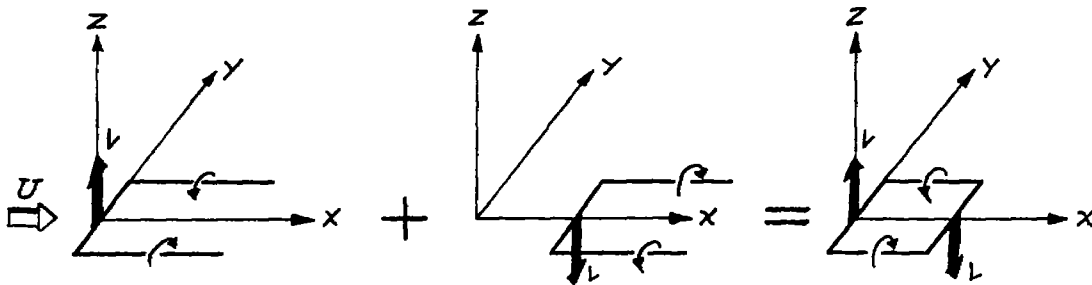


Fig. 3a-3: Formation of doublet or lift transfer element from horseshoe vortices

The horseshoe vortex consists of a bound vortex of infinitesimal length plus two free vortices trailing back to infinity. Since the vortex drag and the lift associated with a finite wing can be evaluated by considering the flow velocities far behind the wing, it is useful to consider the trailing vortices as they appear in the Trefftz plane far downstream from the bound vortex. The Trefftz plane flow represents a two-dimensional doublet or dipole and its potential is obtained by letting  $x \rightarrow \infty$  in Eq. (3a-7). Thus

$$\phi_{2D} = \frac{z}{2\pi(y^2 + z^2)} \quad (3a-10)$$

It should be noted that the potential for this doublet is independent of Mach number, and thus the vortex drag calculations for a given lift distribution are the same for supersonic and incompressible flows. The flow pattern about the doublet will be similar to the planar flow inside the dashed circle in Fig. 3a-2.

#### The Volume Element

Another useful solution is the doublet with its axis in the stream-wise direction; it has as a potential

$$\phi_V = - \frac{\partial \phi_S}{\partial x} = \frac{-x}{2\pi(x^2 - \beta^2 r^2)^{3/2}} \quad x \geq \beta r \quad (3a-11)$$

Equation (3a-11) can be shown to represent the potential for a unit of volume equal to  $1/U$  (see Chapter VII) at the origin. A distribution of volume elements along the  $x$  axis with strength  $f(\bar{x})$  has as a potential

$$\begin{aligned} \phi &= \int_0^{x-\beta r} f(\xi) \phi_V d\xi \\ &= \frac{f(\xi)}{2\pi \sqrt{(x-\xi)^2 - \beta^2 r^2}} \Big|_0^{x-\beta r} - \frac{1}{2\pi} \int_0^{x-\beta r} \frac{f'(\xi) d\xi}{\sqrt{(x-\xi)^2 - \beta^2 r^2}} \end{aligned} \quad (3a-12)$$

The first term in Eq. (3a-12) is infinite; but if only the finite part of the integral is considered (as defined by Hadamard<sup>(5)</sup>), then Eq. (3a-12)

represents the potential for a source distribution of strength  $f'(\xi)$ . Thus a body can be built up from a series of volume elements as well as from a series of sources and sinks.

### The Closed Vortex Line

Equation (3a-11) can be considered not only as a volume element but also as a closed vortex line of circulation strength  $1/\beta^2$  in the  $yz$  plane (Fig. 3a-4a). The line carries a constant intensity of forces directed inward so that the total vector force is zero. The negative of Eq. (3a-11) would represent an element with the forces directed outward from it. The potential for the closed vortex line can also be obtained by applying the standard limiting process to an element composed of two pairs of horseshoe vortices of strength  $1/\beta^2$ , one with its axis in the negative  $z$  and the other in the negative  $y$  direction (Fig. 3a-4b); when added together the trailing vortices cancel leaving the closed vortex line.

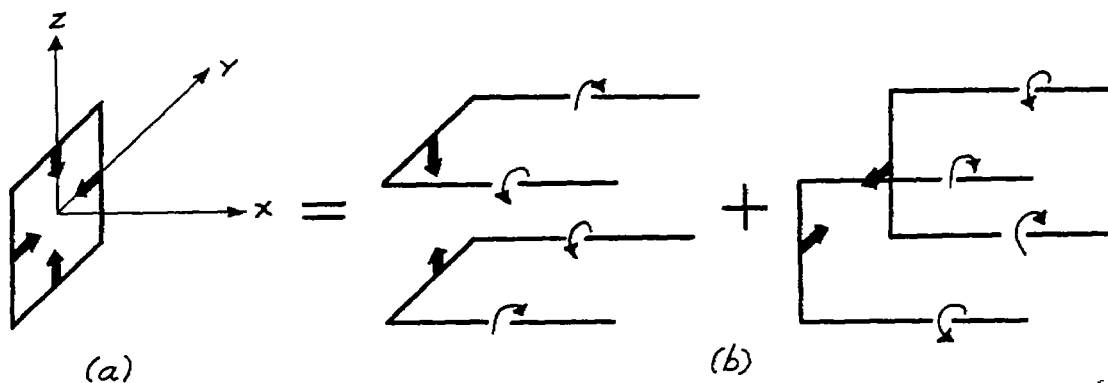


Fig. 3a-4: Formation of closed vortex line from horseshoe vortices

### Two-Dimensional Singularities

In subsonic flow two-dimensional sources, obtained by integrating a line of three-dimensional sources in the lateral direction, have proven useful in many problems; so also has the infinite bound vortex obtained by a lateral integration of horseshoe vortices. The same types of solutions can be derived for supersonic flow and these provide more insight into the nature of the supersonic solutions. The two-dimensional source potential is

$$\phi_{2S} = \int_{-\frac{1}{\beta}\sqrt{x^2-\beta^2z^2}}^{+\frac{1}{\beta}\sqrt{x^2-\beta^2z^2}} \phi_S \, d\eta = -\frac{1}{2\beta} \quad x \geq |\beta z| \quad (3a-13)$$

All of the disturbance created by the two-dimensional source is concentrated on the Mach planes from it, thus creating a potential jump across these planes. The two-dimensional vortex potential is

$$\phi_{2V} = \int_{-\frac{1}{\beta}\sqrt{x^2-\beta^2z^2}}^{+\frac{1}{\beta}\sqrt{x^2-\beta^2z^2}} \phi_{HSV} \, d\eta = \begin{cases} +\frac{1}{2} & z > 0 \\ -\frac{1}{2} & z < 0 \end{cases} \quad x \geq |\beta z| \quad (3a-14)$$

Again all of the disturbance is concentrated on the Mach planes. There is a potential jump across the Mach planes and also across the  $z = 0$  plane, the latter due to the discontinuity in the past history of the fluid particles above and below the plane.

## B. SOME EQUIVALENT SINGULARITY DISTRIBUTIONS

### Statement of the Problem

The first section of this chapter reviewed the basic singularities which represent elements of lift, side force and volume in linearized supersonic flow theory. It was noted that these singularities may all be obtained from the source singularity with the aid of the simple processes of integration and differentiation. The fact that the basic singularities are so related will be shown to imply that certain distributions of singularities are equivalent, i.e. they produce the same flow field, at least outside of a finite region. In the present section an equivalence theorem will be proved regarding constant strength distributions of sources, lifting and side force elements and vortex sheets. Such a theorem will later prove useful in the study of interference between distributions (Ch. IX B,C,F). Note that if the distribution A is part of a larger distribution (A,B) and if A is replaced by an equivalent distribution  $A_1$  then the drag of  $(A_1,B)$  is the same as that of  $(A,B)$ . This follows from the fact that the substitution of  $A_1$  for A does not change the flow field at infinity (Ch. IV).

The distributions to be studied will be located on a cubic shell which has two faces perpendicular to the free stream direction. One face of the cube will be covered by sources of constant strength and the opposite face by sinks of constant strength. The remaining four faces will be encircled by vortex lines of constant strength. Two cases may then be distinguished: (A) The source distribution is on a face parallel to the free stream; (B) The source distribution is on a face normal to the free stream. These two cases are illustrated in Fig. 3b-1. The source, sink and vortex distributions are uniform and of constant intensity as indicated. The vortex lines are continuous around the cube with the circulation directed so as to induce in the interior of the cube downwash velocities in case A and upstream velocities in case B.

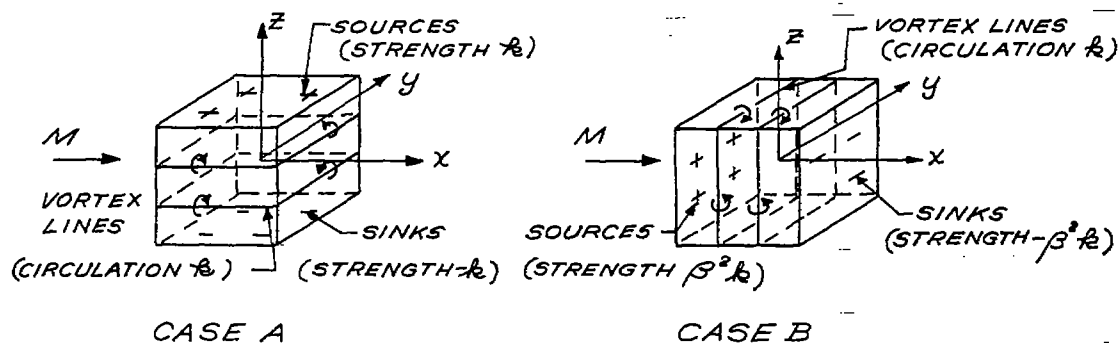


Fig. 3b-1

We shall now prove the following theorem.

### Theorem

In both cases A and B the perturbation velocities are zero everywhere outside the cubic shell. Inside the shell the downwash is constant in case A ( $w = -k$ ) and the pressure is constant in case B ( $u = -k$ ).

This theorem implies in particular that the source sink distribution, say in case A, is equivalent to the negative of the vortex-line distribution in case A, in the sense that the associated flow fields are identical outside the cube. Note that in case A the vortex distribution on the front and rear faces gives rise to a lifting force, whereas the vorticity on the side faces produces no force. In case B the vorticity on the top and bottom produces lift and the vorticity on the side faces produces side force.

The theorem will first be proved by a geometrical argument and then an alternative proof by analytical methods will be outlined.

### Geometrical Proof of Theorem

Consider first case A. We shall construct a geometrical configuration which corresponds to the distribution of singularities indicated in Fig. 3b-1. This construction will proceed in several steps by successively cutting down configurations of infinite extent. The vortex distribution on the front face is equivalent to a distribution of lifting elements of constant strength.

To begin with we shall assume the whole infinite plane containing the front face to be covered by lifting elements. This may be physically realized by a cascade of doubly infinite (two-dimensional) wings of constant angle of attack  $\alpha$  and such that the vertical distance between two neighboring wings is equal to the wing chord divided by  $\sqrt{M^2 - 1}$ , (Fig. 3b-2). In the limiting case of zero chord length the plane  $x = -\bar{x}$  is then covered by vortex lines with the circulation (of strength  $k$ ) oriented as in Fig. 3b-1. The value of the constant  $k$  is then  $k = 2\alpha U$ . The lift per unit area in the plane  $x = -\bar{x}$  is then  $2\alpha\rho U^2$ . Since the wings are spaced so as not to interfere with each other but still influence every point downstream of the cascade, the flow field at any point  $P$  with  $x > -\bar{x}$  may be described as follows (Fig. 3b-2). The point  $P$  receives a unit of downwash ( $-w = \alpha U$ ) from the wings A and B each. It also receives a positive unit of pressure ( $-u = \alpha U / \sqrt{M^2 - 1}$ ) from A and a negative unit

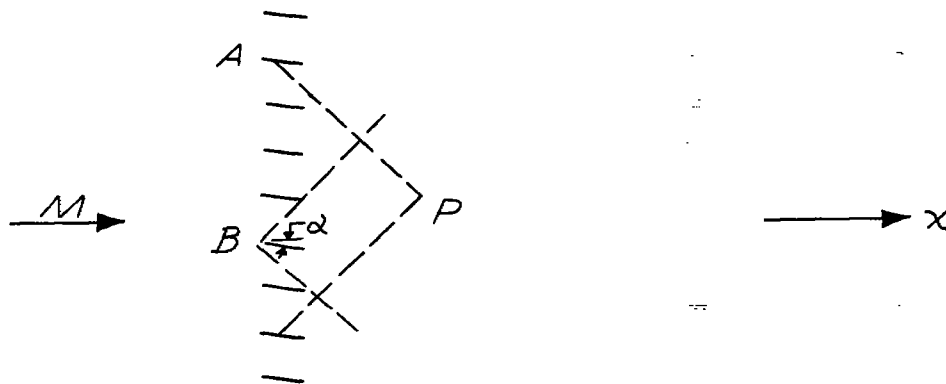


Fig. 3b-2

of pressure from B. The net pressure (referred to  $p_\infty$ ) received at P is then zero and the net downwash is  $-w = 2\alpha U = k$ .

The cascade may now be terminated from above by a wedge of opening angle  $2\alpha$  located in the plane  $z = \bar{z}$  with its exterior surface parallel to the free stream direction (Fig. 3b-3). Actually this wedge corresponds to a source distribution of constant source strength  $k = 2\alpha U$ . If the cascade is removed for  $z > \bar{z}$  the flow field is zero there since the wedge isolates this region from the rest of the cascade and since the exterior surface of the wedge is at zero angle of attack. For  $z < \bar{z}$  the flow field is unaffected by the introduction of the wedge. To see this consider a point P with  $z < \bar{z}$  (Fig. 3b-3). The wing at B acts as before to produce a downwash of  $-\alpha U$  at P. Only the point C on the wedge

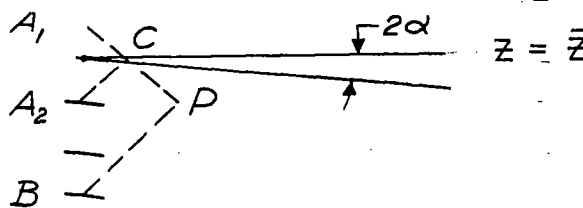


Fig. 3b-3

affects the point P and this point C is already in the downwash field  $-\alpha U$  of wing  $A_2$ . Thus the wedge turns the flow downward only by an angle  $\alpha$

so that the total downwash at P is again  $-2\alpha U$ . Conditions at P are the same as in the infinite cascade.

Similarly the cascade may be terminated from below at  $z = -\bar{z}$  by placing a wedge there of opening angle  $-2\alpha$ . This corresponds to a distribution of sinks of strength  $-k$ .

The cascade may then be cut down to finite width by placing planes of zero thickness parallel to the plane at  $y = \bar{y}$  and removing the part of the wings for  $|y| > \bar{y}$ . Since no sidewash is present the flow field is undisturbed by the introduction of these planes. Thus for  $x > -\bar{x}$ ,  $|y| < \bar{y}$ ,  $|z| < \bar{z}$  the downwash is  $-w = 2\alpha U = k$  and the pressure is zero. Outside this region all perturbation quantities are zero.

Finally one may restrict the flow field to the inside of a cube by taking the negative of the above configuration and placing it at  $x = \bar{x}$ .

Thus the resulting flow field has constant downwash and zero pressure inside the cube  $-\bar{x} < x < \bar{x}$ ,  $-\bar{y} < y < \bar{y}$ ,  $-\bar{z} < z < \bar{z}$ . Outside this cube the perturbation velocity is zero. Thus the front face is a cascade of lifting wings at an angle of attack  $\alpha$ , which bends the flow down. The rear face is a cascade of wings of angle of attack  $-\alpha$  which straighten the flow out again. The top and bottom faces consist of wedges whose inside surfaces follow the direction of the flow which has been bent by the cascade. These outside surfaces are parallel to the free stream. (Note that for the wedge of negative angle the "interior" top surface is directed downward at an angle  $2\alpha$  and the "exterior" bottom surface is parallel to the flow.) Finally the side faces are planes that carry no forces. For each such plane the downwash is  $-w = 2\alpha U$  on the inside and  $w = 0$  on the outside. These planes are then surfaces of constant vorticity. However, the vorticity vector is parallel to the free stream and hence no force results.

Thus a geometric configuration (using a wedge of negative opening angle) corresponding to case A has been constructed and the theorem has been proved for this case.

The corresponding construction for case B will only be indicated. The source distribution on the front face is obtained by placing wedges there (Fig. 3b-4) of half-angle  $\alpha = \beta k/2U$ .

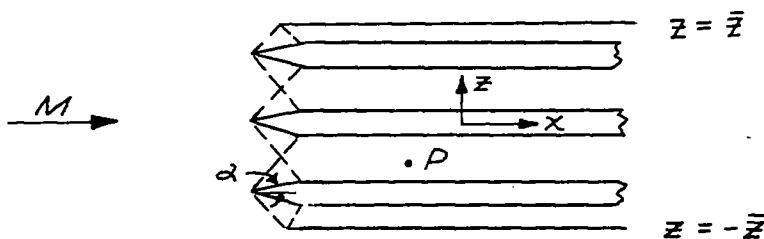


Fig. 3b-4

At a point P then the downwash is zero and the pressure is given by  
 $-u = 2\alpha U \sqrt{M^2 - 1} = k.$

By inserting planes of zero thickness at  $z = \pm \bar{z}$ ,  $y = \pm \bar{y}$  and removing the wedges outside these planes the infinite configuration is cut down to a configuration with a finite cross section. Outside these planes the flow is undisturbed. Inside these planes  $-u$  maintains its value  $2\alpha U \sqrt{M^2 - 1} = k.$  These planes are then pressure discontinuities and hence carry lift and side force respectively. They are also vortex sheets.

Finally the configuration may be terminated by placing its negative at  $x = +\bar{x}.$

A geometric configuration (again using wedges of negative opening angles) corresponding to case B has thus been constructed and the theorem has been proved for case B.

### Analytical Proof of Theorem (Outline)

#### Case A. Source Distribution Face Parallel to Free Stream

Consider a cube with sources of strength  $k$  on the top and  $-k$  on the bottom, and with lifting elements of strength  $\rho U k$  on the front face and  $-\rho U k$  on the rear face. On the side faces of the cube there are no forces associated with the vortex lines parallel to the flow direction; these are the trailing vortex system of the elements on the rear face.

In computing the potential due to the singularities on the cubic shell, various regions of the flow field are considered separately. For the region ahead of the foremost Mach waves from the cube no disturbance is possible in supersonic flow. Behind the cube, if the forward Mach cone from a point includes all of the shell, the potential at that point may be found simply by integrating the total effect of the singularities covering the shell. The potential due to individual unit source elements, lifting elements, and side force elements are given in Eqs. (3a-5), (3a-8), and (3a-9). The strengths of the distributions considered in this case are indicated in Fig. 3b-5.

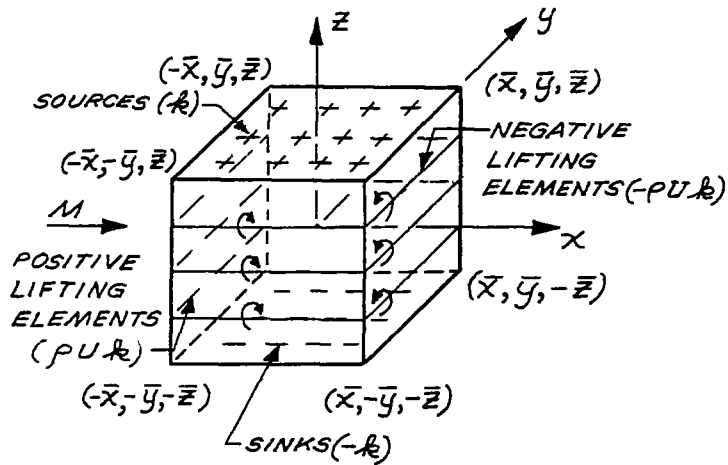


Fig. 3b-5

The potential for the entire shell is then

$$\phi = \frac{k}{2\pi} \left[ (x + \bar{x}) \int_{-\bar{z}}^{\bar{z}} \int_{-\bar{y}}^{\bar{y}} \frac{(z - z_0) dy_0 dz_0}{\left[ (y - y_0)^2 + (z - z_0)^2 \right] \sqrt{(x + \bar{x})^2 - \beta^2 \left[ (y - y_0)^2 + (z - z_0)^2 \right]}} - \right. \\ \left. (x - \bar{x}) \int_{-\bar{z}}^{\bar{z}} \int_{-\bar{y}}^{\bar{y}} \frac{(z - z_0) dy_0 dz_0}{\left[ (y - y_0)^2 + (z - z_0)^2 \right] \sqrt{(x - \bar{x})^2 - \beta^2 \left[ (y - y_0)^2 + (z - z_0)^2 \right]}} - \right. \\ \left. \frac{k}{2\pi} \left[ \int_{-\bar{x}}^{\bar{x}} \int_{-\bar{y}}^{\bar{y}} \frac{dx_0 dy_0}{\sqrt{(x - x_0)^2 - \beta^2 \left[ (y - y_0)^2 + (z - \bar{z})^2 \right]}} - \right. \right. \\ \left. \left. \int_{-\bar{x}}^{\bar{x}} \int_{-\bar{y}}^{\bar{y}} \frac{dx_0 dy_0}{\sqrt{(x - x_0)^2 - \beta^2 \left[ (y - y_0)^2 + (z + \bar{z})^2 \right]}} \right] \right] \quad (3b-1)$$

This, after evaluating the integrals, equals zero.

A third region of the flow field contains points slightly behind and far to the side of the cube, where forward Mach cones from the points include part, but not all, of the cube. For this region, Hayes' method<sup>(1)</sup> can be used to show that the potential again is zero. This method is described in Ch. IVC. It requires that the distance from the cube to any point P where the potential is to be computed must be large compared to the dimensions of the cube. In addition, P must lie near the Mach cones emanating from the singularities on the cube. P is then a point at some angle  $\theta$  (measured from the horizontal plane) on a distant cylindrical control surface surrounding the cubic shell. An "equivalent lineal distribution" of singularities is formed by finding the singularity strength intercepted from the cube by a set of parallel planes originating at angle  $\theta$  on the control cylinder and inclined at the Mach angle to the free stream direction. The singularities intercepted by a given Mach plane are lumped together at the intersection of the Mach plane and the axis of the cylinder, such that the total strength of the equivalent distribution is equal to the total strength of the original distribution. After determining the strength ( $h$ ) of the equivalent lineal distribution which represents the cubic shell for a fixed  $\theta$ , the effect of all those singularities which influence the flow field at P can be summed. Hayes writes the expression for  $h$  as

$$h = +f - g_z \sin \theta - g_y \cos \theta \quad (3b-2)$$

where  $f$  is the source strength (per unit length),  $g_z/\beta$  the circulation strength (per unit length) of the lifting elements, and  $g_y/\beta$  the circulation strength of the side force elements.

Figure 3b-6 indicates the notation to be used in describing the geometry of the intersections of the Mach planes with planes containing the  $x, y, z$  axes. The Mach plane is inclined to the axis of the control cylinder at the Mach angle  $\mu = \sin^{-1}(1/M)$  and it is tangent to a cross-section of the cylinder at angle  $\theta$ . The trace of the Mach plane in a horizontal ( $x-y$ ) plane is inclined to a normal to the flow direction at angle  $\delta$ , where  $\tan \delta = \cot \mu \cos \theta = \beta \cos \theta$ . The trace of the Mach plane in a vertical ( $x-z$ ) plane forms an angle  $\sigma$  with a line parallel to the  $z$ -axis, where  $\tan \sigma = \beta \sin \theta$ .

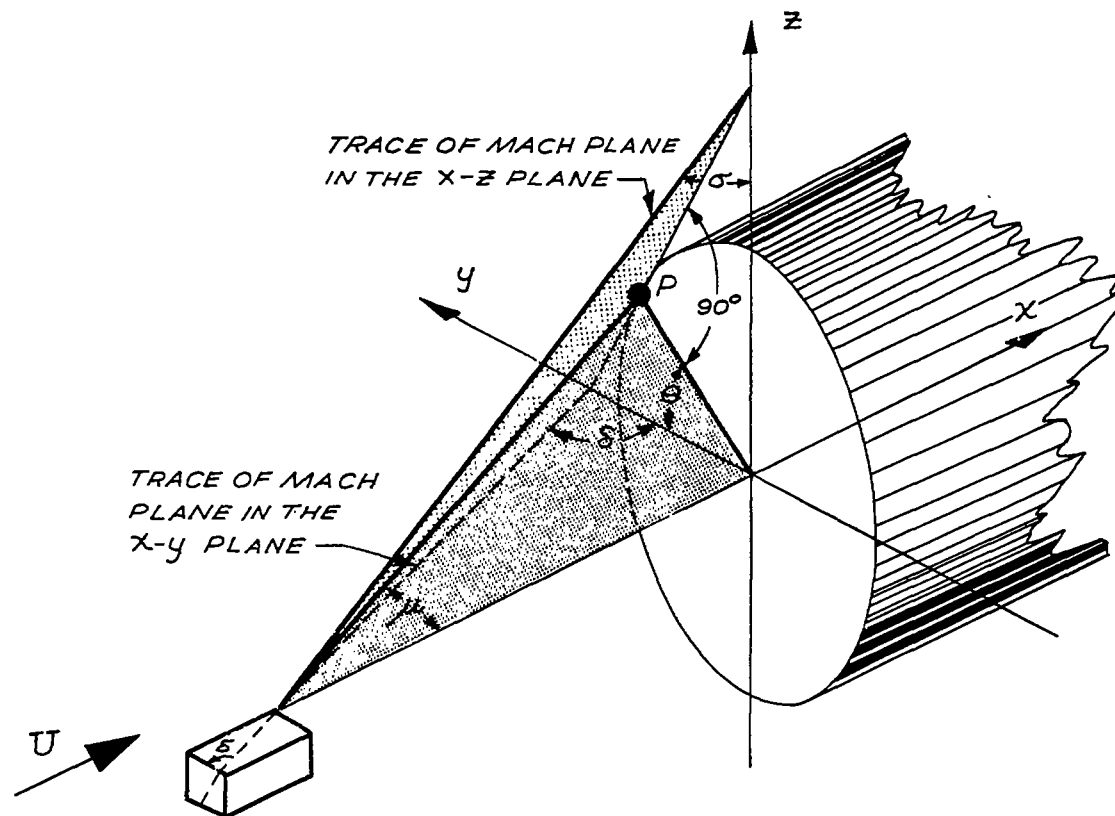


Fig. 3b-6

With this brief description of Hayes' procedure in mind, an equivalent lineal distribution of singularities is now to be computed for the specific case of the cubic shell described previously. Figure 3b-7a shows the intersections of two parallel Mach planes with the shell; the Mach planes are assumed to be separated by an infinitesimal distance. The case illustrated shows only three faces of the cube intersected by the Mach planes since the procedure would be the same if four faces were affected. In order to better define the geometry and notation, Fig. 3b-7b shows the cubic shell as though it were cut along the corner edges and flattened out in one plane.

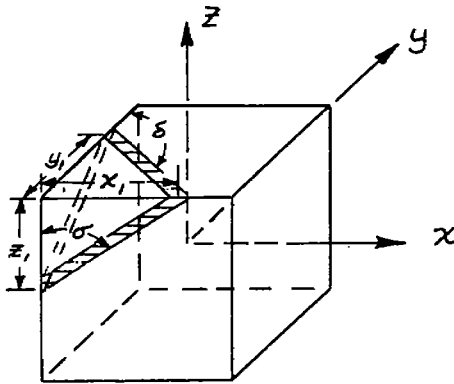


Fig. 3b-7a

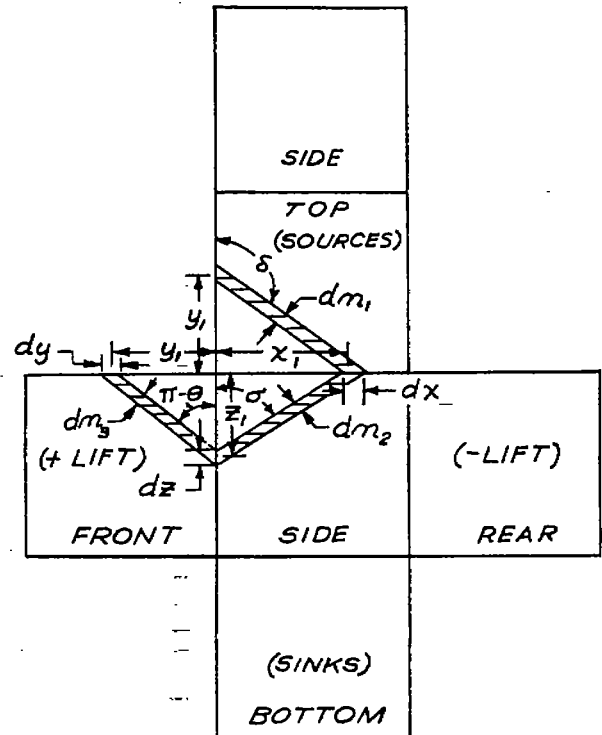


Fig. 3b-7b

The net singularity strength cut out by these Mach planes must be lumped along a length  $dx$  of the axis. The total source strength is the product of the strength per unit area ( $k$ ) and the area intercepted from the top surface of the cube by the Mach planes:

$$f = k \frac{x_1}{\left| \cos \left( \delta - \frac{\pi}{2} \right) \right|} dn_1 = k \frac{x_1}{|\tan \delta|} dx = -k \frac{x_1}{\beta \cos \theta} dx \quad (3b-3a)$$

(The negative sign is inserted because  $\theta$  is in the second quadrant for the example shown, but  $f$  is positive.) The total lifting element strength is  $\rho U k$  multiplied by the area intercepted from the front face:

$$\begin{aligned} l &= \rho U k \frac{z_1}{|\cos(\pi - \theta)|} dn_3 = \rho U k z_1 dz |\tan \theta| \\ &= \rho U k \frac{x_1 dx}{\tan^2 \sigma} |\tan \theta| = -\rho U k \frac{x_1 dx}{\beta^2 \sin \theta \cos \theta} \end{aligned} \quad (3b-3b)$$

Again, a negative sign is inserted because  $\cos \theta$  is negative while  $l$  should be positive. There are no forces on the side faces. In computing the strength of the equivalent lineal distribution from Eq. (3b-2) it must be remembered that  $g_y$ ,  $g_z$  from that formula are circulation strengths multiplied by  $\beta$ ; i.e.,

$$g_z = \frac{\beta l}{\rho U} \quad g_y = \frac{\beta S}{\rho U}$$

Then

$$\begin{aligned} h &= +f - g_z \sin \theta - g_y \cos \theta \\ &= \frac{-kx_1 dx}{\beta \cos \theta} - \frac{\beta}{\rho U} \left( \frac{-\rho U k x_1 dx}{\beta^2 \sin \theta \cos \theta} \right) \sin \theta = 0 \end{aligned} \quad (3b-4)$$

That is, the net singularity strength is zero. This is true for all angles  $\theta$ , and similar calculations show that it is also true for every station  $x$  along the cylinder axis. Therefore, the velocity potential is zero at all distant points for which Hayes' method is applicable.

There remains to find the velocity potential in the neighborhood of the shell. The cube may be subdivided into smaller cubic shells, each similar to the original. Singularities on interfaces of adjoining shells then cancel so the net singularity distribution is unchanged. Those shells which lie behind and outside the forward Mach cone from any point cannot influence the velocity potential at that point. It was shown earlier that those shells which lie completely inside the forward Mach cone from the point also do not influence the potential there. Therefore, only those shells lying along the forward Mach cone need be considered. However, these may be further subdivided into cubic shells of elementary proportions so that the distance from the point to any one of the shells is very large compared to the dimensions of that shell. Then the analysis based on Hayes' procedure shows that these shells do not contribute to the velocity potential at the point either. This indicates that the velocity potential is zero everywhere outside the cubic shell.

To find the velocity perturbations inside the shell, again consider it divided into smaller shells. None of these except the one containing the point  $P$  can influence the potential at  $P$  according to the preceding analysis. Therefore, all of the small shells located more than a distance  $\epsilon$  ahead of  $P$  can be removed without affecting the potential at  $P$ . The forward Mach cone from  $P$  then intersects only the front face of the

remaining part of the original cube, so that, effectively, P is aware only of an infinite distribution of lifting elements. Since this result is independent of the location of P inside the original cubic shell, the downwash inside the shell must be constant.

Case B. Source Distribution Face Normal to the Free Stream

Consider now a cube with lifting elements of strength  $\rho U k$  on the top face and  $-\rho U k$  on the bottom face, with side force elements of strength  $\rho U k$ ,  $-\rho U k$  on the side faces, and with sources of strength  $\beta^2 k$  on the front face and  $-\beta^2 k$  on the rear face.

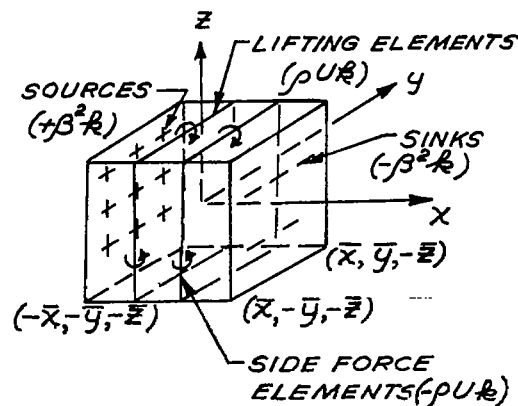


Fig. 3b-8

First, the potential ahead of the foremost Mach waves of the cube is, of course, zero. At a downstream point whose forward Mach cone includes all of the sources and lifting elements, the potential is

$$\begin{aligned}
 \phi = \frac{k}{2\pi} & \left[ (z - \bar{z}) \int_{-\bar{x}}^{\bar{x}} \int_{-\bar{y}}^{\bar{y}} \frac{(x - x_0) dx_0 dy_0}{\left[ (y - y_0)^2 + (z - \bar{z})^2 \right] \sqrt{(x - x_0)^2 - \beta^2 \left[ (y - y_0)^2 + (z - \bar{z})^2 \right]}} - \right. \\
 & (z + \bar{z}) \int_{-\bar{x}}^{\bar{x}} \int_{-\bar{y}}^{\bar{y}} \frac{(x - x_0) dx_0 dy_0}{\left[ (y - y_0)^2 + (z + \bar{z})^2 \right] \sqrt{(x - x_0)^2 - \beta^2 \left[ (y - y_0)^2 + (z + \bar{z})^2 \right]}} + \\
 & (y - \bar{y}) \int_{-\bar{x}}^{\bar{x}} \int_{-\bar{z}}^{\bar{z}} \frac{(x - x_0) dx_0 dz_0}{\left[ (y - \bar{y})^2 + (z - z_0)^2 \right] \sqrt{(x - x_0)^2 - \beta^2 \left[ (y - \bar{y})^2 + (z - z_0)^2 \right]}} - \\
 & \left. (y + \bar{y}) \int_{-\bar{x}}^{\bar{x}} \int_{-\bar{z}}^{\bar{z}} \frac{(x - x_0) dx_0 dz_0}{\left[ (y + \bar{y})^2 + (z - z_0)^2 \right] \sqrt{(x - x_0)^2 - \beta^2 \left[ (y + \bar{y})^2 + (z - z_0)^2 \right]}} \right] + \\
 & \frac{\beta^2 k}{2\pi} \left[ \int_{-\bar{y}}^{\bar{y}} \int_{-\bar{z}}^{\bar{z}} \frac{dy_0 dz_0}{\sqrt{(x - \bar{x})^2 - \beta^2 \left[ (y - y_0)^2 + (z - z_0)^2 \right]}} - \right. \\
 & \left. \int_{-\bar{y}}^{\bar{y}} \int_{-\bar{z}}^{\bar{z}} \frac{dy_0 dz_0}{\sqrt{(x + \bar{x})^2 - \beta^2 \left[ (y - y_0)^2 + (z - z_0)^2 \right]}} \right] \tag{3b-5}
 \end{aligned}$$

Carrying out the integration, it is found that

$$\phi = -2k\bar{x} \quad \text{for } -\bar{y} < y < \bar{y} \text{ and } -\bar{z} < z < \bar{z}$$

$$\phi = 0 \quad \text{Elsewhere}$$

By Hayes' procedure, when forward Mach cones from distant points include only part of the singularities, the potential at those points is the same as would be contributed by a lineal distribution whose strength,  $h$ , can be computed in the manner described previously. For Mach planes intersecting the cube in the same location illustrated for another case in Fig. 3b-7, one finds that

$$f = -k \frac{x_1 dx}{\sin \theta \cos \theta}, \quad S = -\rho U k \frac{x_1 dx}{\beta \sin \theta}, \quad z = -\rho U k \frac{x_1 dx}{\beta \cos \theta} \quad (3b-6)$$

and so

$$h = -k \frac{x_1 dx}{\sin \theta \cos \theta} - \frac{\beta}{\rho U} \left( -\rho U k \frac{x_1 dx}{\beta \sin \theta} \right) \cos \theta - \frac{\beta}{\rho U} \left( -\rho U k \frac{x_1 dx}{\beta \cos \theta} \right) \sin \theta = 0 \quad (3b-7)$$

Thus, the potential due to the cubic shell is zero at all distant points of the flow field which lie near the Mach cone of the shell.

In the neighborhood of the cube, the same arguments used for the first cubic shell show that the perturbation velocities for this case are zero there also. Therefore, the perturbation velocities are proved to be zero in every region of the flow field external to the cubic shell.

To find the potential at a point inside the shell, the shell is subdivided as before into smaller shells, each similar to the original. The analysis just completed shows that the velocity perturbations at  $P$  cannot be influenced by any of these shells except the one containing  $P$ . Therefore, all of the small shells located more than a distance  $\epsilon$  ahead of  $P$  can be removed. The net singularity strength intersected by the forward Mach cone from  $P$  then includes only sources on the front face of the remaining group of cubes. Effectively, then, conditions at  $P$  are the same as behind an infinite distribution of sources of constant intensity. This result is independent of the location of  $P$  inside the cubic shell, so the pressure must be constant inside the shell and the potential is of the form  $\phi = cx$ .

CHAPTER IV. THE EVALUATION OF DRAGA. THE "CLOSE" AND THE "DISTANT" VIEWPOINTS

The non-viscous drag for a wing and body moving at supersonic speeds may be obtained from two different points of view<sup>(1)</sup>, using linearized theory. First, the drag can be evaluated by integrating the local pressure times frontal area over the wing and body surfaces. Second, the drag can be evaluated from momentum or energy considerations involving the flow field at a great distance from the aircraft. These two procedures are actually variations of the same basic method.

In the latter case part of the drag due to lift is associated with the production of kinetic energy in the trailing vortex system, and is called "vortex drag." This drag is identical with that produced by the same spanwise lift distribution in an incompressible flow, (frequently called "induced drag").

The remainder of the drag due to lift and all of the drag due to thickness is associated with the production of energy near the surface of a downstream Mach cone whose vertex is in or near the aircraft. This is called wave drag, and the associated energy is half kinetic and half potential<sup>(1)</sup>.

The wave drag plus the vortex drag is equal to the drag evaluated at the wing and body surfaces by the first method. (It may be necessary to retain nonlinear terms in the expression for pressure coefficient to get this agreement.)

The momentum theorem is utilized in both of the above methods but different "control surfaces" are used. In the first case the control surface is close to the aircraft surface, but in the second case the control surface is a distant one. For example Hayes<sup>(1)</sup> uses a circular cylinder with axis passing through the aircraft and parallel to the free stream direction. The radius of the cylinder is chosen to be very large compared to the aircraft dimensions since this simplifies the calculations.

The wave drag of the aircraft is then evaluated from the rate at which momentum (in the free stream direction) is carried across the surface of the cylinder. (If the control surface had been chosen as a surface containing streamlines instead of a perfect cylinder, then the wave drag would have appeared as pressure on the streamline surface.)

The cylindrical control surface is closed far downstream by a plane normal to the flow direction. The vortex drag is then determined, as in incompressible flow, by the rate at which the kinetic energy of the trailing vortex system passes through this plane, or alternatively through momentum and pressure considerations.

### B. GENERAL MOMENTUM THEOREM FOR EVALUATION OF DRAG

In the present section a momentum integral for the drag, as given by linearized theory, will be derived (Eqs. 4b-33,34). The drag will be given as an integral over an arbitrary control surface enclosing the solid. The integrand is a quadratic expression in the velocity components as given by linearized theory.

First a more general momentum integral will be considered. Consider a control surface  $S$  enclosing a solid (Fig. 4b-1). A surface element on  $S$  of area  $dS$  will be represented by its outward normal  $d\vec{n}$  where the length of  $d\vec{n}$  is equal to the area of the surface element. Thus  $d\vec{n} = (dS)\vec{n}$  if  $\vec{n}$  is the outward normal of unit length. Let the hydrodynamical stress

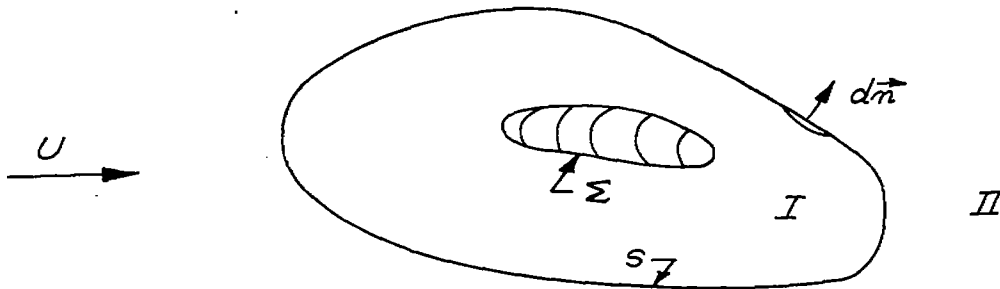


Fig. 4b-1

tensor be denoted by  $\sigma$ , and let I be the region inside  $S$  and II the region outside  $S$ . Then

$$\vec{f} = \sigma d\vec{n} = \text{Force exerted by II on I across surface element} \quad (4b-1)$$

If a system of coordinates  $x_1, x_2, x_3$  is chosen  $d\vec{n}$  may be represented by its three components  $(dn)_j$  and  $\sigma$  by a  $3 \times 3$  matrix  $\sigma_{ij}$ . The above equation may then be written

$$f_i = (\sigma d\vec{n})_i = \sum_{j=1}^3 \sigma_{ij} (dn)_j \quad (4b-2)$$

where  $(\sigma d\vec{n})_i$  is the  $i^{\text{th}}$  component of the force.

For a non-viscous fluid the only hydrodynamical force is the pressure  $p$  and the stress tensor is

$$\sigma = -pI = -(p\delta_{ij}) \quad (4b-3)$$

where  $I$  is the identity tensor whose matrix is the Kronecker delta  $\delta_{ij}$ . In this case the force across the element is

$$\vec{f} = -p(I d\vec{n}) = -p d\vec{n} \quad (4b-4)$$

or

$$f_i = -p(dn)_i$$

The hydrodynamical momentum equation states that the stress tensor is balanced by flow-of-momentum tensor. (This is actually a restatement of Newton's law that force = (mass) times (acceleration).) To define the flow-of-momentum tensor we first introduce the concept of a dyadic product of two vectors. Let  $\vec{a}$  and  $\vec{b}$  be two vectors with components  $(a_i)$  and  $(b_i)$ . The dyadic product is then the tensor whose  $ij$  component  $(\vec{a} \cdot \vec{b})_{ij}$  is  $a_i b_j$ , i.e.

$$\vec{a} \cdot \vec{b} = (a_i \cdot b_j) \quad (4b-5)$$

Note that if  $\vec{c}$  is any vector then

$$(\vec{a} \cdot \vec{b})\vec{c} = (\Sigma a_i b_j) c_j = (a_i \Sigma b_j c_j) = \vec{a}(\vec{b} \cdot \vec{c}) \quad (4b-6)$$

where  $\vec{b} \cdot \vec{c}$  is the ordinary dot product.

The flow of momentum tensor is then the dyadic product of  $\rho\vec{q}$  (momentum per unit volume) and  $\vec{q}$  velocity:

$$\text{Flow-of-momentum tensor} = \rho\vec{q} \cdot \vec{q} \quad (4b-7)$$

Its physical interpretation may be seen by applying this tensor to the normal  $d\vec{n}$

$$(\rho\vec{q} \cdot \vec{q})d\vec{n} = \rho\vec{q}(\vec{q} \cdot d\vec{n}) = \text{Momentum transported through } dS \text{ per unit time.} \quad (4b-8)$$

The basic momentum equation for stationary flow for a surface  $S_1$  which does not enclose a body is then

$$\int_{S_1} (\rho\vec{q} \cdot \vec{q})d\vec{n} = \int_{S_1} \sigma d\vec{n} \quad (4b-9)$$

This is analogous to the law of conservation of mass which states that

$$\int_{S_1} \rho\vec{q} \cdot d\vec{n} = 0 \quad (4b-10)$$

Consider now the composite surface consisting of the surface  $S$  in Fig. 4b-1 and the body surface  $\Sigma$ . Let  $d\vec{n}$  denote normals on  $\Sigma$  which point outwards with respect to the body (i.e. into region I). From the definition of the stress tensor  $\sigma$

$$\vec{F} = \text{Total force exerted by fluid on body} = \int_{\Sigma} \sigma d\vec{n} \quad (4b-11)$$

Since the flow through  $\Sigma$  is zero one obtains by applying Eq. (4b-9) to the composite surface  $S_1 = S + \Sigma$

$$\int_S (\rho\vec{q} \cdot \vec{q})d\vec{n} = \int_S \sigma d\vec{n} - \int_{\Sigma} \sigma d\vec{n} \quad (4b-12)$$

The minus sign in the last term is due to the convention that on the surface  $\Sigma$  the quantity  $d\vec{n}$  denotes the inward normal with respect to the region I. Comparing Eqs. (4b-11) and (4b-12) one obtains

$$\vec{F} = - \int_S (\rho \vec{q} \cdot \vec{q}) d\vec{n} + \int_S \sigma d\vec{n} \quad (4b-13)$$

This is the fundamental momentum formula which gives the total hydrodynamical force on the solid as an integral over a control surface enclosing the solid.

Note that in Eq. (4b-11), the force is given by an integral of the stresses on the body surface. This is the "close" point of view for evaluating the force. Eq. (4b-13) shows how the same force may be evaluated from the distant point of view.

A slight modification of Eq. (4b-13) will be needed later. Denote the flow quantities at infinity as follows

$$\vec{q}, \rho, p, \sigma \text{ at infinity} = \vec{U}, \rho_0, p_0, \sigma_0, \text{ respectively} \quad (4b-14)$$

The difference between a flow quantity and its value at infinity will be denoted by a "prime." Thus

$$\vec{q}' = \vec{q} - \vec{U}, p' = p - p_0, \rho' = \rho - \rho_0, \sigma' = \sigma - \sigma_0 \quad (4b-15)$$

From the continuity equation (Eq. 4b-10) it follows that

$$\vec{U} \int_S \rho \vec{q} \cdot d\vec{n} = \int_S (\rho \vec{U} \cdot \vec{q}) d\vec{n} = 0 \quad (4b-16a)$$

Furthermore, since  $\sigma_0 = \text{Constant}$

$$\int_S \sigma_0 d\vec{n} = 0 \quad (4b-16b)$$

Subtracting Eqs. (4b-16a, b) from Eq. (4b-13) one obtains

$$\vec{F} = - \int_S (\rho \vec{q}' \cdot \vec{q}') d\vec{n} + \int_S \sigma' d\vec{n} \quad (4b-17a)$$

where, for a non-viscous fluid,

$$\int_S \sigma' d\vec{n} = - \int_S p' d\vec{n} \quad (4b-17b)$$

This is the fundamental momentum formula in terms of perturbation quantities. Note that the latter are not assumed to be small.

The drag is the component of  $\vec{F}$  in the free stream direction. We shall take this direction as the x-direction and use the following notation.

$$\vec{U} = U_1, \quad \vec{q} = (u, v, w), \quad \vec{q}' = (u', v', w') \quad (4b-18)$$

where

$$u = U + u', \quad v' = v, \quad w' = w$$

From Eq. (4b-17a) then follows the fundamental momentum formula for drag:

$$\text{Drag} = \vec{F} \cdot \vec{i} = - \int_S \rho u' \vec{q} \cdot d\vec{n} + \vec{i} \cdot \int_S \sigma' d\vec{n} \quad (4b-19)$$

The momentum integrals may be further simplified for special choices of the control surface S, in particular by letting S recede to infinity. However, we shall first derive an approximate form of the drag formula, valid within linearized theory. In the following section this linearized formula will then be specialized to a special infinitely distant control surface (method of Hayes<sup>(1)</sup>).

#### Inviscid Second-Order Drag

It will be shown below that for a thin or slender body the largest contribution to the drag may be evaluated by an integral of a quadratic expression of the linearized perturbation velocities. It is usually stated that the drag is of second order. However, it should be remembered that the values of the perturbation velocities are computed from first-order (linearized) theory. The result is a formula for drag according to first-order theory. The term "second-order drag" refers to the fact

the integrand is quadratic in  $u'$ ,  $v'$  and  $w'$  and hence of second order if  $u'$ ,  $v'$  and  $w'$  are themselves of first order. Furthermore, the second-order correction to  $u'$ ,  $v'$  and  $w'$  will contribute nothing to the second-order expression for drag. The final formula is given by Eqs. (4b-33,34) and the reader interested only in the final result may skip the derivation now presented below.

We shall first assume non-viscous flow, so that the stress tensor is given by Eq. (4b-3). Furthermore, we shall assume that the solid is characterized by a parameter  $\epsilon$ , which is small, e.g. the fineness or thickness ratio. We shall furthermore assume that the flow quantities may be expressed by power series in  $\epsilon$ :

$$u = U + \epsilon u_1 + \epsilon^2 u_2 + \dots \quad (4b-20)$$

$$v = \epsilon v_1 + \epsilon^2 v_2 + \dots$$

$$w = \epsilon w_1 + \epsilon^2 w_2 + \dots$$

$$p = p_0 + \epsilon p_1 + \epsilon^2 p_2 + \dots$$

$$\rho = \rho_0 + \epsilon \rho_1 + \epsilon^2 \rho_2 + \dots$$

Such an expansion is valid at a distance from the body. It should be remembered, however, that in slender body theory, terms involving  $\log \epsilon$  are of importance very near the body.

The coefficients of  $\epsilon$  are the first order terms and are given by linearized theory. The coefficients of  $\epsilon^2$  are the second order terms, etc. The lowest order term in the expression for the drag will now be found using the isentropic pressure-density relation and Bernoulli's law.

From isentropy it follows that density is a function of pressure alone. One defines

$$\left( \frac{dp}{d\rho} \right)_{\text{constant entropy}} = a^2$$

where  $a$  is the isentropic speed of sound. Then

$$\rho = \rho_0 + \frac{1}{a_0^2} (p - p_0) + \dots \quad (4b-21)$$

from which then follows

$$\rho_1 = \frac{p_1}{a_0^2} \quad (4b-22)$$

Bernoulli's law may be written

$$\frac{d(u^2 + v^2 + w^2)}{2} + dP = 0$$

where

$$P = \int_{p_0}^p \frac{dp}{\rho}$$

or

$$(u' + U)^2 + v^2 + w^2 + 2P = U^2 \quad (4b-23)$$

Using Eq. (4b-21) P may be expanded to second order

$$P \doteq \int \frac{dp'}{\rho_0 + \frac{p'}{a_0^2}} = \frac{1}{\rho_0} \int \left( 1 - \frac{p'}{\rho_0 a_0^2} \right) dp' = \frac{1}{\rho_0} \left[ p' - \frac{(p')^2}{2\rho_0 a_0^2} \right] \quad (4b-24)$$

Expanding the terms in Eq. (4b-23) to second order one obtains

$$\epsilon U u_1 + \epsilon^2 U u_2 + \epsilon^2 \frac{u_1^2 + v_1^2 + w_1^2}{2} + \frac{1}{\rho_0} \left( \epsilon p_1 + \epsilon^2 p_2 - \frac{\epsilon^2 p_1^2}{2\rho_0 a_0^2} \right) = 0$$

Collecting the terms of order  $\epsilon$  one finds the linearized Bernoulli's law

$$p_1 + \rho_0 u_1 U = 0 \quad (4b-25)$$

Comparing with Eq. (4b-22) one sees that

$$\rho_1 = -\rho_0 \frac{Uu_1}{a_0^2} \quad (4b-26)$$

The terms of order  $\epsilon^2$  yield the following expression for  $p_2$

$$\rho_0 Uu_2 + \rho_0 \frac{u_1^2 + v_1^2 + w_1^2}{2} + p_2 - \frac{\rho_0 u_1^2 M^2}{2} = 0 \quad (4b-27)$$

where Eq. (4b-25) has been used and

$$M = \frac{U}{a_0}$$

In the momentum formula, Eq. (4b-17), the stress and momentum flow tensors may be combined to form a tensor A

$$A = -\rho \bar{q}' \cdot \bar{q} - p' I$$

Using Eqs. (4b-20, 25, 26) one may evaluate  $A_{11}$

$$\begin{aligned} A_{11} &= -\rho u'(U + u') - p' \\ &= -\epsilon(\rho_0 u_1 U + p_1) - \epsilon^2(\rho_0 u_2 U + \rho_1 u_1 U + \rho_0 u_1^2 + p_2) \\ &= -\epsilon^2 \rho_0 \left( Uu_2 - M^2 u_1^2 + u_1^2 - Uu_2 - \frac{u_1^2 + v_1^2 + w_1^2}{2} + \frac{u_1^2 M^2}{2} \right) \end{aligned}$$

Finally

$$A_{11} = \epsilon^2 \rho_0 \frac{1}{2} \left[ (M^2 - 1) u_1^2 + v_1^2 + w_1^2 \right] \quad (4b-28)$$

Similarly

$$A_{12} = -\rho u'v' = -\epsilon^2 \rho_0 u_1 v_1 \quad (4b-29)$$

$$A_{13} = -\rho u'w' \doteq -\epsilon^2 \rho_0 u_1 w_1 \quad (4b-30)$$

Since only the first row ( $A_{11}$ ,  $A_{12}$ ,  $A_{13}$ ) enters in the drag computation we have proved the following:

1. The dominant term in the drag formula is of second order in  $\epsilon$
2. The integrand in the drag formula is, to second order, a second degree polynomial in the first order velocity perturbations. The velocity perturbations of second order, or pressure and density perturbations of second order, do not enter into this expression.

Thus while drag is of second order, it may be computed on the basis of first order theory (linearized theory). On the other hand, one may easily check from the above expressions that in general the lift has a first order term. Furthermore to compute lift to second order one needs to know  $u_2$ , that is,  $u$  to second order.

In the remainder of this report we shall only be concerned with the drag as given by linearized theory. It is then convenient to introduce a change of notation. We shall let  $u$ ,  $v$ ,  $w$  stand for the linearized velocity perturbation; in other words

$$\epsilon u_1, \epsilon v_1, \epsilon w_1 \quad \text{are replaced by} \quad u, v, w \quad (4b-31)$$

Furthermore a velocity potential  $\phi$  will be introduced such that

$$\text{Grad } \phi = u, v, w \quad (4b-32)$$

The above results may then be summarized as follows. The drag to second order is given by the formula

$$D = \int_S \vec{A}_1 \cdot d\vec{n} \quad (4b-33)$$

where  $S$  = Control surface enclosing the body

$$\vec{A}_1 = (A_{11}, A_{12}, A_{13})$$

$$A_{11} = +\rho_0 \frac{1}{2} (\beta^2 u^2 + v^2 + w^2), \quad \beta^2 = M^2 - 1 \quad (4b-34)$$

$$A_{12} = -\rho_0 uv$$

$$A_{13} = -\rho_0 uw$$

and  $u$ ,  $v$  and  $w$  are the components of the perturbation velocity given by linearized theory.

### C. HAYES METHOD FOR DRAG EVALUATION

The method developed by Hayes in Ref. 1 consists in applying the drag formula Eq. (4b-33) to a special control surface, a truncated circular cylinder, surrounding the body and in considering the limiting case when the control surface recedes to infinity. The general momentum integral for the drag then assumes a simplified form. (This results in certain simplifications in the integrand.) Furthermore, if the body is represented by singularities (sources, lifting elements, etc.) as discussed in Ch. III, the velocities at large distances may be represented very simply in terms of the strength of the singularities. As a result the drag may also be represented as an integral over the singularities (distribution of source strength, etc.). This result of Hayes' generalizes a previous result by von Kármán<sup>(7)</sup> for a body of revolution.

First a somewhat detailed demonstration of the method of Hayes will be given for the case of a lineal source distribution. This part may be skipped by a reader not interested in mathematical details. Then the results of Hayes and related results will be stated in intuitive terms for general three-dimensional distribution of sources, lifting elements and side-force elements. Detailed proofs will not be given. However, the results may be proved by methods closely analogous to the method exhibited for the case of a lineal source distribution.

#### Hayes Method for Lineal Source Distribution

We shall consider a distribution of sources along the  $x$ -axis between  $x = 0$  and  $x = L$ . The corresponding solid is then a body of revolution. The source strength will be denoted by  $f$ . It will be assumed that

$$f(0) = 0, \quad f(L) = 0 \quad (4c-1)$$

These assumptions lead to certain restrictions on the body shape. Let the radius of the body be  $r(x)$ . The cross sectional area  $S(x)$  is then  $\pi r^2(x)$ . Since  $f(x) = U S'(x)$ ,  $f(0)$  means that  $r(0) \cdot r'(0) = 0$ . This is fulfilled if  $r \sim x^n$ ,  $n > 1/2$  near the origin. In particular,  $f(0)$  is equal to zero if the body starts in a point with finite slope, i.e.  $r \sim x$  near  $x = 0$ . The analogous condition at  $x = L$  insures  $f(L) = 0$ . In addition,  $f(L) = 0$  if the body ends smoothly in a cylinder with constant radius, i.e. if  $S(x) = \text{Constant}$  for  $x \geq L$  and  $S'(x)$  is continuous and hence zero at  $x = L$ . It will be indicated in the proof below why the restrictions on  $f$  are necessary.

#### Expression for Velocities

The potential due to the source distribution is then

$$\phi(x_1 r) = - \frac{1}{2\pi} \int_0^{x-\beta r} \frac{f(\xi) d\xi}{\sqrt{(x-\xi)^2 - \beta^2 r^2}} \quad (4c-2)$$

where  $r^2 = y^2 + z^2$ . For  $x - \beta r \geq L$  the upper limit may be replaced by  $L$ .

Using the condition  $f(0) = 0$  one finds by partial integration of Eq. (4c-2) and differentiation that the perturbation velocities are

$$\phi_x = - \frac{1}{2\pi} \int_0^{x-\beta r} \frac{f'(\xi) d\xi}{\sqrt{(x-\xi)^2 - \beta^2 r^2}} \quad (4c-3a)$$

$$\phi_r = \frac{1}{2\pi r} \int_0^{x-\beta r} - \frac{(x-\xi) f'(\xi) d\xi}{\sqrt{(x-\xi)^2 - \beta^2 r^2}} \quad (4c-3b)$$

In Eqs. (4c-3), the upper limit is replaced by  $L$  for  $x - \beta r \geq L$ .

We shall introduce the notation

$$t_\xi = \frac{\beta r}{x - \xi} \quad (4c-4)$$

Then  $t_\xi = 1$  on the downstream Mach cone from  $x = \xi$  and  $0 \leq t \leq 1$  inside this Mach cone. For  $x - \beta r \geq L$  one may also write the velocity components as

$$\begin{aligned}\phi_x &= \frac{1}{2\pi} \int_0^L f(\xi) \left[ (x - \xi)^2 - \beta^2 r^2 \right]^{-3/2} (x - \xi) d\xi \\ &= \frac{1}{2\pi} \int_0^L f(\xi) (x - \xi)^{-2} (1 - t_\xi^2)^{-3/2} d\xi\end{aligned}\quad (4c-5a)$$

$$\begin{aligned}\phi_r &= \frac{-1}{2\pi} \int_0^L f(\xi) \left[ (x - \xi)^2 - \beta^2 r^2 \right]^{-3/2} \beta^2 r d\xi \\ &= \frac{-\beta}{2\pi} \int_0^L f(\xi) (x - \xi)^{-2} t_\xi (1 - t_\xi^2)^{-3/2} d\xi\end{aligned}\quad (4c-5b)$$

#### Hayes' Control Surface

Following Hayes we now introduce the control surface shown in Fig. 4c-1. It consists of a circular cylinder of radius  $r_1$ , truncated by a front disc  $x = \text{Constant} < 0$  and a rear disc  $x = x_1 > L$ . The drag

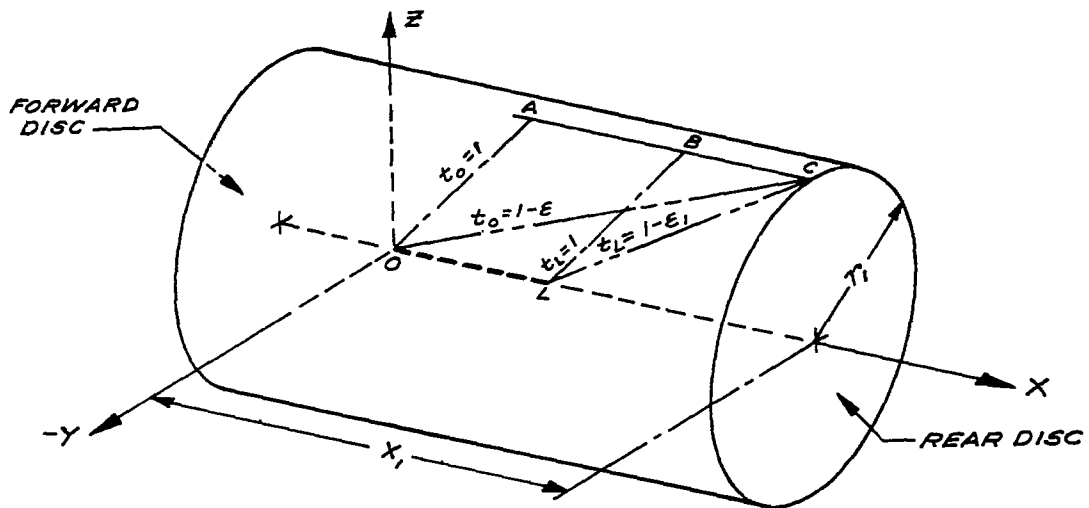


Fig. 4c-1

integral (Eq. 4b-33) will be evaluated for this control surface as  $r_1$  and  $x_1$  tend to infinity. The ratio between  $x_1$  and  $r_1$  will be determined later in such a way that the contribution of the rear disc to the drag will vanish in the limit.

#### Contribution of Rear Disc

According to Eqs. (4b-33,34) the contribution of the rear disc to the drag is

$$D = \frac{\rho_0}{2} \int_0^{r_1} (\beta^2 \phi_x^2 + \phi_r^2) 2\pi r dr \quad (4c-6)$$

The velocity components may be evaluated as follows. Write  $f(\xi)$  as a difference of two positive functions

$$f(\xi) = f_+(\xi) - f_-(\xi), \quad f_+(\xi), f_-(\xi) \geq 0 \quad (4c-7)$$

Then by the mean value theorem and Eqs. (4c-5a,b)

$$\phi_x = \frac{\int_0^L f_+(\xi) d\xi}{2\pi(x - \xi_3)^2(1 - t_{\xi_3}^2)^{3/2}} - \frac{\int_0^L f_-(\xi) d\xi}{2\pi(x - \xi_2)^2(1 - t_{\xi_2}^2)^{3/2}} \quad (4c-8)$$

where  $0 \leq \xi_3, \xi_2 \leq L$ . A similar expression is valid for  $\phi_r$ . Note that in Eq. (4c-8) the continuous source distribution is replaced by a positive source at  $\xi_3$  and a sink at  $\xi_2$ . However,  $\xi_3$  and  $\xi_2$  depend on  $x$  and  $r$ .

As is easily seen

$$0 \leq x - L \leq x - \xi_1, \quad t_L \geq t_{\xi_1}, \quad i = 2, 3 \quad (4c-9)$$

$$1 \leq 1 + t_{\xi_3}, \quad 1 + t_{\xi_2} \leq 2$$

Hence, replacing  $\xi_3$  and  $\xi_2$  by  $L$  increases the absolute magnitude of both terms in Eq. (4c-8). Hence, on the rear disc  $x = x_1$ ,  $0 \leq r \leq r_1$ ,

$$\phi_x^2 \leq \frac{2\beta^2 A}{(x_1 - L)^4 (1 - t_L^2)^3} \quad (4c-10)$$

where  $A$  is independent of  $x_1$  and  $r_1$ , and

$$\int_0^{r_1} r\beta^2 \phi_x^2 dr \leq \frac{A}{(x_1 - L)^2} \int_0^{r_1} \frac{\beta r}{x_1 - L} \frac{1}{(1 - t_L^2)^3} \frac{2\beta dr}{x_1 - L} \quad (4c-11)$$

If one puts  $y = 1 - t_L^2$ , then  $dy = -2t_L dt_L = -t_L \cdot 2\beta dr / (x_1 - L)$ . Hence

$$\int_0^{r_1} r\beta^2 \phi_x^2 dr \leq \frac{A}{(x_1 - L)^2} \int_{y_1}^1 \frac{dy}{y^3} = \frac{A}{2(x_1 - L)^2} \left[ \frac{1}{y^2} \right]_1^{y_1} \quad (4c-12)$$

where  $y_1 = 1 - (1 - \epsilon_1)^2 = 2\epsilon_1 - \epsilon_1^2$  and  $\epsilon_1$  is explained in Fig. 4c-1. Equation (4c-12) may be written

$$\int_0^{r_1} r\beta^2 \phi_x^2 dr < \frac{B}{(x_1 - L)^2 \epsilon_1^2} \leq \frac{C}{r_1^2 \epsilon^2} \quad (4c-13)$$

where  $C$  is independent of  $r_1$  and  $x_1$  for  $r_1$  and  $x_1$  sufficiently large;  $\epsilon$  is explained in Fig. 4c-1. The fact that  $x_1 / (x_1 - L) \rightarrow 1$ ,  $\epsilon / \epsilon_1 \rightarrow 1$  as  $r \rightarrow \infty$  has been used above. It is then clear that if  $\epsilon$  is constant or if  $\epsilon = r^{-a}$ ,  $a < 1$ , then the integrand in Eq. (4c-13) tends to zero as  $r \rightarrow \infty$ . A similar estimate may be shown for  $\int r \phi_r^2 dx$ . A comparison with Eq. (4c-6) shows that:

Contribution of rear disc to drag is zero even if  $\epsilon$  decreases as  $r$  increases. However,  $\epsilon$  should decrease more slowly than  $r^{-1}$ .

Since the distance BC is of the order  $\epsilon r$  it follows that this distance becomes infinite in the limit.

#### Contribution of Cylindrical Part

Since the contribution of the forward disc to the drag integral is identically zero it follows then in the limit  $r_1, x_1 \rightarrow \infty$  the entire drag contribution comes from the cylindrical part, provided  $\epsilon$  varies as prescribed above. Thus

$$D = \text{Limit } D_2 \quad (4c-14)$$

where  $D_2$ , the contribution of the cylindrical part, is

$$D_2 = -\rho_0 2\pi r_1 \int_{\beta r_1}^{x+\beta r_1 \epsilon} \phi_x \phi_r dx' \quad (4c-15)$$

(Note that the radial component  $A_{1r}$  of the vector  $A_1$  in the drag formula Eq. (4b-34) is  $-\rho_0 \phi_x \phi_r$ .) In the above equation  $1/1 - \epsilon$  has been replaced by  $1 + \epsilon$  which may be done without loss of generality.

To evaluate  $D_2$ , we write Eq. (4c-3a,b) in the following form

$$\phi_x = \frac{-1}{2\pi} \int_0^{x',L} \frac{f'(\xi_1) d\xi_1}{\sqrt{x' - \xi_1} \sqrt{x' - \xi_1 + 2\beta r_1}}$$

$$\phi_r = \frac{1}{2\pi} \int_0^{x',L} \frac{f'(\xi_2) \beta}{\sqrt{x' - \xi_2} \sqrt{x' - \xi_2 + 2\beta r_1}} \frac{x' + \beta r_1 - \xi_2}{\beta r_1} d\xi_2 \quad (4c-16)$$

where  $x' = x - \beta r_1$ .

The upper limit is  $x'$  for  $x' \leq L$  and  $L$  for  $x' \geq L$ . Hence

$$D_2 = \frac{\rho_0}{2\pi} \int_0^{\beta \epsilon r_1} \int_0^{x_1', L} \int_0^{x_1', L} \frac{1}{2} \left[ \frac{f'(\xi_1) f'(\xi_2)}{\sqrt{x' - \xi_1} \sqrt{x' - \xi_2}} \right] \left[ \frac{\sqrt{2\beta r_1}}{\sqrt{x' - \xi_1 + 2\beta r_1}} \cdot \frac{\sqrt{2\beta r_1}}{\sqrt{x' - \xi_2 + 2\beta r_1}} \cdot \frac{x' + \beta r_1 - \xi_2}{\beta r_1} \right] d\xi_1 d\xi_2 dx' \quad (4c-17)$$

Limiting Case for Infinitely Distant Control Surface

We shall now evaluate  $D_2$  as  $r_1 \rightarrow \infty$ . The three ratios within the second bracket all tend to unity as  $r_1 \rightarrow \infty$  and may hence be neglected in the limit. Note that this approximation implies

$$\frac{1}{\sqrt{(x - \xi_1)^2 - \beta^2 r^2}} \sim \frac{1}{\sqrt{(x - \xi_1) - \beta r}} \frac{1}{\sqrt{2\beta r}} = \frac{1}{\sqrt{x' - \xi_1}} \frac{1}{\sqrt{2\beta r}} \quad (4c-18a)$$

Furthermore, applying the same approximation to Eq. (4c-16) one obtains that

$$\phi_r \sim -\beta \phi_x \quad (4c-18b)$$

$\phi_r$  and  $\phi_x$  both vanish as  $1/\sqrt{2\beta r_1}$ . Their ratio, however, is given by the above equation. The corresponding relation with  $\phi_r$  replaced by  $\phi_y$  is exact for two-dimensional flow. Thus the flow is approximately two-dimensional at large distances near the Mach cone from the leading edge ( $\epsilon$  small, i.e.  $t_\xi$  almost unity for  $0 \leq \xi \leq L$ ).

Hence

$$D = \text{Limit } D_2 = \frac{\rho_0}{4\pi} I \quad (4c-19a)$$

where

$$I = \int_0^{\beta \epsilon r_1} \int_0^{x', L} \int_0^{x', L} \frac{f'(\xi_1) f'(\xi_2)}{\sqrt{x' - \xi_1} \sqrt{x' - \xi_2}} d\xi_1 d\xi_2 dx'$$

The domain of integration is a region in  $x'$ ,  $\xi_1$ ,  $\xi_2$  space whose cross-section for  $x' = \text{Constant}$  is the square  $0 \leq \xi_1 \leq x'$ ,  $0 \leq \xi_2 \leq x'$  for  $0 \leq x' \leq L$  and the square  $0 \leq \xi_1, \xi_2 \leq L$  for  $L \leq x' \leq \beta \epsilon r_1$ . Let  $I_1$  be the integral where  $0 \leq y \leq L$  and  $I_2$  the integral over the domain  $L \leq y \leq \beta \epsilon r_1$ . Since the integrand is symmetric in  $\xi_1$  and  $\xi_2$ , half its value is obtained by integrating only over the triangle ABC in the  $\xi_1, \xi_2$  plane (i.e.  $\xi_1 \leq \xi_2$ ) as shown in Fig. 4c-2. In evaluating  $I_1$  over

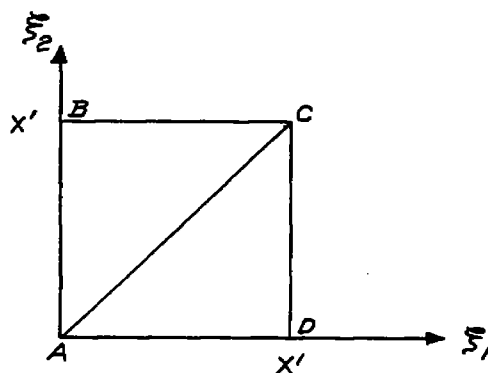


Fig. 4c-2

its domain (a truncated triangular cylinder with base at  $x = L$  and vertex at  $x' = 0$ ) we shall first integrate along a line parallel to the  $y$ -axis. For  $\xi_1, \xi_2$  fixed this line is inside the pyramid only when  $\xi_1 \leq x' \leq L$ .  $\xi_1$  may vary inside the triangle between 0 and  $\xi_2$ , and for  $\xi_2$  any value between 0 and  $L$  may be chosen. Hence  $I_1$  may be written

$$I_1 = 2 \int_0^L \int_0^{\xi_2} \int_{\xi_2}^L \frac{f'(\xi_1)f'(\xi_2)}{\sqrt{x' - \xi_1}\sqrt{x' - \xi_2}} dx' d\xi_1 d\xi_2 \quad (4c-20)$$

The integral  $I_2$  is (domain is triangular cylinder)

$$I_2 = 2 \int_L^{\beta \epsilon r_1} \int_0^L \int_0^{\xi_2} \frac{f'(\xi_1)f'(\xi_2)}{\sqrt{x' - \xi_1}\sqrt{x' - \xi_2}} d\xi_1 d\xi_2 dx' \quad (4c-21)$$

Interchanging the order as above one obtains

$$I = I_1 + I_2 = 2 \int_0^L \int_0^{\xi_2} f'(\xi_1) f'(\xi_2) \left[ \int_{\xi_2}^{\beta \epsilon r_1} \frac{dx'}{\sqrt{x' - \xi_1} \sqrt{x' - \xi_2}} - \log C \right] d\xi_1 d\xi_2 \quad (4c-22)$$

Here C is a constant and it has been introduced under the assumption that

$$\int_0^L f'(\xi) d\xi = 0, \text{ which, since } f(0) = 0 \text{ means } f(L) = 0$$

(cf. Eq. 4c-1). (Note that the limit of integration for  $\xi_1$  may be replaced by L if the factor 2 is omitted.)

Now

$$\begin{aligned} \int_{\xi_2}^{\beta \epsilon r_1} \frac{dx'}{\sqrt{x' - \xi_1} \sqrt{x' - \xi_2}} - \log C &= \left[ \log(2x' - \xi_1 - \xi_2 + 2\sqrt{(x' - \xi_1)(x' - \xi_2)}) \right]_{\xi_2}^{\beta \epsilon r_1} - \log C \\ &= -\log(\xi_2 - \xi_1) + \log \frac{2\beta \epsilon r_1 - \xi_1 - \xi_2 + 2\sqrt{(\beta \epsilon r_1 - \xi_1)(\beta \epsilon r_1 - \xi_2)}}{C} \end{aligned} \quad (4c-23)$$

Hence if one chooses  $C = 4\beta \epsilon r_1$ , the second term will tend to  $\log 1 = 0$  as  $r_1 \rightarrow \infty$ . Note that for this it is essential that  $\epsilon r_1 \rightarrow \infty$  as  $r_1 \rightarrow \infty$  (cf. pg. IV16). In other words the simplicity of the proof depends on the fact that  $\epsilon \rightarrow 0$  as  $r_1 \rightarrow \infty$  (cf. Eqs. 4c-18). On the other hand  $\epsilon$  may not tend to zero so fast that  $\epsilon r_1$  remains bounded. In this case the above proof would be invalidated. Actually a drag contribution would come from the rear disc in that case.

By combining the Eqs. 4c-19a, 22, 23 one obtains the final drag formula

$$D = \frac{-\rho_0}{2\pi} \int_0^L \int_0^{\xi_2} f'(\xi_1) f'(\xi_2) \log(\xi_2 - \xi_1) d\xi_1 d\xi_2 \quad (4c-24)$$

This is von Kármán's drag formula for a lineal source distribution such that  $f(0) = f(L) = 0$ . It has been derived above by the method of Hayes. This derivation has the advantage that it may be extended immediately to cases of a more general distribution of singularities.

Such generalizations will now be discussed.

#### General Three-Dimensional Source Distributions

We shall now consider a more general case of a spatial distribution of sources. It will still be assumed that no lifting or side force elements are present. The source strength will be denoted by  $f(x,y,z)$ . It will be assumed that  $f = 0$  outside a certain finite region  $V$ . A special case is a planar distribution, say in the plane  $z = 0$  in which case  $f(x,y,z) = f_2(x,y)\delta(z)$ . Another special case is the lineal distribution on the  $x$ -axis which was discussed above. In this case  $f(x,y,z) = f_1(x)\delta(r)$ . It will be shown below how in a certain sense the drag evaluation for the general three-dimensional case may be reduced to a consideration of certain equivalent lineal distributions. In the course of this discussion certain restrictions on  $f(x,y,z)$  will be made in addition to the requirement that it vanish outside a finite region.

Consider a line in the streamwise direction passing through  $V$ . The position of the line which will be taken as the  $x$ -axis is actually arbitrary, but for practical purposes it will be assumed that it is "well centered." This is, of course, a somewhat vague requirement. However, if for example  $f$  has rotational symmetry, the  $x$ -axis will be its axis of symmetry. On the  $x$ -axis choose as origin a point,  $O$ , whose downstream Mach cone contains  $V$ . For convenience choose this point as far downstream as possible. Also choose the point,  $L$ , for convenience as far upstream as possible, whose upstream Mach cone contains  $V$ . An equivalent requirement is that the downstream Mach cone from  $L$  is contained within the downstream Mach cones from every point in  $V$ . Let the value of  $x$  at point  $L$  be  $L$ . Thus the downstream Mach cone from  $x = 0$  and the upstream Mach cone from  $x = L$  touch but do not penetrate  $V$ . We now introduce a control surface and define  $\epsilon$  and  $\epsilon_1$  as in the lineal case (cf. Fig. 4c-1). This is shown in Fig. 4c-3. It will be assumed that  $r_1$  and  $x_1$  tend to infinity as described in discussion of the lineal case.

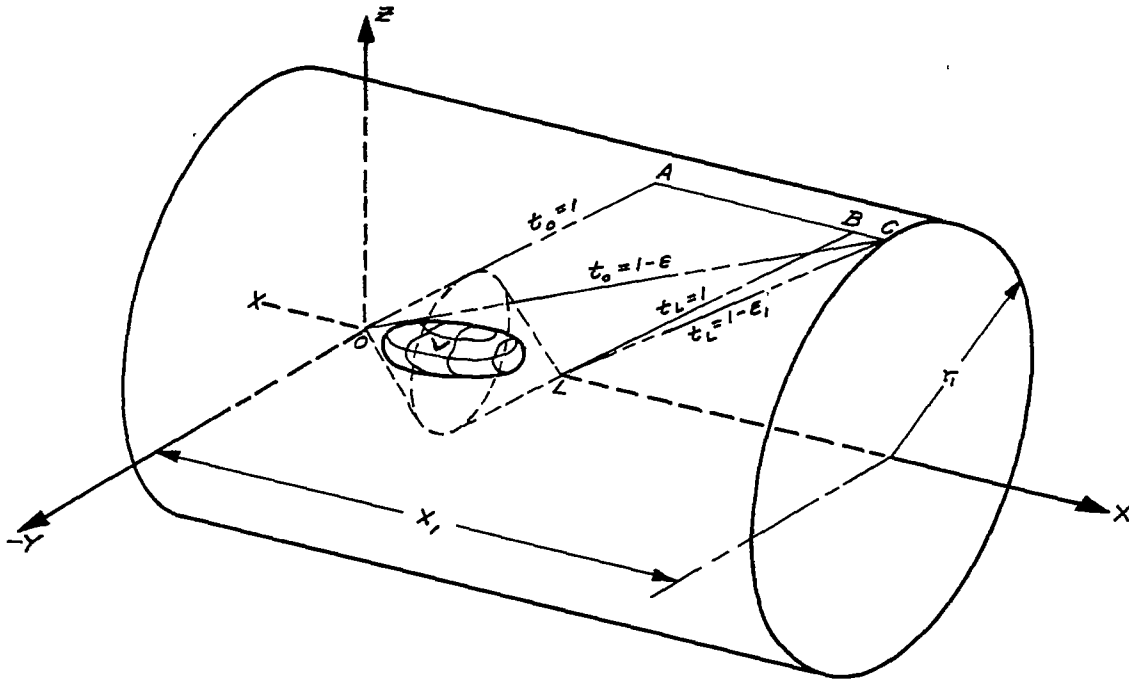


Fig. 4c-3: Hayes control surface in three-dimensional space

That is as  $x_1$  and  $r_1$  tend to infinity  $\epsilon$  and  $\epsilon_1$  will tend to zero. In that sense the line AC will come arbitrarily near the Mach cone from the origin. On the other hand  $\epsilon$  and  $\epsilon_1$  will tend to zero slower than  $1/r_1$  so that the line AC becomes infinitely long as  $r_1 \rightarrow \infty$ .

By the same methods that were used in the lineal case, it may be easily seen that the contribution of the rear disc,  $x = x_1$ , becomes zero in the limit. All the drag thus comes from a portion on the cylindrical surface arbitrarily near the Mach cone from the origin and is hence pure wave drag.

To evaluate the drag contribution from the cylindrical surface we introduce cylindrical coordinates  $x, r, \theta$  where

$$x = r \cos \theta, \quad z = r \sin \theta \quad (4c-25)$$

Let the drag contribution of a strip on the cylinder between  $\theta = \theta_0$  and  $\theta = \theta_0 + \Delta\theta$  be  $\Delta D$ . We define

$$\frac{dD}{d\theta} = \text{Drag contribution per unit angle} = \lim_{\Delta\theta \rightarrow 0} \frac{\Delta D}{\Delta\theta} \quad (4c-26a)$$

Then

$$D = \text{Total drag} = \int_0^{2\pi} \frac{dD}{d\theta} d\theta \quad (4c-26b)$$

Consider now a fixed meridian plane  $\theta = \theta_0$ , and a point  $P = (x_0, r_1, \theta_0)$  on the cylinder between A and C (Fig. 4c-3). The potential  $\phi(P)$  depends on the contribution from all sources inside the upstream Mach cone from P. The contribution from a source at  $Q = (\xi, \eta, \zeta)$  is proportional to the source strength  $f(Q)$  and inversely proportional to the hyperbolic distance  $r_h(P, Q)$  between P and Q where

$$r_h^2 = (x_0 - \xi)^2 - \beta^2 \left[ (r_1 \cos \theta_0 - \eta)^2 + (r_1 \sin \theta_0 - \zeta)^2 \right] \quad (4c-27)$$

This hyperbolic distance is constant on hyperboloids of revolution with  $r = r_1$ ,  $\theta = \theta_0$  as axis. Consider now the sources between two such hyperboloids which intersect the x-axis at  $x = \xi$  and  $x = \xi + d\xi$ . To evaluate the contribution to  $\phi(P)$  of these sources one may transfer their total source strength to the axis. In this way the distribution in V is replaced by an equivalent lineal distribution i.e. by an equivalent body of revolution. So far this lineal distribution depends on  $x_0$  and  $r_1$  as well as  $\theta_0$ .

Consider now, still for fixed  $\theta = \theta_0$ , the limit as  $r_1 \rightarrow \infty$ . Then the hyperboloids may be replaced by Mach planes which intersect the meridian plane  $\theta = \theta_0$  orthogonally along Mach lines. Note that for this it is necessary that as  $r_1 \rightarrow \infty$  any point between A and C comes arbitrarily near the downstream Mach cone from the origin in the sense described above. The source strength between two such neighboring planes

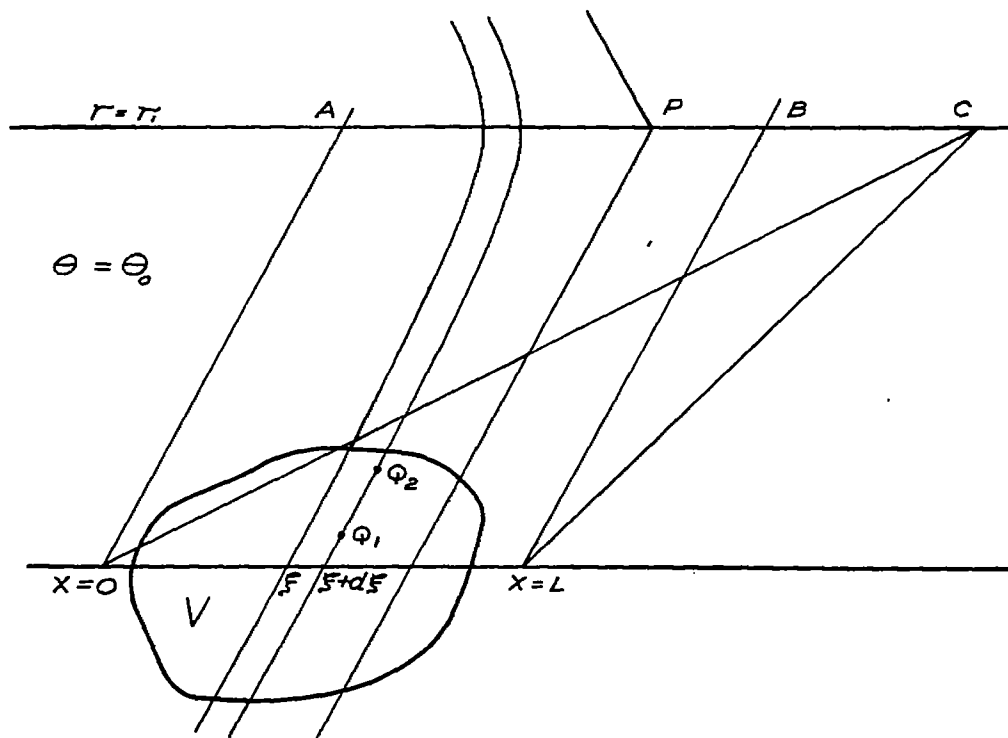


Fig. 4c-4: Evaluation of  $\phi(P)$

may then be transferred to the x-axis as above. However, in this limiting case the resulting equivalent body of revolution depends at most on  $\theta_0$ . It becomes independent of  $r_1$  and  $x_0$ . The corresponding lineal source distribution will be denoted by  $f(x; \theta_0)$ . A consequence of the independence of  $x_0$  and  $r_1$  is that  $f(x; \theta)$  may be used for computing  $\phi_r$  and  $\phi_x$  as well as  $\phi$  at P. In general it may not be used for computing  $\phi_\theta$ . Clearly  $\phi_\theta$  is zero for a lineal distribution, whereas the  $\phi_\theta$  resulting from the original volume distribution is not. On the other hand  $\phi_\theta$  is not needed for drag evaluation on the cylindrical surface.

Since  $\phi_r$  and  $\phi_x$  may be computed from the equivalent body of revolution for fixed  $\theta$  it follows that  $dD/d\theta$  may be computed in exactly the same way as the drag of a body of revolution was computed. The result will differ from Eq. (4c-24) only by a factor  $2\pi$ . Hence we have proved the following: The drag D of a volume distribution of sources of strength  $f(\xi, \eta, \zeta)$  is given by the formulas

$$D = \int_0^{2\pi} \frac{dD}{d\theta} d\theta \quad (4c-28a)$$

$$\frac{dD}{d\theta} = \frac{-\rho}{4\pi^2} \int_0^L \int_0^{\xi_2} f'(\xi_1; \theta) f'(\xi_2; \theta) \log(\xi_2 - \xi_1) d\xi_1 d\xi_2 \quad (4c-28b)$$

$$f(\xi; \theta) d\xi = \iiint_{V(\xi, \theta)} f(Q) dQ \quad (4c-28c)$$

where  $V(\xi, \theta_0)$  is the region contained between two Mach planes perpendicular to  $\theta = \theta_0$  and intersecting the x-axis at  $x = \xi$  and  $x = \xi + d\xi$ .

This result was obtained by Hayes in Ref. 1. It is thus seen how Hayes' derivation of von Kármán's drag formula for bodies of revolution admits an easy generalization to the general three-dimensional case.

This proof obviously presupposes the following requirement on the strength distribution  $f(Q)$  in addition to the requirement that it vanish outside a finite volume:  $f(Q)$  must be such that for each  $\theta$   $f(x; \theta)$  satisfies the same requirements as  $f(x)$  in the lineal case. In particular for each  $\theta$ :  $f(0; \theta) = f(L; \theta) = 0$  and  $f(x; \theta)$  must be differentiable with respect to  $x$ .

If  $f(Q)$  has rotational symmetry, i.e. depends on  $r$  and  $x$  only then it may obviously be replaced by one equivalent lineal distribution, independent of  $\theta$ , for computing the distant flow field and the drag. In the special case when  $f(Q)$  is lineal to begin with, Eqs. (4c-28) reduce to the previously established formula (Eq. 4c-24).

#### Extension to Include Lift and Side Force Elements

For simplicity only sources have been considered in the preceding development. However lift and side force elements can be included and were included by Hayes in his original report. We will not go into the details here, but merely indicate the final results, since the fundamental ideas of the method have been illustrated in the discussion of source distributions.

Following Hayes we define a function  $h$  such that

$$h = f - (g_z \sin \theta + g_y \cos \theta) \quad (4c-29)$$

where

$$f = f(\xi; \theta) = \text{Source strength}$$

$$\rho U g_z / \beta = l(\xi; \theta) = \text{Lifting element strength}$$

$$\rho U g_y / \beta = s(\xi; \theta) = \text{Side force strength}$$

The term  $(g_y \sin \theta + g_x \cos \theta)$  is proportional to the component of force in the direction  $\theta$ , and is the only component contributing to the wave drag in the Hayes calculation. Equation (4c-28b), as extended to include lift and side force elements, is

$$\begin{aligned} \left( \frac{dD}{d\theta} \right)_{\text{wave}} &= \frac{-\rho}{4\pi^2} \int_0^L \int_0^{\xi_2} h'(\xi_1; \theta) h'(\xi_2; \theta) \log(\xi_2 - \xi_1) d\xi_1 d\xi_2 \\ &= \frac{-\rho}{8\pi^2} \int_0^L \int_0^L h'(\xi_1; \theta) h'(\xi_2; \theta) \log |\xi_2 - \xi_1| d\xi_1 d\xi_2 \quad (4c-30) \end{aligned}$$

where  $h(\xi; \theta)$  is the equivalent lineal distribution (for a given station  $\theta$ ) of the original spatial distribution of singularities.

This equation makes it possible to determine the wave drag of an arbitrary spatial system containing thickness and carrying both lift and side forces. In order to determine the total pressure drag of the system it is necessary to evaluate the vortex drag produced by the lift and side force. In Hayes method the vortex drag appears as a momentum outflow through and a pressure on the end of the cylindrical control surface. It can be evaluated by calculating this momentum and pressure or by determining the kinetic energy associated with the vortex system in the Trefftz plane. Since this is identical with the induced drag problem of incompressible flow, we will not discuss it further.

#### D. LEADING EDGE SUCTION

The evaluation of the drag of a lifting wing of zero thickness by integrating local pressure times frontal area over the wing surface is not theoretically complete until leading edge suction is accounted for.

This means that the infinite negative pressures acting on subsonic leading edges should be included. In practical applications this leading edge suction is sometimes discarded since in many cases only a fraction of the theoretical value is actually realized.

However, from the distant viewpoint, leading edge suction cannot be isolated. This is true because there is no point-to-point correspondence between the close and the distant control surfaces. At the distant control surface the velocity field created by the wing leading edges is merged with the fields created by other areas on the wing and body.

From the distant point of view leading edge suction is automatically assumed to be fully effective, and therefore it must be so assumed from the close viewpoint to get correspondence in the drag values.

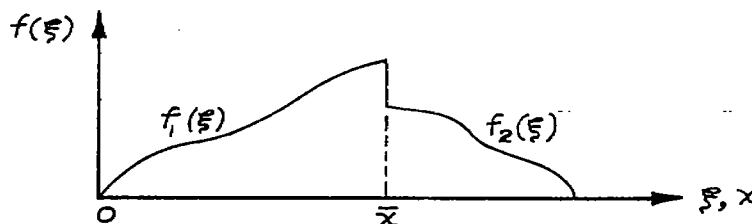
#### E. DISCONTINUITIES IN LOADINGS

For a planar wing, vortex drag is dependent only on the spanwise lift distribution. A discontinuity in the ordinates of this lift distribution produces a concentrated vortex of finite strength and infinite energy, which corresponds to infinite drag.

Wave drag is similarly affected by discontinuities in loadings. For example, consider a distribution of sources on a streamwise line. If there is a discontinuity in source strength, then the drag evaluated on the distant control surface is infinite.

To prove this, assume a source distribution with a discontinuity at the point  $x = \bar{x}$  (see sketch). The velocity potential at a point  $(x, r)$  downstream of the rearward Mach cone from  $\bar{x}$  may be written

$$\phi = -\frac{1}{2\pi} \int_0^{x-\beta r} \frac{f(\xi) d\xi}{\sqrt{(x-\xi)^2 - \beta^2 r^2}} = -\frac{1}{2\pi} \left\{ \int_0^{\bar{x}} \frac{f_1(\xi) d\xi}{\sqrt{(x-\xi)^2 - \beta^2 r^2}} + \int_{\bar{x}}^{x-\beta r} \frac{f_2(\xi) d\xi}{\sqrt{(x-\xi)^2 - \beta^2 r^2}} \right\} \quad (4e-1)$$



The u-component of velocity at the point (x,r) is found by differentiating Eq. (4e-1) axially. (In order to avoid indeterminate forms in the differentiation, the equation is first transformed by means of the relation  $\xi = x - \beta r \cosh u$ .) This process gives the result (assuming  $f(0) = 0$ ):

$$u = \frac{\partial \phi}{\partial x} = -\frac{1}{2\pi} \left\{ \int_0^{\bar{x}} \frac{f_1'(\xi) d\xi}{\sqrt{(x-\xi)^2 - \beta^2 r^2}} + \int_{\bar{x}}^{x-\beta r} \frac{f_2'(\xi) d\xi}{\sqrt{(x-\xi)^2 - \beta^2 r^2}} - \frac{\Delta f(\bar{x})}{\sqrt{(x-\bar{x})^2 - \beta^2 r^2}} \right\} \quad (4e-2)$$

where  $\Delta f(\bar{x}) = f_1(\bar{x}) - f_2(\bar{x})$ .

At the distant control surface it previously was shown (Ch. IV-C) that one need consider only conditions very near the Mach cones from the source distribution. Introducing the approximations used in Hayes' method (i.e.,  $(x - \xi)/\beta r \cong 1$ ), Eq. (4e-2) can be expressed

$$u = -\frac{1}{2\pi\sqrt{2}\beta r} \left\{ \int_0^{\bar{x}} \frac{f_1'(\xi) d\xi}{\sqrt{x' - \xi}} + \int_{\bar{x}}^{x'} \frac{f_2'(\xi) d\xi}{\sqrt{x' - \xi}} - \frac{\Delta f(\bar{x})}{\sqrt{x' - \bar{x}}} \right\} \quad (4e-3)$$

where  $x' = x - \beta r$  and  $x' - \xi \ll \beta r$ . Since the radius of the control surface is large compared to the length of the source distribution, the Mach cones originating at the sources are essentially plane waves when they intersect the control surface, so that the radial component of velocity (at the control surface) is (Eq. 4c-18b)

$$v = \beta u \quad (4e-4)$$

The drag, being equal to the transport of horizontal momentum across the control surface, is proportional to the product of u and v integrated axially along the control surface. From Eqs. (4e-3) and (4e-4) it is readily seen that the drag includes a term of the form

$$\int_{\bar{x}}^{\infty} \frac{[\Delta f(\bar{x})]^2}{(x' - \bar{x})} dx'$$

The integral is non-convergent. An infinite drag contribution therefore results from a discontinuity in the strength of the source distribution.

#### F. THE USE OF SLENDER BODY THEORY WITH THE DISTANT VIEWPOINT

If slender body theory is applied, then the source strength is assumed proportional to the rate of change of cross-sectional area,  $dS/dx$ , for a corresponding body of revolution. This means that infinite drag will be predicted (by the distant procedure) for all bodies of revolution having discontinuities in  $dS/dx$ . Such a prediction is, of course, incorrect, and the error is caused by the application of slender body theory to bodies which are not sufficiently smooth.

The use of slender body theory requires that smoothness should be maintained at the nose and tail of the body and therefore  $dS/dx$  should be zero at these locations. In order that  $dS/dx$  should be zero at the nose or tail of a closed body of revolution it is necessary that the variation of body radius,  $R$ , with distance,  $d$ , from the nose or tail should be of the form  $R \sim |d|^{(1/2)+k}$  where  $k > 0$ . This does not eliminate blunt noses or tails entirely, but excludes "excessive" bluntness. (Note that the Sears-Haack optimum shape is blunt.)

The linearized theory requirement that all velocity perturbations be small theoretically excludes all bluntness, but this is unimportant if very small regions of the flow field are affected.

Bodies which begin or end in cylinders also may satisfy the smoothness requirements.

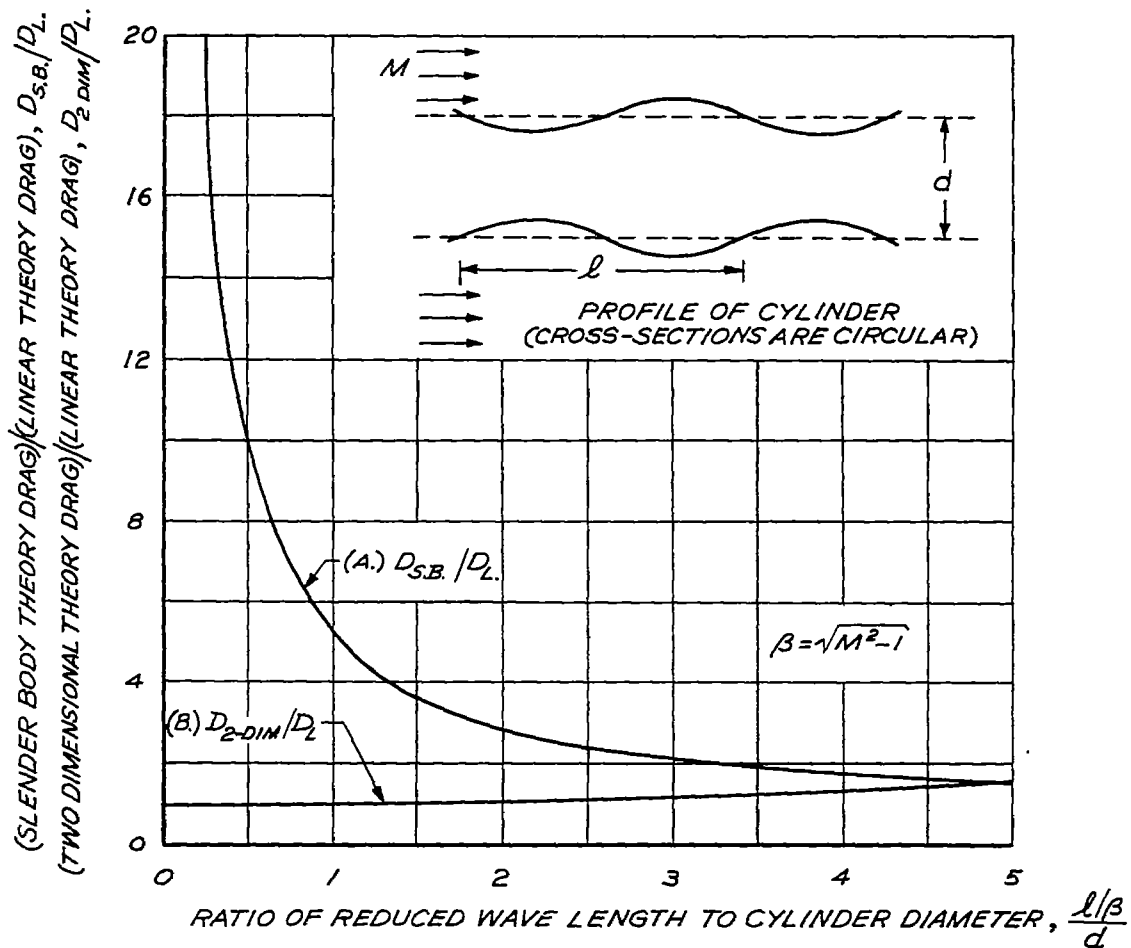
For a body to be sufficiently smooth to permit the use of slender body theory, it is necessary to restrict the "short" wave length fluctuations in the plot of cross-sectional area versus length. (The word "short" cannot be defined exactly here, but should probably apply to all wave lengths less than the body diameter times  $\sqrt{M^2 - 1}$ .)

Figure 4f-1 illustrates the effect of wave length on the accuracy of the slender body theory. The drag for an infinitely long corrugated cylinder according to strict linear theory was found by von Kármán<sup>(7)</sup>. Slender body theory is in good agreement with these results only where the reduced wave lengths are large compared to the cylinder radius. At the other extreme two-dimensional theory is approached.

It should be remembered that when the distant viewpoint is used the drag of a singularity distribution is evaluated. The body shape corresponding to the singularities may be determined either by "exact" linear theory or approximated by slender body theory. For example in Fig. 4f-2 a specific source distribution is considered, and is interpreted as a "bump" on a cylinder by "exact" linear theory and by the slender body approximation. For this ratio of wave length to cylinder

### COMPARISON OF THEORETICAL CALCULATIONS FOR DRAG OF CORRUGATED CYLINDER

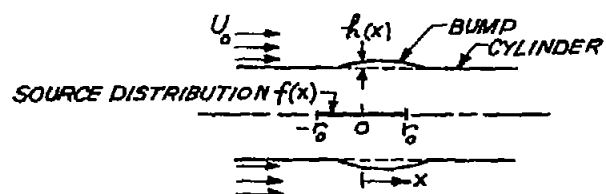
- (A.) RATIO OF THE DRAG COMPUTED BY SLENDER BODY THEORY TO THE DRAG COMPUTED BY LINEAR THEORY
- (B.) RATIO OF THE DRAG COMPUTED BY TWO-DIMENSIONAL LINEAR THEORY (ASSUMING TWO-DIMENSIONAL FLOW IN EACH MERIDIAN PLANE) TO THE DRAG COMPUTED BY THREE-DIMENSIONAL LINEAR THEORY



(FOR LINEAR THEORY DRAG OF CORRUGATED CYLINDER, SEE REF:7)

Fig. 4f-1

COMPARISON OF BUMP SHAPES OBTAINED FROM A GIVEN SOURCE DISTRIBUTION  
ACCORDING TO SLENDER BODY THEORY AND LINEARIZED THEORY



$$f(x) = -0.12 \pi U_0 r_0 \frac{x}{r_0} \sqrt{1 - \left(\frac{x}{r_0}\right)^2}$$

(THIS SOURCE DISTRIBUTION COULD BE USED  
TO FORM (ALONG THE AXIS) A SEARS-HAACK  
BODY OF FINENESS RATIO 5, LENGTH  $2r_0$ )

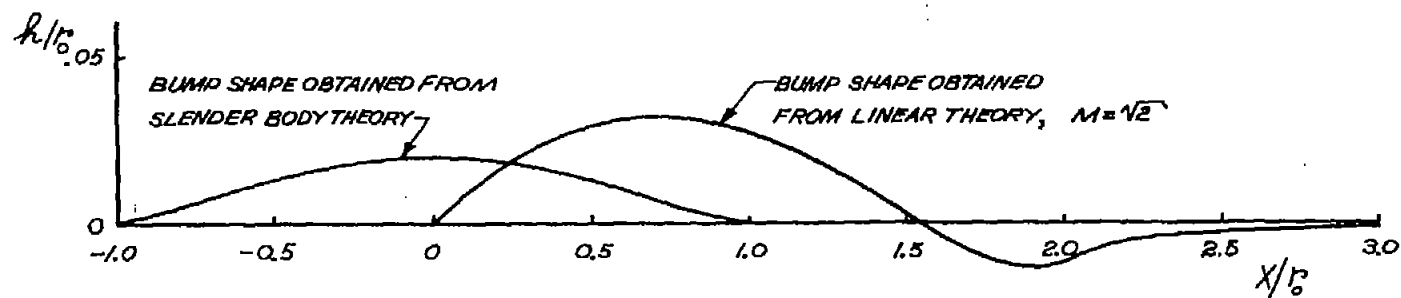


Fig. 4f-2

diameter the bump shapes and locations are quite different. It is of interest however that the net volumes contained in the bumps are identical. This has been proved by Lagerstrom and Bleviss and generalized by Bleviss in Ref. 22. (This suggests that "volume elements" may retain their significance even when slender body theory does not apply.)

#### G. THE DEPENDENCE OF DRAG COEFFICIENT ON MACH NUMBER

Hayes<sup>(1)</sup> has pointed out that, for a distribution of singularities on a single streamwise line, the drag, evaluated from the distant viewpoint, is independent of Mach number. If the singularities are sources, and slender body theory is applied, this indicates that the drag of a given body of revolution is independent of Mach number. However the application of slender body theory in conjunction with the distant viewpoint requires that  $dS/dx = 0$  at the tail of the body.

Hayes' result is therefore consistent with a fact previously determined, that the drag coefficient of a slender body satisfying the "closure" condition ( $dS/dx = 0$  at the tail) is independent of Mach number.

If the singularities are not confined to a single streamwise line, then the distant viewpoint gives a drag coefficient which varies with Mach number. This can be seen from the fact that the projection of the singularity distribution onto a single streamwise line varies with the inclination of the Mach planes used for the projection.

#### H. SUPERPOSITION PROCEDURES AND INTERFERENCE DRAG

In all the developments discussed in this report the linearized supersonic flow equation is used. This means that one flow field and the lift (or volume) distribution which causes it can be superimposed on a second flow field with its corresponding lift (or volume) distribution. If the individual flow fields satisfy the linearized flow equation, then their sum does also.

For example, let a pressure field,  $p_1$ , correspond to a downwash field,  $\alpha_1$ , and a second pressure field,  $p_2$ , correspond to a second downwash field,  $\alpha_2$ , then the pressure field  $p_1 + p_2$  corresponds to the downwash field  $\alpha_1 + \alpha_2$ .

However, the drag of the sum of the two fields is not in general the sum of the drags of the individual fields. For example, the drag of the first field would be  $D_1 = \int p_1 \alpha_1 dS$ , where the integration extends

over the wing and body surfaces, and similarly the drag of the second field is  $D_2 = \int p_2 \alpha_2 dS$ . However, the drag of the combination is

$D_{1+2} = \int (p_1 + p_2)(\alpha_1 + \alpha_2) dS$ . The terms involving cross products give

the interference drag,  $D_i = \int (p_1 \alpha_2 + p_2 \alpha_1) dS$ .

#### I. ORTHOGONAL DISTRIBUTIONS AND DRAG REDUCTION PROCEDURES

If the interference drag is zero then the two distributions are said to be orthogonal. The use of orthogonal distributions for reducing drag has been studied in Refs. 8, 9, 10, and 11.

For example consider two types of lift distributions which are orthogonal and assume that each one carries a net lift. It has been shown (see for example Ref. 9) that some combination of the two will carry a given total lift with less drag than would be produced if either one of the individual types of distribution carried all of the lift.

On the other hand, any given (non-optimum) lift distribution can be improved by adding the proper amount of a non-orthogonal type of distribution which carries zero net lift. The improvement is obtained by utilizing negative interference drag. This can be seen as follows. The total drag of the combination is the sum of the individual drags plus the interference drag. The interference drag can always be made negative by proper choice of the sign of the distribution that carries zero net lift. Also, since the strength of the zero lift distribution enters linearly into the interference drag, but enters quadratically into its individual drag, the magnitude can be so chosen that the interference drag dominates. Thus the total drag of the combination can be made less than the drag of the given (non-optimum) lift distribution.

#### J. THE PHYSICAL SIGNIFICANCE OF INTERFERENCE DRAG

It has been stated that the interference drag,  $D_i$ , is  $\int (p_1 \alpha_2 + p_2 \alpha_1) dS$

where the subscripts designate the two flow fields which have been superimposed, and the integration is to be carried over all surfaces. Assume that both flow fields are produced by thickness distributions. Then the  $\alpha$  values are the body surface inclinations which correspond to  $dS/dx$ ,

the rate of change of cross-sectional area for the body. The  $\int p_1 \alpha_2 dS$

gives the drag produced by the pressure field of the first body acting on the cross-sectional area distribution of the second. The term  $\int p_2 \alpha_1 dS$  has a similar interpretation.

Assume that both flow fields are produced by lift distributions.

Then  $\int p_1 \alpha_2 dS$  is the drag created by the downwash field of the second distribution acting on the lifting elements of the first distribution. (The surface which supports the lift corresponding to  $p_1$  must be inclined further because of the downwash due to  $p_2$ .)

Let the first field be produced by a lift distribution and the second by a thickness distribution (a body). Then  $\int p_1 \alpha_2 dS$  is the drag produced by the downwash field of the thickness distribution acting on the lift elements plus the drag caused by the pressure field of the lift distribution acting on the cross-sectional area distribution of the body. The  $\int p_2 \alpha_1 dS$  gives no contribution to the drag in this case.

Assume that the first field is produced by a lift distribution and the second by a side force distribution. The  $\int p_1 \alpha_2 dS$  is drag corresponding to the downwash field of the side force distribution acting on the lift elements, while the  $\int p_2 \alpha_1 dS$  is produced by the sidewash field of the lift elements acting on the side force distribution.

#### K. INTERFERENCE AMONG LIFT, THICKNESS, AND SIDE FORCE DISTRIBUTIONS

For planar distributions of lift and thickness (the lift being normal to the plane) there are no interference drag terms, and the two problems can be studied independently. However, for spatial distributions, interference generally exists. This has been discussed by Hayes, and the physical meaning of the interference drag has been discussed in the preceding sections.

Suppose that a source and a lifting element are located as shown in Fig. 4k-1, the direction of flow being perpendicular to the page. Then the component of the lift which lies in the line connecting the two singularities causes all of the interference. If the lift element were located on the  $y$ -axis (corresponding to a planar wing problem) there would be no interference.

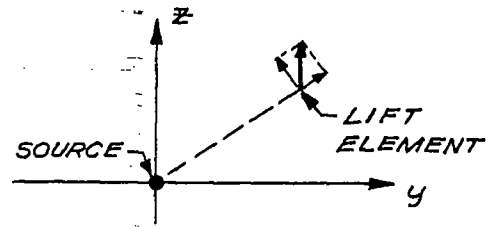


Fig. 4k-1

For lift and side force elements, as shown in Fig. 4k-2, there is interference between the force components which lie in the line connecting the singularities, and also interference between the components normal to the connecting line.

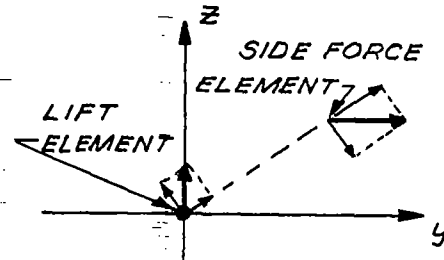


Fig. 4k-2

If the side force element lies either on the  $y$ -axis or on the  $z$ -axis (as shown in Fig. 4k-3a and b), then there is no interference. This can also be seen from symmetry considerations, which show that the lift element produces no sidewash at the side force element and similarly the side force element produces no downwash at the lift element.

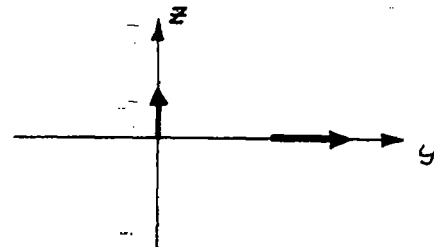


Fig. 4k-3a

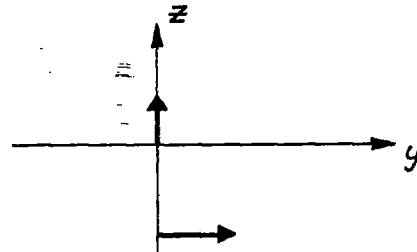


Fig. 4k-3b

L. REDUCTION OF DRAG DUE TO LIFT BY ADDITION OF A THICKNESS DISTRIBUTION

Consider the two-dimensional system sketched in Fig. 47-1. The cross-hatched area is a thickness distribution lying partly in the pressure field of a flat-plate wing. The relative geometry of the thickness distribution and the lifting surface are indicated in the figure. Also, the pressure distributions, relative to the two-dimensional pressure  $2\alpha q/\beta$ , are shown in parentheses.

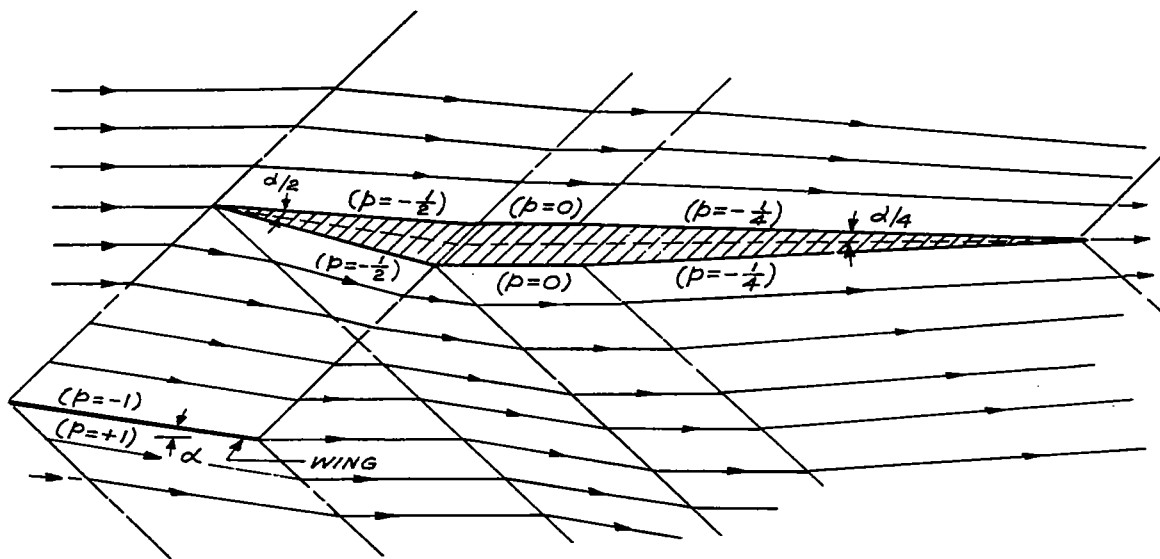


Fig. 47-1

As long as the pressure field of the thickness distribution does not intersect the flat-plate, the lift of the system is the same as for the flat-plate by itself. On the other hand, the interference between the pressure field of the flat-plate and the thickness distribution produces a negative drag contribution, so that the total drag of the system (omitting friction) is 12-1/2 percent less than the drag of the flat-plate alone. Thus, the total lift in this case is unaffected by introduction of the thickness distribution and a drag reduction is obtained.

This example is related to the Busemann biplane. The result obtained illustrates the fact that, in the general case (non-planar systems), sources and lifting elements have an interference drag.

CHAPTER V. THE CRITERIA FOR DETERMINING OPTIMUM DISTRIBUTIONS  
OF LIFT OR VOLUME ELEMENTS ALONE

A. THE "COMBINED FLOW FIELD" CONCEPT

The idea of the "combined flow field" was introduced by Munk<sup>(12)</sup> and extended by R. T. Jones<sup>(13,14)</sup>. Consider a distribution of lifting elements in a free stream of given velocity. A certain downwash velocity and pressure are produced at each point in the field. If the direction of the free stream is now reversed without moving the lift elements or altering the directions and magnitude of these lift contributions, then in general different downwash velocities and pressures are produced at each point in the field.

One-half the sum of the downwash velocities produced at a given point in the forward and reverse flows is called the downwash velocity of the combined flow field at that point. A similar definition applies to sidewash velocity. One-half the difference of the pressures in the forward and reverse flows is called the pressure in the combined flow field. These definitions follow from the super-position of the perturbation velocity fields for forward and reverse flow. It should be remembered that in the flow reversal the lift distribution (not the wing geometry) is fixed.

The same ideas may be applied if other singularities such as sources, side force elements and volume elements are considered. When sources are used the signs must be reversed when the flow direction is reversed. A source in forward flow becomes a sink in reverse flow.

B. COMBINED FLOW FIELD CRITERION FOR IDENTIFYING OPTIMUM LIFT DISTRIBUTIONS

A necessary and sufficient condition for minimum wave plus vortex drag was given by R. T. Jones<sup>(13)</sup> in connection with planar systems. The condition is that the downwash in the combined flow field shall be constant at all points of the planform. This result depends on the fact that a pair of lifting elements has the same drag in forward and reverse flow, which is also true when the lifting elements are not in the same horizontal plane. Hence the above criterion can be extended immediately to lift distributions in space by requiring constant downwash (in the combined flow field) throughout the space.

C. THE COMBINED FLOW FIELD CRITERION FOR IDENTIFYING OPTIMUM VOLUME DISTRIBUTIONS

A necessary and sufficient condition for minimum wave drag due to thickness was given by R. T. Jones<sup>(13)</sup> in connection with planar systems. If total volume is fixed then the optimum distribution of volume gives a pressure gradient in the combined flow field which is constant over the planform.

As in the case of lifting elements this criterion can be extended to cover thickness distributions in space. It is then necessary for the pressure gradient in the combined flow field to be constant throughout the space.

D. UNIFORM DOWNWASH CRITERION FOR MINIMUM VORTEX DRAG

A necessary and sufficient condition for vortex drag alone to be a minimum is that the downwash velocity throughout the wake of the wing system shall be constant in the Trefftz plane. (The wake cross-section is the projection of the wing system on the Trefftz plane.) This condition was given by Munk<sup>(15)</sup>.

If the wake of the wing system has an elliptical cross-section then a constant intensity of lift over the cross-section satisfies the above condition and gives the minimum possible vortex drag. (See Appendix V-1). In particular when the cross-section of the wing wake degenerates into a horizontal line, (corresponding to a planar wing) the familiar requirement of elliptic spanwise load distribution is obtained.

E. ELLIPTICAL LOADING CRITERION FOR MINIMUM WAVE DRAG DUE TO LIFT

In special cases elliptic loadings identify minimum drag configurations, as has been shown by Jones<sup>(14)</sup>. Let the space containing the lifting elements be cut by a series of parallel planes each inclined at the Mach angle to the flow axis. Consider all the lift intensity cut by any one plane to be located at the intersection of the plane with the flow axis. If the resulting load distribution on the axis is elliptical, and if this is true for all possible sets of parallel planes (inclined at the Mach angle), then the wave drag is a minimum.

In Hayes<sup>(1)</sup> procedure for calculating drag (see Ch. IV) this condition corresponds to obtaining the minimum possible drag contribution at every angular position on the cylindrical control surface.

Such minima cannot be attained in general since the condition is sufficient but not necessary. However if they are attained and if the vortex drag is also a minimum then the more general criterion (constant downwash in the combined flow field) is satisfied.

F. THE "ELLIPTICAL LOADING CUBED" CRITERION FOR MINIMUM WAVE DRAG DUE TO A FIXED TOTAL VOLUME

Sears<sup>(16)</sup> and Haack<sup>(17)</sup> in determining optimum shapes for bodies of revolution in supersonic flow have also determined sufficient conditions for identifying optimum distributions of volume elements within a prescribed space.

We consider a distribution of volume elements within a prescribed space and ask how these elements should be arranged in order that they should cause the least wave drag while providing a fixed total volume. If the equivalent body of revolution for a given angular position  $\theta_1$  on the distant control surface (see Ch. IV) conforms to the Sears-Haack optimum shape then the wave drag contribution at  $\theta_1$  is a minimum. Therefore if the equivalent bodies of revolution for all values of  $\theta$  are optimum shapes the total wave drag is a minimum.

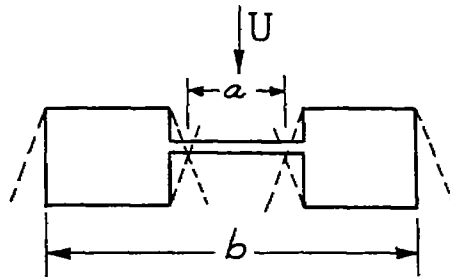
The density of the lineal distribution of volume elements representing the Sears-Haack optimum shape corresponds to the cube of an elliptical distribution over the length of the line. Hence if all the equivalent lineal distributions have this form an optimum is ensured.

Such minima cannot be attained in general since the "Elliptical Loading Cubed" criterion is a sufficient, but not a necessary condition for minimum drag. When such minima are attained the more general criterion (constant pressure gradient in the combined flow field) is also satisfied.

G. COMPATABILITY OF MINIMUM WAVE PLUS VORTEX DRAG WITH MINIMUM WAVE OR MINIMUM VORTEX DRAG

It is possible for minimum wave plus vortex drag to be obtained when neither the wave nor the vortex drag is individually a minimum.

For example consider that the "space" within which lifting elements may be distributed is the planform shown in the figure. For the vortex drag to be a minimum it is necessary to maintain an elliptic spanwise loading over  $b$ . This requires a finite load on "a" which in turn produces infinite wave drag if the chord for "a" goes to zero. However



the minimum drag due to lift for the planform is certainly finite (load the end pieces only and consider them as isolated wings) hence minimum vortex drag is not consistent with minimum total drag in this case.

On the other hand, for a planar wing of elliptical planform minimum wave drag and minimum vortex drag are obtained with the same (constant intensity) lift distribution.

#### H. ORTHOGONAL LOADING CRITERIA

Optimum distributions can be identified also through orthogonality considerations<sup>(8,9)</sup>. The optimum distribution of lifting elements in a space is orthogonal to every distribution carrying zero net lift and is not orthogonal to any other distributions.

A similar statement can be made for the optimum distribution of volume elements alone (assuming for the moment that negative local volumes are not excluded). However if lifting (and side force) elements are introduced in addition to volume elements, then the criterion must be modified. For example the rotationally symmetric wing plus central body having zero wave drag is orthogonal to all singularity distributions although it contains a net volume.\*

The criteria discussed in preceding sections of this chapter have not been thoroughly investigated for cases involving lift and volume elements simultaneously. However, some material on interference between lift and volume distributions is given in Ch. IX.

---

\* See p. 103 ff. Since the wave drag is zero the disturbances on a distant control cylinder are identically zero. Hence its interference with any other singularity distribution is zero.

## APPENDIX V

DISTRIBUTION OF LIFT IN A TRANSVERSE  
PLANE FOR MINIMUM VORTEX DRAG

As stated by Munk's Stagger Theorem<sup>(15)</sup>, the vortex drag of a spatial wing system is not changed if all lift and side force elements in the system are projected onto a single plane normal to the flight direction (see Fig. A5-1). Furthermore, if there are no side force elements,

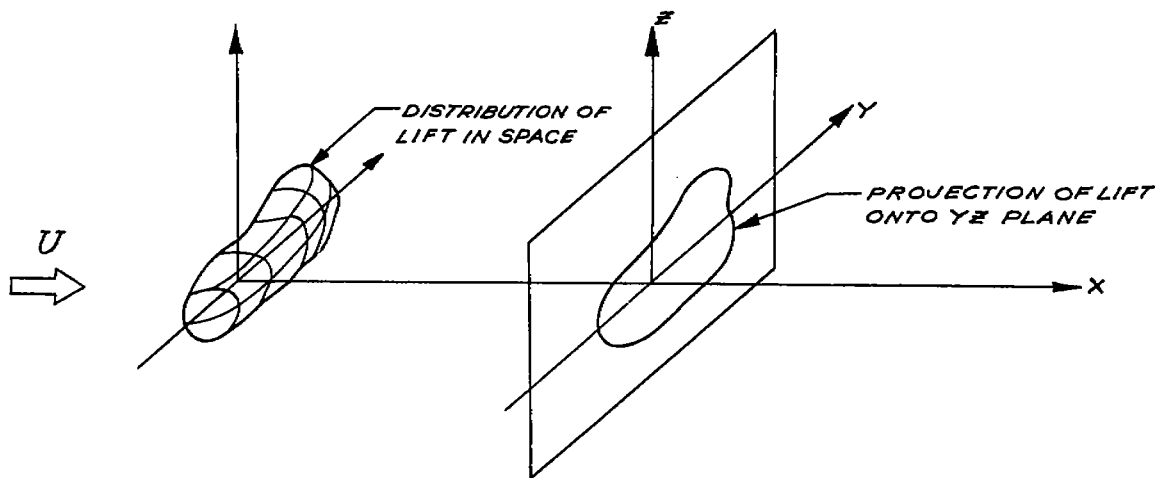


Fig. A5-1

then Munk's criterion for minimum vortex drag is that in the Trefftz plane, the downwash in the wake must be constant. (The wake cross-section is defined as the projection of the wing system on the Trefftz plane.) Assume that the downwash field associated with the optimum lift distribution is  $w = -w_0$  and that a uniform field  $w = +w_0$  is superimposed on the original field in the Trefftz plane; then the resulting two-dimensional flow pattern is equivalent to a uniform flow around a solid body. Munk gives the expression for the lift distribution in the transverse plane in terms of the velocity potential of this new flow for

certain bodies symmetrical with respect to the x-z plane; for example, if  $\phi$  is the two-dimensional potential flow around an elliptic cylinder, then

$$l_{opt} = 2\rho U \left( \frac{d\phi}{dz} \right)_{boundary}$$

and

$$d_{vortex_{min}} = \left( \frac{w_0}{U} \right) l_{opt}$$

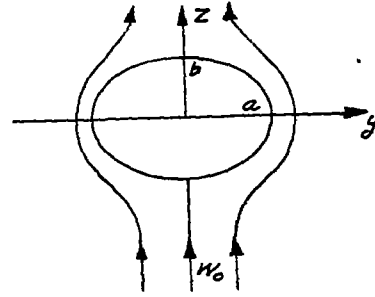


Fig. A5-2

where  $l$  and  $d$  are the lift and drag intensities per unit area in the transverse plane. For an ellipse oriented as in Fig. A5-2, the potential is<sup>(18)</sup>

$$\phi = w_0(a + b) \cosh(\xi - \xi_0) \sin \eta$$

where

$$y + iz = \sqrt{a^2 - b^2} \cosh(\xi + i\eta)$$

The curve  $\xi = \xi_0$  corresponds to the boundary of the lift distribution in the transverse plane. From the above equations one obtains

$$l = 2\rho U \left( \frac{\partial\phi}{\partial\eta} \frac{d\eta}{dz} \right)_{\xi=\xi_0} = \frac{2\rho U w_0 (a + b)}{b}$$

so that the lift intensity in the transverse plane must be constant to obtain minimum vortex drag. With  $S = \pi ab$ , the drag is

$$D_{vortex_{min}} = \left( \frac{w_0}{U} \right) L = \frac{L^2}{4qS(1 + a/b)}$$

where  $L$  is the total lift generated. Thus to obtain minimum vortex drag for a spatial distribution of lift whose Trefftz plane projection is an ellipse with one axis vertical, the lift should be distributed so as to give a constant intensity when projected on the Trefftz plane.

This proof can be extended to cases in which the projected lift distribution covers a rolled ellipse, as shown in Fig. A5-3. If only lift (and no sideforce) elements are allowed, Munk's criterion of constant downwash still holds, but the lack of symmetry precludes use of the formulas given above. However, the optimum lift distribution can be determined by a superposition of two symmetrical optimum distributions, as shown in Fig. A5-4.  $L_1$  and  $L_2$

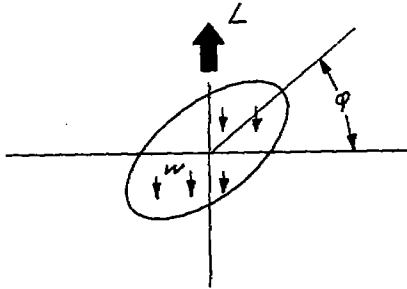


Fig. A5-3

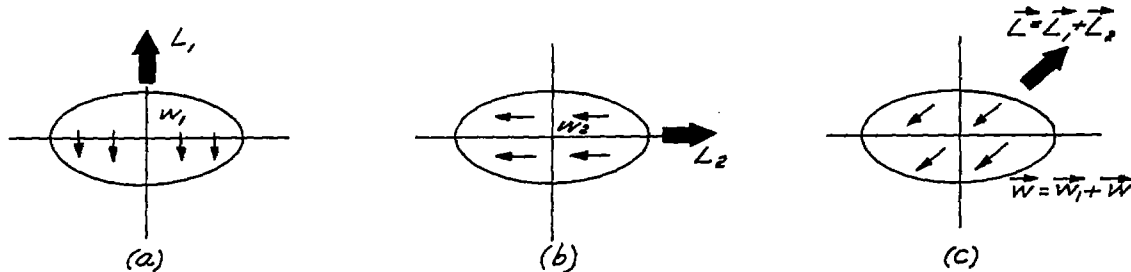


Fig. A5-4

are constant intensity lift distributions over the elliptic areas which produce constant downwashes  $w_1$  and  $w_2$  over those areas. Because the governing equation is the Laplace equation, which is linear, the lift distributions  $L_1$  and  $L_2$  and the flow fields they produce can be superimposed. If  $L_1 = L \cos \phi$  and  $L_2 = L \sin \phi$  and Fig. A5-4c is rotated through the angle  $\phi$ , then Fig. A5-4c corresponds to Fig. A5-3. There is a uniform downwash  $w$  corresponding to the uniform lift  $L$ . Thus Munk's criterion is satisfied and the drag is a minimum. It can be shown by symmetry that the total interference drag between the lift distributions  $L_1$  and  $L_2$  is zero so that the drag of  $L$  is obtained simply by adding the drags of  $L_1$  and  $L_2$ ; that is

$$D_{\text{vortex min}} = \frac{L_1^2}{4qS(1 + a/b)} + \frac{L_2^2}{4qS(1 + b/a)} = \frac{L^2(a \sin^2\phi + b \cos^2\phi)}{4qS(a + b)}$$

It should be noted that for this optimum rolled ellipse case there is also a uniform sidewash generated. If a distribution of side force elements were available, it would be possible to utilize the uniform sidewash to reduce the vortex drag below the value given above.

CHAPTER VI. THE OPTIMUM DISTRIBUTION OF LIFTING ELEMENTS ALONE

A. THE OPTIMUM DISTRIBUTION OF LIFT THROUGH A SPHERICAL SPACE

Consider a sphere of radius "R" with its center at the origin, and let a total lift "L" be distributed through the sphere with local intensity "λ." If  $\lambda = \frac{L}{\pi 2R^2 \sqrt{R^2 - r^2}}$ , r being the radial distance from the

origin, then elliptic loadings are obtained when the sphere is cut by any set of parallel planes (see Appendix VI for derivation). The fact that elliptic loadings are produced when the planes are inclined at the Mach angle (to the free stream direction) insures that the wave drag is a minimum (Ch. V). The cross-section of the wake is circular, and if the lift intensity is projected onto a plane normal to the free stream direction it can be shown that the lift is uniformly distributed over this circular cross section. This insures that the vortex drag is also a minimum (Ch. V).

The lift distribution  $\lambda = \frac{L}{\pi 2R^2 \sqrt{R^2 - r^2}}$  then gives the minimum possible wave and vortex drag. By Hayes' procedure it can be found that the minimum wave drag is  $D_{\min \text{ wave}} = \frac{L^2 \beta^2}{2\pi q (2R)^2 M^2}$ ; the minimum vortex

drag<sup>(15)</sup> is  $D_{\min \text{ vortex}} = \frac{L^2}{2\pi q (2R)^2}$  and the minimum total drag is

$$D_{\min} = \frac{1}{2} \frac{L^2}{\pi q (2R)^2} \left[ \frac{2M^2 - 1}{M^2} \right].$$

The largest planar wing of circular planform contained in the sphere has a minimum drag<sup>(14)</sup> which is greater by the ratio  $\frac{2M^3}{2M^2 - 1}$ . This is a factor of 1.885 at  $M = \sqrt{2}$ . However, the drag comparison is, of course, not complete without consideration of the viscous drag (and thickness drag). For the spatial lift distribution described above, the required wing area is infinite and so, then, is the viscous drag. But the same minimum of wave and vortex drag can be achieved with a number of wing systems having finite wing area. For example, consider the infinite set of cascades enclosed in a spherical space as shown in Fig. 6a-1. At

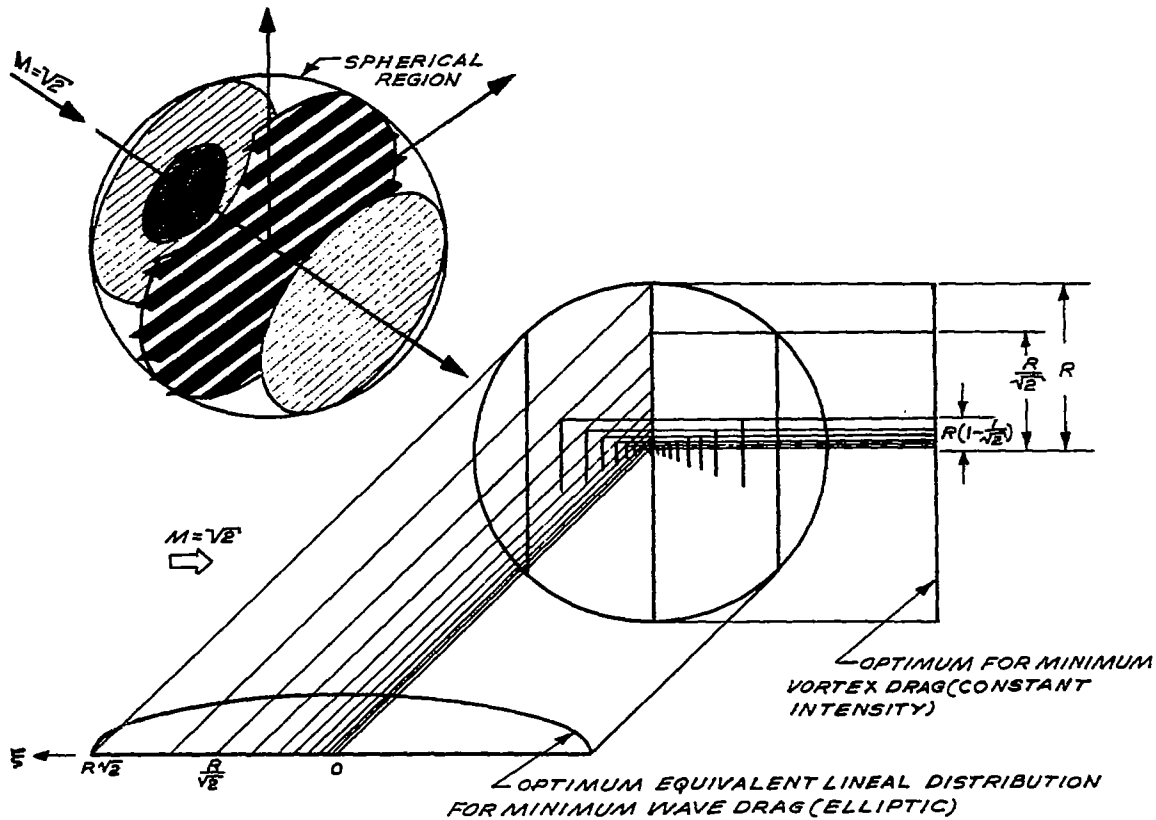


Fig. 6a-1: Cross-sectional view of an optimum set of finite area lifting surfaces in a spherical space

$M = \sqrt{2}$  this set of cascades covers the region adequately so that the equivalent linear distribution will be continuous. Determining the lift distributions for the cascades is essentially a stepwise process in that the vortex drag criterion is satisfied over part of the space and then the wave drag criterion over part, alternating back and forth until both conditions are satisfied everywhere. In this example rotational symmetry is assumed and the center cascade is used to satisfy the vortex drag requirements; thus, the outer region  $\frac{R}{\sqrt{2}} \leq r \leq R$  of this cascade must

carry a constant intensity of lift. The cascades of radius  $R/\sqrt{2}$  are used to give the equivalent linear distribution the required elliptic shape for  $R/\sqrt{2} \leq \xi \leq R\sqrt{2}$ . The next step is to evaluate the distribution over another section of the center cascade to give constant lift intensity when elements are summed up in the free stream direction, then satisfy the wave drag criterion with the next cascade, etc. This process is continued working inward to the center of the space; although an infinite number of cascades are required the total wing area is finite. Each of the small cascades has a radius  $1/\sqrt{2}$  times the radius of the next larger one and the total wing area is  $S = 2.172\pi R^2$  (Ch. VI B). It should be noted that this is not necessarily the minimum wing area that could be used, so the distribution obtained is an optimum one with respect to wave and vortex drag only and not with respect to friction drag.

#### B. THE OPTIMUM DISTRIBUTION OF LIFT THROUGH AN ELLIPSOIDAL SPACE

The spherical space with its optimum lift distribution can be changed into an ellipsoidal space with a corresponding lift distribution by a scale transformation of one of the cartesian coordinates. This transformation transforms planes into planes so that elliptical loadings are preserved for the ellipsoid and minimum wave drag is obtained.

Also a constant intensity of lift over the wake cross-section is maintained for the ellipsoid so that the vortex drag is also a minimum.

Although the optimum lift distribution for an ellipsoid is obtainable from the spherical case, the value of the minimum drag is not necessarily the same. For an ellipsoid formed by revolving an ellipse of semi-major axis B and semi-minor axis R about the free stream (major) axis, the optimum distribution of lift is

$$l_{opt} = \frac{L}{\pi^2 R^2 B \left[ 1 - (x/B)^2 - (y/R)^2 - (z/R)^2 \right]^{1/2}}$$

The wave drag, computed by Hayes' method, is

$$D_{min \text{ wave}} = \frac{\beta^2 L^2}{8\pi q R^2 \left[ (B/R)^2 + \beta^2 \right]}$$

and the vortex drag is also a minimum,

$$D_{\text{min vortex}} = \frac{L^2}{8\pi\alpha R^2}$$

so that the total drag is

$$D_{\text{min}} = \frac{L^2}{8\pi\alpha R^2} \left\{ \frac{\beta^2}{\left[ \left( \frac{B}{R} \right)^2 + \beta^2 \right]} + 1 \right\}$$

For  $B = R$  the results reduce to the spherical case.

Several limiting cases can be examined; in one an ellipsoid is collapsed into a horizontal planar wing of elliptic planform carrying constant pressure. Optimum cases of this type were first discussed by R. T. Jones<sup>(14)</sup>. Another limiting case which gives minimum drag occurs when an ellipsoid is collapsed into a plane normal to the flow direction ( $B/R \rightarrow 0$ ). Then the wing system can be interpreted as a uniformly loaded airfoil cascade (of zero chord and gap) within the elliptical cross-section. The entire cascade can be analyzed as a two-dimensional system. If the chord is chosen to be  $\beta$  times the gap then the airfoils in the cascade are non-interfering but the lift distribution is sufficiently continuous (Fig. 6b-1). In other words, when the cascade is cut by planes inclined at the Mach angle, the resulting load distributions used in Hayes' method will be continuous. The total wing area is then  $\beta$  times the area of the ellipse..

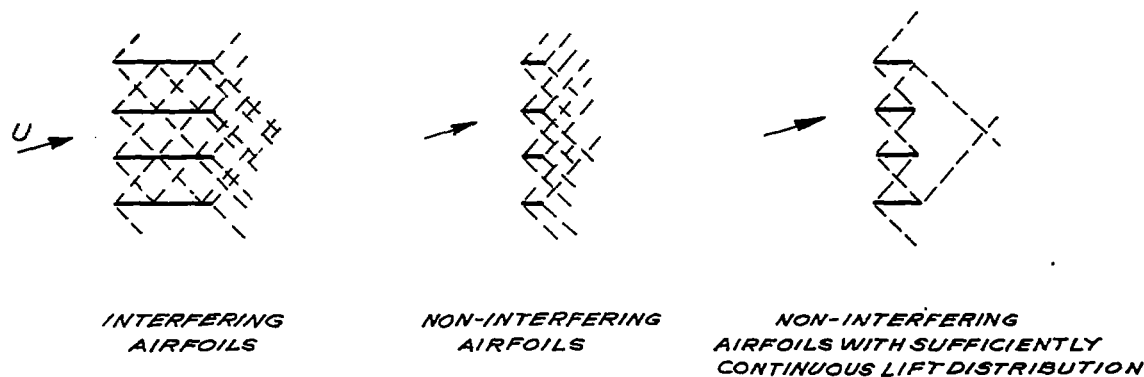


Fig. 6b-1: Examples of airfoil spacing in cascades

A third limiting case is the slender body obtained when  $B/R \rightarrow \infty$ ; then

$$D_{\min} = \frac{L^2}{2\pi q(2R)^2} + \frac{\beta^2 L^2}{2\pi q(2B)^2} = \bar{D}_{\text{vortex}} + \bar{D}_{\text{wave}}$$

The wave drag portion is the same as that obtained by Jones for a planar slender wing<sup>(13)</sup>, while the vortex drag for the spatial distribution is one-half that obtained by Jones for the planar distribution.

### C. THE OPTIMUM DISTRIBUTION OF LIFT THROUGH A "DOUBLE MACH CONE"

Consider a space consisting of two Mach cones placed base to base (Fig. 6c-1). If a uniformly loaded cascade of airfoils (with zero gap and chord) is placed at the maximum cross-section of this space then

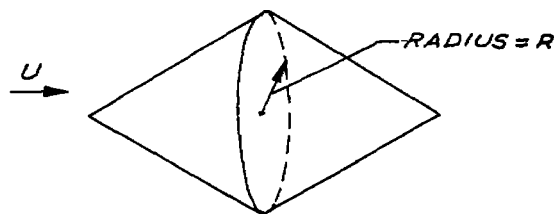


Fig. 6c-1: Double Mach cone space with optimum cascade

elliptic loadings will be obtained when the space is cut by planes inclined at the Mach angle. This airfoil cascade consequently produces the minimum possible wave drag for wing systems contained within the space and carrying a specified lift. The uniform distribution of load over the circular cross-section insures minimum vortex drag also, so the lift distribution is an optimum for the double Mach cone.

The value of the minimum wave drag (obtained by Hayes' method) is

$D_{\text{wave}} = \frac{1}{2} \frac{L^2}{\pi q(2R)^2}$  and the vortex drag has the same magnitude in this case.

The wave plus vortex drag is then  $D = \frac{L^2}{\pi q (2R)^2}$ . This is equal to the minimum vortex drag alone for a planar wing of span  $2R$ . If the airfoil cascade is compared to the largest planar wing of diamond planform which can be contained within the double Mach cone, the minimum wave plus vortex drag of the diamond planform is approximately 1.52 times greater than for the cascade<sup>(2)</sup>.

Again it must be emphasized that the drag comparison is not complete without the inclusion of viscous drag and thickness drag for the wing system.

Since the circular cascade is an optimum arrangement, it satisfies Jones' criterion (Ch. V). This can be checked as follows: By two-dimensional analysis the downwash,  $\epsilon$ , in the aft Mach cone is  $2\alpha$  where  $\alpha$  is the angle of attack of each airfoil (Fig. 6c-2). Since the downwash is zero in the fore Mach cone, the downwash velocity in the combined field is constant and equal to  $\alpha U$  throughout the double Mach cone.

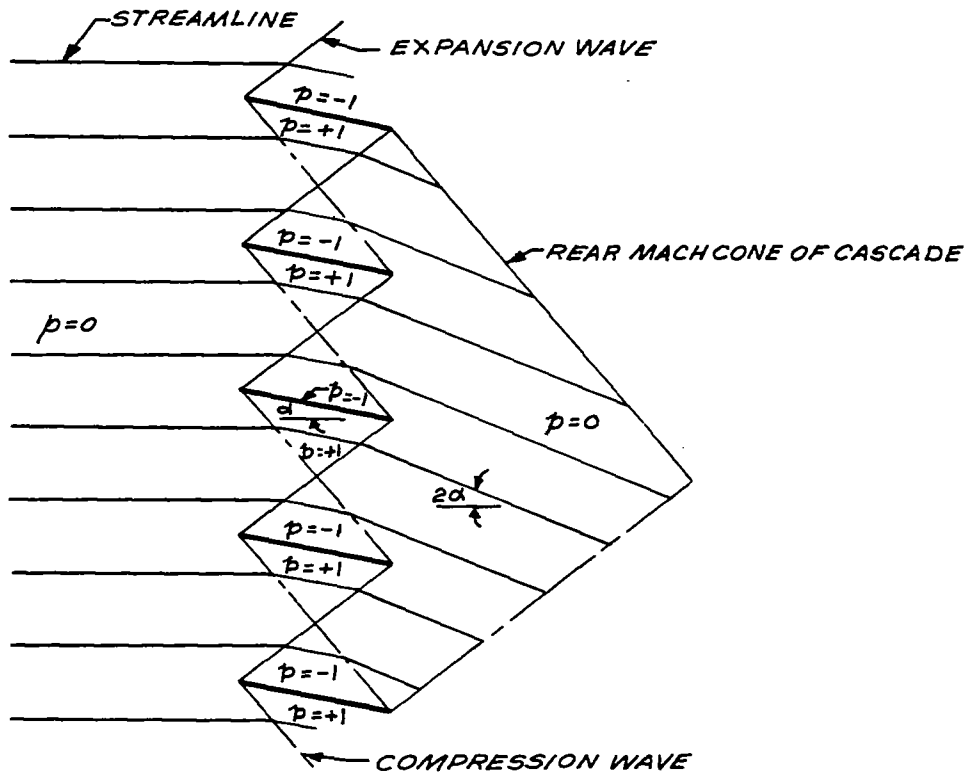


Fig. 6c-2: Two-dimensional analysis of downwash in rear Mach cone of an optimum cascade

Far behind the cascade in the wake of the wing system  $\epsilon = \alpha$ ; this can be shown by equating lift to rate of change of vertical momentum. The individual wings of the cascade are non-interfering and, in the limit as gap and chord go to zero, have two-dimensional wing characteristics. The wing area for a sufficiently continuous lift distribution (Ch. VIB) is equal to the cascade cross-sectional area  $A$  times  $\beta$ . Consequently  $L = C_L q S = (4\alpha/\beta) q (\beta A)$ . By Munk's criterion (see Ch. V and Ref. 12) the downwash in the Trefftz plane over the area behind the cascade is constant; thus, the vertical momentum of the fluid in the downwash region behind the cascade is  $(\rho AU) (\epsilon U)$ . The vertical momentum of the surrounding fluid can be evaluated from the known "virtual mass" of a solid circular cylinder of cross-sectional area  $A$  moving downward in the fluid; this latter momentum is equal to that of the downwash region itself. Thus, by the momentum theorem,  $L = 2\rho AU(\epsilon U)$  and equating the two expressions for  $L$  gives  $\epsilon = \alpha$ .

The airfoil cascade is not the only distribution of lift in the double Mach cone which has minimum wave drag. A true lineal distribution of lift distributed as an elliptic loading along the axis of the double Mach cone will produce the same minimum value of wave drag. So also will a lift distribution of constant intensity throughout the entire double Mach cone. However, the latter two cases will not give the minimum value of vortex drag; in fact, the true lineal distribution will have infinite vortex drag.

## APPENDIX VI

DERIVATION OF OPTIMUM DISTRIBUTION OF LIFT THROUGH A SPHERICAL SPACE

A sufficient condition for minimum drag is that each equivalent lineal distribution of lift should be elliptic (Ch. V). For the spherical space these equivalent lineal distributions will be the same at all angular stations if the optimum lift distribution is rotationally symmetric. For simplicity, examine the problem from the angular position  $\theta$  (on the control surface) equal to  $90^\circ$ ; then the Mach planes will be parallel to the  $y$  axis. The notation to be used is illustrated in Fig. A6-1; cylindrical coordinates  $(\zeta, S, \phi)$  and the radial coordinate  $r$  will be used.

If the spatial lift distribution is  $l(r) = l(\sqrt{\zeta^2 + S^2})$  then the equivalent lineal distribution along the  $\zeta$  axis will be

$$F(\zeta) = \int_{S=0}^{\sqrt{R^2 - \zeta^2}} \int_{\phi=0}^{2\pi} l(\sqrt{\zeta^2 + S^2}) S \, d\phi \, dS = 2\pi \int_0^{\sqrt{R^2 - \zeta^2}} S l(\sqrt{\zeta^2 + S^2}) \, dS$$

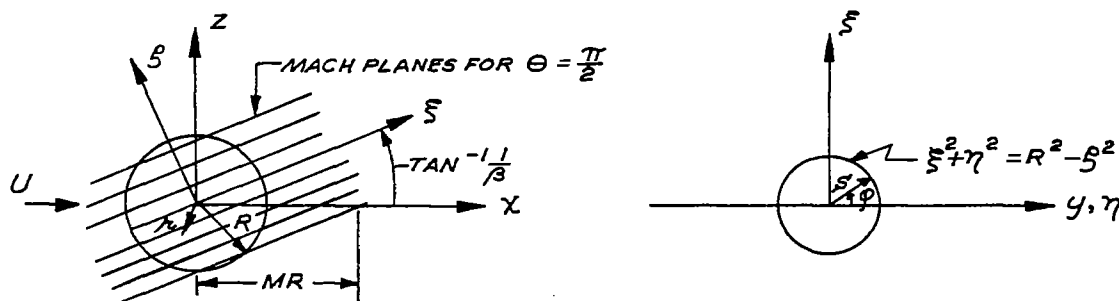


Fig. A6-1

However,

$$F(\zeta)_{\text{opt}} = K \sqrt{1 - (\zeta/R)^2}$$

where  $K$  depends on the total lift of the sphere. Introducing the radial coordinate  $r$ , the integral equation to be solved is

$$K\sqrt{1 - (\xi/R)^2} = 2\pi \int_{\xi}^R r\lambda(r)dr$$

The solution to this equation, found by differentiation with respect to  $\xi$ , is

$$\lambda(r) = \frac{K}{2\pi R\sqrt{R^2 - r^2}}$$

The total lift of the sphere is

$$L = 2 \int_0^R K\sqrt{1 - (\xi/R)^2} d\xi = \frac{\pi RK}{2}$$

so that the distribution of lift for minimum wave drag is

$$\lambda(r) = \frac{L}{\pi^2 R^2 \sqrt{R^2 - r^2}}$$

For application of Hayes' method, the equivalent lineal distribution along the  $x$  axis is needed. A plane  $\xi = \xi'$  intersects the  $x$  axis at  $x = -M\xi'$ ; since the distribution is spread out over a larger distance along the  $x$  axis, its maximum intensity will be less; thus,

$$F(x)_{\text{opt}} = \frac{K}{M}\sqrt{1 - (x/MR)^2} = \frac{2L}{\pi MR}\sqrt{1 - (x/MR)^2}$$

Hayes defines two functions such that for the lifting case (Ch. IV)

$$F = \frac{\rho U g_z}{\beta}$$

$$h = -g_z \sin \theta = \frac{-2\beta L \sin \theta}{\pi \rho U M R} \sqrt{1 - (x/MR)^2}$$

The expression for the wave drag contribution at each angular station  $\theta$  is, from Eq. (4c-30),

$$\frac{dD}{d\theta} = \frac{-\rho}{8\pi^2} \iint h'(x_2)h'(x_1) \ln|x_2 - x_1| dx_1 dx_2$$

and the total wave drag is

$$D_{\text{wave}} = \int_0^{2\pi} \frac{dD}{d\theta} d\theta$$

The integration for  $dD/d\theta$  has been carried out by Sears<sup>(16)</sup> in terms of a Fourier series expansion of an arbitrary function  $h$ . For the wave drag optimum the distribution  $h$  is elliptic and only the first term in the series for  $h$  appears. (Note the similarity to the vortex drag optimums in incompressible flow.) If  $h = C\sqrt{1 - (x/MR)^2}$  then  $dD/d\theta = \rho C^2/16$ . Substituting in the equations above leads to the final result,

$$D_{\text{wave}} = \frac{\beta^2 L^2}{8\pi q R^2 M^2}$$

CHAPTER VII. THE OPTIMUM DISTRIBUTION OF VOLUME ELEMENTS ALONE\*

A. THE SINGULARITY REPRESENTING AN ELEMENT OF VOLUME

The investigation of lift distributions is simplified by the use of a singularity which represents an element of lift. This singularity is the elementary horseshoe vortex. The intensity of lift corresponds to the strength of the singularity and the location of the lift force is identical with that of the bound vortex. The study of volume (or thickness) distributions is similarly simplified by identifying the singularity which corresponds to an element of volume.

Consider a source and sink of equal strength and located on the same streamwise line. In each unit of time a certain quantity of fluid is introduced into the flow pattern by the source and the same quantity is removed by the sink. The volume occupied by the fluid flowing from source to sink depends on the strength of the source and sink and the distance between them, and also depends on the velocity and density of the fluid flowing from source to sink. However, if the volume is to be considered a linear function of the strength of the singularities, then the mean value of density times velocity must be unaffected by the perturbation velocities created by the source and sink. This means that in a linearized treatment of the problem the fluid flowing from source to sink may be considered to have free stream density and velocity.

Let  $m$  = Mass of fluid introduced per unit time

$d$  = Distance between source and sink

$\rho_0$  = Free stream density

$U_0$  = Free stream velocity

Then the volume occupied by the fluid is

$$\text{vol} = md / (\rho_0 U_0)$$

Since the volume is proportional to  $md$ , doubling the intensity of source and sink and halving the distance between them should produce a shorter, but thicker volume of the same magnitude. This suggests proceeding to the limiting case (as in incompressible flow) where the source

---

\* The contents of this chapter have appeared in the paper "The Drag of Non-Planar Thickness Distributions in Supersonic Flow," published in the Aeronautical Quarterly, Vol. VI, May 1955.

and sink are combined in a dipole with axis in the free stream direction. This singularity should represent an element of volume, although the fineness ratio of the element is zero.

The potential for a unit source at  $(\xi, 0)$  in supersonic flow is

$$\phi_S = \frac{-1}{2\pi \sqrt{(x - \xi)^2 - \beta^2 r^2}}$$

where  $\beta = \sqrt{M^2 - 1}$ ;  $x$  and  $\xi$  are coordinates in the streamwise direction and  $r$  is radial distance from the  $x$  axis.

Differentiating with respect to  $x$  gives

$$\phi_{S_x} = \frac{(x - \xi)}{2\pi \left[ (x - \xi)^2 - \beta^2 r^2 \right]^{3/2}} = \phi_v$$

where  $\phi_v$  is the potential for the unit dipole or an element of volume equal to  $1/U_0$ .

#### B. THE DISTRIBUTION OF VOLUME ELEMENTS

For a distribution of volume elements along the  $\xi$  axis with intensity  $f(\xi)$ , starting at  $\xi = 0$ , the potential is

$$\phi = \frac{1}{2\pi} \int_0^{x-\beta r} \frac{f(\xi)(x - \xi)d\xi}{\left[ (x - \xi)^2 - \beta^2 r^2 \right]^{3/2}}$$

Integration by parts gives

$$\phi = \frac{f(\xi)}{2\pi \sqrt{(x - \xi)^2 - \beta^2 r^2}} \Big|_0^{x-\beta r} - \frac{1}{2\pi} \int_0^{x-\beta r} \frac{f'(\xi)d\xi}{\sqrt{(x - \xi)^2 - \beta^2 r^2}}$$

The first term in the expression for the potential is infinite, and apparently corresponds to the "roughness" of the body, which is an assembly of blunt elements (see illustration).



The smoothly faired body (indicated by dash lines) is all that we are concerned with, and this creates the finite part of the potential. This finite part is also the potential for a source distribution of intensity equal to  $+f'(\xi)$ . This source distribution can be used to construct a body of revolution extending from  $-l/2$  to  $+l/2$ .

The shape of the body of revolution created by the singularity distribution may be obtained approximately by slender body theory or more accurately by "exact" linear theory. In the first case the volume is

$$\int_{-l/2}^{+l/2} \frac{f(\xi)d\xi}{U_0}$$

which agrees exactly with the sum of the volume elements.

An example of the second case is shown in Fig. 4f-2 where a singularity distribution on the axis is interpreted first by slender body theory then by "exact" linear theory as a "bump" on a cylinder. The bump shapes and locations are quite different but the volumes are identical. This has been proved by Lagerstrom and Bleviss and generalized by Bleviss in Ref. 22.

A planar distribution of volume elements may be interpreted by ("exact") linear theory as a thin planar wing. The volume contained in this wing is exactly equal to the sum of the volume elements.

The concept of the volume element is not necessary for the study of smooth slender bodies of revolution and planar wings, since these configurations are relatively simple. However the use of the volume element does help to clarify problems involving more general spatial distributions of thickness.

The points to be emphasized are that fixing the sum of the volume elements fixes the total volume, and fixing the distribution of volume elements determines the drag. It is therefore possible to study the drag of a distribution of volume elements without calculating the exact shape of the corresponding body. This is analogous to the fact that the drag of a distribution of lifting elements can be studied without calculating the twist and camber of the corresponding wing surfaces.

### C. THE DRAG OF VOLUME DISTRIBUTIONS ON A STREAMWISE LINE AND THE SEARS-HAACK BODY

A body of revolution may be constructed from a distribution of volume elements along a streamwise line, or from the equivalent distribution of sources. The body constructed from volume elements is an "infinitely rough" body and has infinite drag. However, discarding the infinite part of the potential leaves a "smooth" body (with finite drag) which is equivalent in every respect to the body created by a source distribution.

If  $f(x)$  is the intensity of the volume element distribution for a body of revolution of length " $l$ " then the drag is given by<sup>(16)</sup>

$$D = \frac{-\rho}{4\pi} \int_{-l/2}^{+l/2} \int_{-l/2}^{+l/2} f''(x_1) f''(x_2) \ln|x_1 - x_2| dx_1 dx_2$$

To maintain constant total volume according to linearized theory it is necessary that  $\int_{-l/2}^{+l/2} f(x) dx = \text{Constant}$ . The body shape giving minimum drag for a given length and volume has been determined by Sears<sup>(16)</sup> and Haack<sup>(17)</sup> independently. The corresponding  $f(x)$  (which is proportional to the cross-sectional area) is given by

$$f_{\text{opt}}(x) = \frac{16}{3\pi} \left[ 1 - \left( \frac{2x}{l} \right)^2 \right]^{3/2} \frac{\int_{-l/2}^{+l/2} f(x) dx}{l} = \frac{8U_0}{3\pi} \frac{\text{volume}}{l/2} \left[ 1 - \left( \frac{2x}{l} \right)^2 \right]^{3/2}$$

Thus the optimum distribution of volume elements along the axis corresponds to the cube of an elliptical distribution. (For lifting elements the optimum distribution is elliptical.)

The value of the minimum drag is

$$D_{\text{min}} = \frac{8q}{\pi} \left( \frac{l}{2} \right)^2 \left[ \frac{\int_{-l/2}^{+l/2} f(x) dx}{U_0 (l/2)^3} \right]^2 = \frac{8q}{\pi} \left( \frac{l}{2} \right)^2 \left[ \frac{\text{volume}}{(l/2)^3} \right]^2$$

#### D. THE SEARS-HAACK BODY AS AN OPTIMUM VOLUME DISTRIBUTION IN SPACE

If the volume elements are not confined to a single streamwise line, then the drag contributions at different angles,  $\theta$ , on Hayes' cylindrical control surface are not necessarily the same. For any one angle,  $\theta$ , the drag is given by

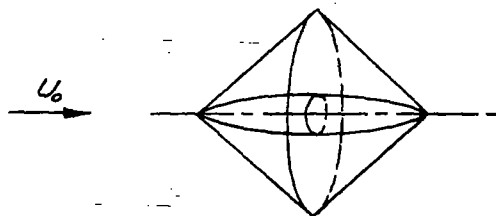
$$\frac{\partial D}{\partial \theta} = \frac{-\rho}{8\pi^2} \int_{-l/2}^{+l/2} \int_{-l/2}^{+l/2} f''(x_1, \theta) f''(x_2, \theta) \ln|x_1 - x_2| dx_1 dx_2$$

Here  $f(x, \theta)$  is determined by the use of "Mach planes" for the angle  $\theta$ . All the volume elements intercepted by any one "Mach plane" are transferred (in the plane) to the streamwise axis. The resulting distribution along the axis is  $f(x, \theta)$ . The problem of finding the minimum drag contribution at the one angle  $\theta$  is then similar to the Sears-Haack problem. If  $f(x, \theta)$  corresponds to the cube of an elliptical distribution for every  $\theta$ , then the total drag is a minimum, and the drag contribution at each  $\theta$  is a minimum and corresponds to that of an equivalent Sears-Haack body.

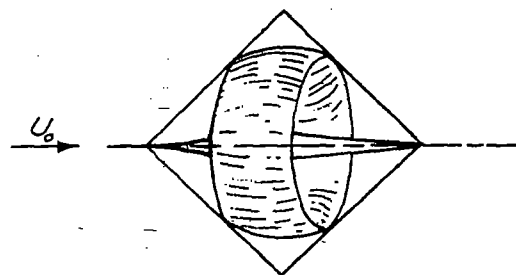
It is not always possible to simultaneously minimize the drag contributions at all angles  $\theta$ . However if we consider the optimum distribution of thickness within a space which has rotational symmetry about a streamwise axis, then it may be possible that all the equivalent bodies are Sears-Haack bodies having the same length.

For example, consider that a double Mach cone bounds the space within which thickness is to be distributed. The Sears-Haack body placed on the axis is an optimum for this space. It has the same drag contribution at every angle on the cylindrical control surface, and of course, the "equivalent" body of

revolution for any angle  $\theta$  is identical with the real body. However, a "ring" wing (which carried no radial forces) plus a central body of revolution can be designed to have exactly the same drag as the Sears-Haack body. The equivalent bodies of revolution are all identical with the Sears-Haack body. This is discussed in the next section. (For the case in which radial forces are carried on the ring wing see Ch. IX.)



**SEARS-HAACK BODY BOUNDED  
BY DOUBLE MACH CONE SPACE**



**RING WING PLUS CENTRAL  
BODY HAVING SAME DRAG  
AS SEARS-HAACK BODY**

E. RING WING AND CENTRAL BODY OF REVOLUTION  
COMBINATION HAVING THE SAME DRAG AS A SEARS-HAACK BODY

Consider a ring-wing plus a central body of revolution contained within the space bounded by a double Mach cone. Because of the rotational symmetry of this particular system, the equivalent body of revolution is independent of the angle  $\theta$  on the cylindrical control surface. In this case, if the local radial force on the wing is everywhere zero, the drag of the equivalent body of revolution is, according to Hayes' formula, identical to the drag of the original system. Thus, a ring-wing (which carries no radial force) plus a central body of revolution will have exactly the same drag as a Sears-Haack body if the equivalent body of revolution is a Sears-Haack body.

To design such a system, we may select any smooth, slender profile for the ring-wing and compute the cross-sectional areas cut from this wing by a set of parallel Mach planes. These areas must then be subtracted from the cross-sectional areas which would be cut from a central Sears-Haack body by the corresponding Mach planes. The resulting area difference defines the area distribution (in the Mach planes) of the correct central body. (This area must be projected normal to the flow direction to obtain the cross-sectional area of the central body defined in the usual way.) This body, together with the ring-wing originally selected, is an optimum distribution of thickness within the double Mach cone space.

As an example, consider a ring-wing with thickness distribution corresponding to a bi-parabolic arc profile. The camber necessary for zero local radial force need not be determined, since it does not affect the shape of the central body. Assume that the wing is six percent thick and located half-way between the axis and the apex of the space. If the central body of revolution is designed so that the equivalent Sears-Haack body is of fineness ratio 5, the resulting shape of the central body of revolution is as shown in Fig. 7e-1.

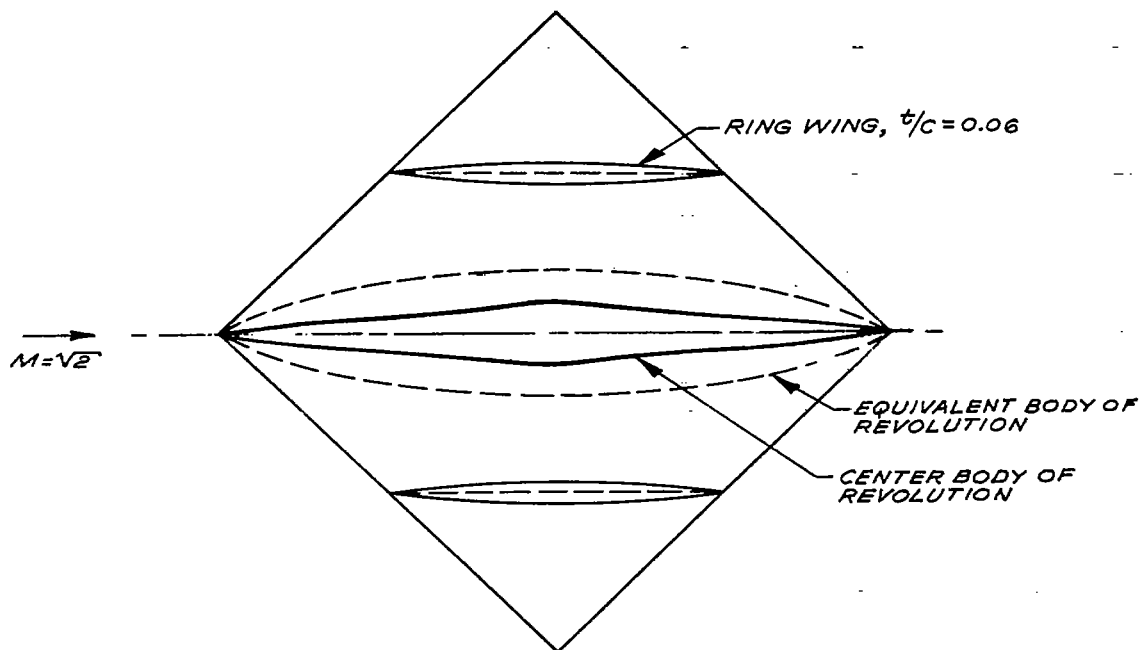


Fig. 7e-1: Cross-sectional view of ring-wing and central body (an optimal distribution of thickness within the double Mach cone space)

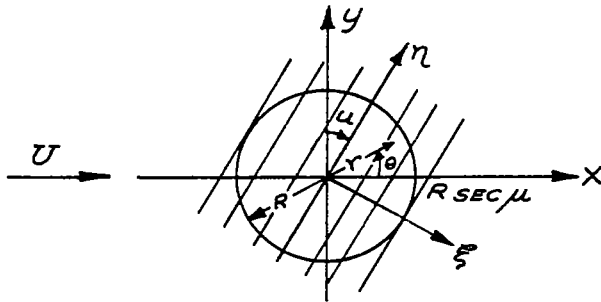
F. OPTIMUM THICKNESS DISTRIBUTION FOR A PLANAR WING OF ELLIPTICAL PLANFORM

It is desired to find the optimum thickness distribution for a planar wing of elliptic planform and given volume; this problem was first solved by R. T. Jones<sup>(14)</sup>. A geometrically simpler problem, which will be examined first, is to find the optimum thickness distribution for a circular wing of given volume. The method of Hayes<sup>(1)</sup> in which the drag is evaluated by summing increments of drag at each angular station around a cylindrical control surface far away from the body, will be used. For the total drag to be a minimum, the increment of drag at each angular station should also be a minimum.

If the thickness distribution of the circular planform is rotationally symmetric, then the equivalent bodies at each angular station will have the same shape (although different "fineness ratios") due to symmetry. If  $t(r)$  is the thickness distribution to be optimized for a given volume  $V$ , then

$$V = 2\pi \int_0^R t(r)r dr \quad (7f-1)$$

where  $R$  is the radius of the circular wing and  $r, \theta$  are polar coordinates from the wing center (Fig. 7f-1). The area cut out at each point along the  $\xi$  axis by planes normal to that axis is



$$\begin{aligned} S(\xi) &= \int_{-\sqrt{R^2-\xi^2}}^{+\sqrt{R^2-\xi^2}} t d\eta \\ &= 2 \int_{\xi}^R \frac{t(r)r dr}{\sqrt{r^2 - \xi^2}} \quad (7f-2) \end{aligned}$$

The equivalent lineal distribution along the  $x$  axis is

$$S(x) = 2 \cos \mu \int_{x \cos \mu}^R \frac{rt(r)dr}{\sqrt{r^2 - x^2 \cos^2 \mu}} \quad (7f-3)$$

with

$$\int_{-R \sec \mu}^{+R \sec \mu} S(x)dx = V$$

For minimum drag, this distribution should be (Ch. VF)

$$S(x) \propto \left[ 1 - (x/R \sec \mu)^2 \right]^{3/2} \quad (7f-4)$$

Thus the integral equation to be solved for  $t(r)$  is

$$K \left[ 1 - (x/R \sec \mu)^2 \right] = 2 \cos \mu \int_{x \cos \mu}^R \frac{t(r)r dr}{\sqrt{r^2 - x^2 \cos^2 \mu}} \quad (7f-5)$$

where  $K$  is a constant dependent upon the given wing volume. By a suitable transformation of coordinates, Eq. (7f-5) may be written in the form

$$\frac{K\phi^{3/2}}{R \sec \mu} = \int_0^\phi \frac{t(\alpha) d\alpha}{\sqrt{\phi - \alpha}} \quad (7f-6)$$

where

$$\phi = 1 - (x/R \sec \mu)^2$$

$$\alpha = 1 - (r/R)^2$$

Eq. (7f-6) is called Abel's equation and its solution is well known, c.f., Ref. 19. The solution to Eq. (7f-6) is

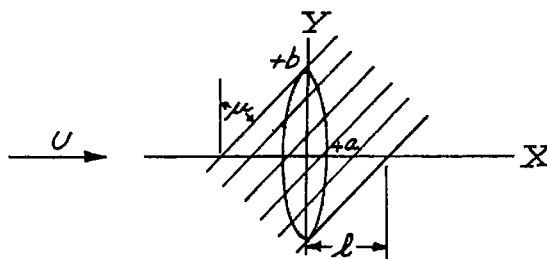
$$t(r) = \frac{3K}{4R \cos \mu} \left[ 1 - (r/R)^2 \right]$$

and substitution of this in Eq. (7f-1) determines  $K$ ; then

$$t(r) = \frac{2V}{\pi R^2} \left[ 1 - (r/R)^2 \right] \quad (7f-7)$$

Equation (7f-7) thus gives the distribution of thickness which will result in minimum drag for the circular planform wing of given volume.

To apply the circular planform solution to the original problem of finding the optimum thickness for an unyawed elliptic planform, make the following change of coordinates:



$$X = \frac{ax}{R} \quad (7f-8)$$

$$Y = \frac{by}{R}$$

Fig. 7f-2

The circular wing is then transformed into an elliptic wing whose equation is

$$\left(\frac{X}{a}\right)^2 + \left(\frac{Y}{b}\right)^2 = 1$$

It can be verified that the thickness distribution

$$t = \frac{2V}{\pi ab} \left[ 1 - \left(\frac{X}{a}\right)^2 - \left(\frac{Y}{b}\right)^2 \right] \quad (7f-9)$$

obtained from Eq. (7f-7) through the transformation Eq. (7f-8) is the optimum for this more general case; that is, the equivalent linear distribution for Eq. (7f-9) with a set of Mach planes inclined at the angle  $\mu$  as shown in Fig. 7f-2 is

$$s(X) = \frac{8V}{3\pi l} \left[ 1 - \left(\frac{X}{l}\right)^2 \right]^{3/2} \quad (7f-10)$$

where

$$l = \sqrt{a^2 + b^2 \tan^2 \mu}$$

Since Eq. (7f-10) represents a Sears-Haack body, the thickness given by Eq. (7f-9) is optimum for the unyawed elliptic wing.

Determination of the total drag in this optimum case involves an integration of the drag increments from these Sears-Haack bodies as seen at each angular reference station. If the reference station is at an angle  $\theta$  from the horizontal, then the Mach planes cut the elliptic planform at an angle  $\mu$  defined as (Ch. IVC).

$$\tan \mu = \sqrt{M^2 - 1} \cos \theta \quad (7f-11)$$

and the total drag is

$$D = \int_0^{2\pi} \frac{dD}{d\theta} d\theta$$

The increment of drag at each reference station is (Ch. IVC)

$$\begin{aligned} \frac{dD}{d\theta} &= -\frac{q}{4\pi} \int_0^\infty \int_0^\infty S''(x)S''(\xi) \ln|x-\xi| dx d\xi \\ &= \frac{4qV^2}{\pi^2 \lambda^4} \end{aligned} \quad (7f-12)$$

and the total drag for the optimum thickness distribution Eq. (7f-9) is

$$D_{\text{opt}} = \frac{4qV^2}{\pi a^3 b} \left[ \frac{M^2 - 1 + \frac{2a^2}{b^2}}{\left(M^2 - 1 + \frac{a^2}{b^2}\right)^{3/2}} \right] \quad (7f-13)$$

Defining

$$t = t_0 \left[ 1 - \left(\frac{X}{a}\right)^2 - \left(\frac{Y}{b}\right)^2 \right]$$

and

$$D = C_D q \pi a b$$

then

$$C_{D_{\text{opt}}} = \frac{\left(M^2 - 1 + \frac{2a^2}{b^2}\right) t_0^2}{\left(M^2 - 1 + \frac{a^2}{b^2}\right)^{3/2} a^2} \quad (7f-14)$$

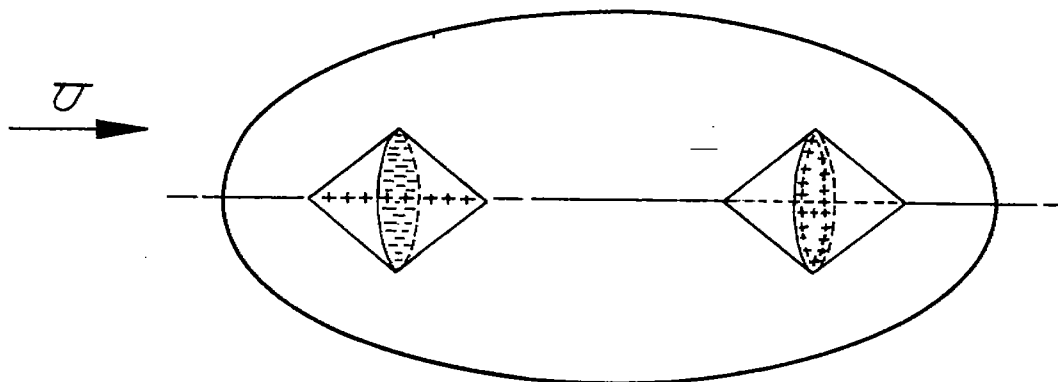
This result agrees with that given by Jones<sup>(14)</sup>.

CHAPTER VIII. UNIQUENESS PROBLEMS FOR OPTIMUM DISTRIBUTIONS IN SPACEA. THE NON-UNIQUENESS OF OPTIMUM DISTRIBUTIONS IN SPACE - "ZERO LOADINGS"

In the subsonic flow of a perfect fluid the only drag caused by a lifting wing is vortex drag. The minimum possible vortex drag for a planar wing is obtained when the spanwise lift distribution is elliptical. According to Munk's stagger theorem<sup>(15)</sup> the chordwise location of the lifting elements is unimportant, so there are infinitely many distributions of lift over a given planform which produce the minimum drag.

In supersonic flow lift causes both vortex drag and wave drag. The chordwise location of lifting elements is still unimportant in determining vortex drag, but does affect the wave drag. For this reason the optimum lift distribution for a planar wing is generally unique in supersonic flow. However, spatial lift distributions offer more freedom in the arrangement of lifting elements and the optimum distributions in space are not generally unique even in supersonic flow.

For example, the minimum wave drag due to lift in a double Mach cone space can be attained with each of three different simple lift distributions. (See VI-C.) The first is a constant intensity over the circular disc located at the maximum cross-section of the space. The second is an elliptical intensity concentrated on the axis of the double Mach cone. The third is a constant intensity throughout the entire double Mach cone. If the first two distributions are superimposed, one carrying a unit of positive lift and the other a unit of negative lift, the result is a net lift equal to zero. Also, the net strength of the lifting elements intercepted by any cutting plane inclined at the Mach angle is zero. This means that the combined distribution has zero wave drag. Furthermore, there are no disturbances whatsoever produced on the distant control surface near the Mach cone and no wave drag interference can exist with any other loading. If another such combined distribution with opposite sign is placed on the same streamwise line with the first one, then, by Munk's stagger theorem, the vortex drag is zero also. This is one example of a "zero loading" (see illustration), and many others can be constructed.



*A "ZERO LOADING" PLACED WITHIN AN ELLIPSOIDAL SPACE*

Such a "zero loading" placed within any space alters neither the lift nor the drag of the original lift distribution. For this reason optimum lift distributions in three dimensions are never unique (unless the space degenerates into a surface).

Similar arguments can be applied to optimum distributions of volume. For an example of non-uniqueness in such cases see Ch. VII.

B. UNIQUENESS OF THE DISTANT FLOW FIELD  
PRODUCED BY AN OPTIMUM FAMILY

It has been shown that optimum lift or volume distributions in space are not generally unique, since a group of optimum distributions can be obtained from one given optimum distribution by superposition of "zero loadings." Each member of the group produces the same (minimum) value of drag for a given total lift or volume.

From the method of construction of this group (by the use of "zero loadings") it follows that each member produces the same velocity perturbation field in the Trefftz plane and on the distant control surface near the Mach cone. It can also be shown that there are no optimum distributions outside this group, since all possible optimum distributions are indistinguishable from the "distant" viewpoint.

Assume that  $f_{1\text{opt}}(\xi, \eta, \zeta)$  and  $f_{2\text{opt}}(\xi, \eta, \zeta)$  are members of the optimum family not included in the original group (whose members were related through "zero loadings"). Assume also that  $f_{1\text{opt}}$  and  $f_{2\text{opt}}$  do not produce identical perturbation velocity fields far from the singularity

distribution. Then the drag of  $f_{1\text{opt}}$  equals the drag of  $f_{2\text{opt}}$  (or  $D_{1\text{opt}} = D_{2\text{opt}}$ ) by definition of the optimum family. Also  $f_{2\text{opt}}$  may be set equal to  $f_{1\text{opt}} + \Delta f$ , where  $\Delta f$  carries zero net lift (or volume), but has a velocity perturbation field which is not identically zero far from the singularities.

The distribution  $\Delta f$  is orthogonal to (does not interfere with)  $f_{1\text{opt}}$ . This follows because any given lift or volume distribution can be improved through combining it with a distribution having zero net lift or volume if there is interference drag. However  $f_{1\text{opt}}$ , by definition, cannot be improved, and must, therefore, be orthogonal to  $\Delta f$ .

Since  $\Delta f$  is orthogonal to  $f_{1\text{opt}}$ ,  $D_{2\text{opt}} = D_{1\text{opt}} + D_{\Delta f}$ , but we also know that  $D_{2\text{opt}} = D_{1\text{opt}}$  and, therefore,  $D_{\Delta f}$  must equal zero. Here we can obtain a contradiction since both the vortex drag and the wave drag depend on the squares of velocity perturbations (in the Trefftz plane and far out on the Mach cone) and the drag contribution from each portion of the control surface is non-negative. If  $\Delta f$  produces any disturbances far from the lifting system it must have positive drag, and so  $\Delta f$  must produce identically zero disturbances to have zero drag.

The above contradiction shows that all the members of the optimum family are indistinguishable from the distant viewpoint.

If drag is computed from the "close" viewpoint the above argument cannot be made. Drag contributions then appear as the product of local pressure times angle of attack on the wing surfaces, and these quantities are not necessarily non-negative at every point on the surface.

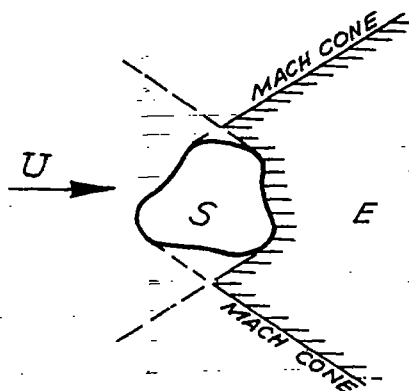
### C. UNIQUENESS OF THE ENTIRE "EXTERNAL" FLOW FIELD PRODUCED BY AN OPTIMUM FAMILY

It has been shown that any two members of an optimum family produce identical velocity perturbations on the distant control surface.

If  $f_{1\text{opt}}(\xi, \eta, \zeta)$  and  $f_{2\text{opt}}(\xi, \eta, \zeta)$  are two members of an optimum family, then  $f_{1\text{opt}} - f_{2\text{opt}}$  must produce identically zero velocity perturbations on the distant control surface, and the drag will be zero.

Let "S" designate the space within which the singularity distribution  $f_{1\text{opt}} - f_{2\text{opt}}$  exists, and let "E" represent the external flow field

consisting of points whose aft Mach cones do not intersect "S." Assume that at some point in the external field "E" the resultant velocity vector is inclined to the free stream direction. Then an elementary wing can be inserted at that point with the angle of attack adjusted to give negative drag on the wing. Since the singularities in "S" are outside the aft Mach cones of all points in "E," the net drag change produced by the elementary wing is negative. However,  $f_{1\text{opt}} - f_{2\text{opt}}$  is a singularity distribution causing zero drag, so  $f_{1\text{opt}} - f_{2\text{opt}}$  plus the elementary



wing is a system having negative drag, although it is an isolated system inserted in a uniform flow field. However, the drag of this system evaluated on a distant control surface comes from a summation of positive quantities and cannot be negative. This contradiction shows that the external flow field "E" produced by  $f_{1\text{opt}} - f_{2\text{opt}}$  must consist of velocity vectors aligned with the free stream direction. These vectors must also have the magnitude of the free stream velocity; hence, the external flow field is completely undisturbed, and it can be concluded that all members of the optimum family produce the same flow pattern in the external field "E."

It is of interest that a similar proof cannot be made for subsonic flows. In such cases there is no external region where an elementary airfoil can be inserted without producing interference effects at the original singularities.

#### D. EXISTENCE OF SYMMETRICAL OPTIMUM DISTRIBUTIONS IN SYMMETRICAL SPACES

It can be shown that, if the boundary of a space has a horizontal plane of symmetry, then there is one member of the family of optimum lift distribution within the space which is symmetrical about the plane. The proof is as follows:

Let  $l_{\text{opt}}(x,y,z)$  represent an optimum lift distribution in the space. The distribution  $l_{\text{opt}}(x,y,-z)$  has the same drag and lift (the drag of

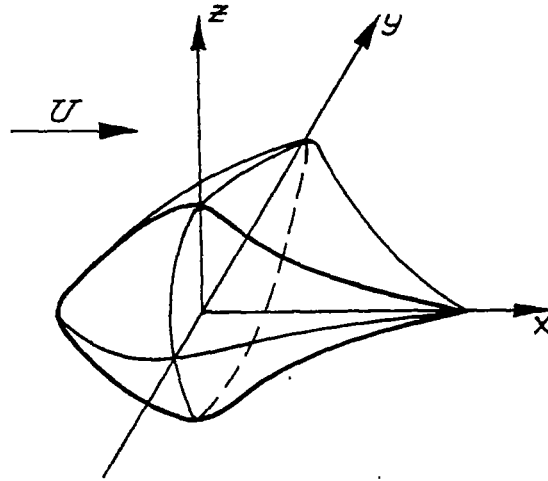
the individual lifting elements is unaltered by the change of position, and the interference drag of any element pair is unaltered also).

Since  $l_{\text{opt}}(x,y,-z)$  has the same lift and drag as  $l_{\text{opt}}(x,y,z)$  it is also a member of the optimum family. All members of the optimum family produce the same external flow field, and any distribution producing that field is an optimum. The distribution,

$\frac{1}{2}l_{\text{opt}}(x,y,-z) + \frac{1}{2}l_{\text{opt}}(x,y,z)$  pro-

duces the same external flow field as  $l_{\text{opt}}(x,y,z)$ . It is, therefore, an optimum, and since it is also symmetrical about the horizontal plane the proof is completed.

Similar proofs can be developed for cases where lift, thickness, and side force elements are present. Also certain other planes of symmetry can be used.



CHAPTER IX. INVESTIGATION OF SEPARABILITY OF LIFT,  
THICKNESS AND SIDEFORCE PROBLEMS\*

A. THE SEPARABILITY OF OPTIMUM  
DISTRIBUTIONS PROVIDING LIFT AND VOLUME

Separability Questions

For the purpose of drag evaluation a complete aircraft is represented by a distribution of lift elements, volume elements and possibly sideforce elements in space. A certain net lift must be provided to support the weight and a net volume must be provided to house payload, fuel, structure, etc. The drag should then be made as small as possible with the net lift and volume equal to the prescribed values.

Several questions arise. Can we first study the problem of how best to provide the required lift (with no net volume), then determine the best way to provide the required volume (with no net lift), and finally by superposition obtain the optimum distributions of singularities for simultaneously providing the net lift and volume? If this procedure is possible will the drag of the combination be the sum of the drags of the two superimposed distributions? Does the optimum way of providing the lift with no net volume require only lifting elements or are volume and sideforce elements necessary? Similarly does the optimum way of providing the volume with no net lift require singularities other than volume elements?

For horizontal planar systems the answers to these questions are comparatively simple. The lift and volume problems can be studied separately and the optimum singularity distributions superimposed. The drag of the combination is the sum of the drags of the individual distributions. Finally, the optimum way of providing the lift requires only lifting elements and the optimum way of providing volume requires only volume elements.

All of the above results follow from the fact that in horizontal planar systems there is no interference drag among lift, sideforce, and volume elements. However this is not true in general for non-planar systems, and consequently the above problems must be re-investigated for these more general configurations.

---

\* Portions of this chapter have appeared in the paper "The Drag of Non-Planar Thickness Distributions in Supersonic Flow," published in the Aeronautical Quarterly, Vol. VI, May 1955.

Optimum Distributions Providing Lift and Volume

In non-planar distributions of lift, sideforce and thickness there is generally interference among the different singularities. This means that the drag for a given net lift may in some cases be decreased by adding thickness or sideforce elements and taking advantage of negative interference drag.

In order to study such cases let  $l(x,y,z)$ ,  $t(x,y,z)$ , and  $s(x,y,z)$  represent respectively distributions of lift, thickness and sideforce in  $x,y,z$  space within some boundary. Here we will exclude, without loss of generality, those distributions of  $l$  and  $s$  which are completely equivalent to elements of volume or thickness (see III-A, the closed vortex line). Let  $l_1^1(x,y,z) + t_1^0(x,y,z) + s_1^0(x,y,z)$  give the minimum possible drag for one unit of net lift and zero net thickness and sideforce. (The superscript simply indicates the net lift or thickness or sideforce of the distribution.) Also let  $l_2^0(x,y,z) + t_2^1(x,y,z) + s_2^0(x,y,z)$  give the minimum possible drag for one unit of net volume and zero net lift and side force. We ask what distribution gives the minimum drag when both the net lift and net volume are simultaneously prescribed and equal to  $L_0$  and  $V_0$  respectively?

Consider the distribution  $A(x,y,z) = L_0 [l_1^1 + t_1^0 + s_1^0] + V_0 [l_2^0 + t_2^1 + s_2^0]$

which gives the prescribed net lift and volume. For this to be the optimum it is necessary and sufficient that it be orthogonal to every distribution  $l^0 + t^0 + s^0$ , which contains zero net lift, zero net volume and zero net sideforce. For example, any loading  $l^0 + t^0 + s^0$  multiplied by an arbitrary constant  $C$  can be superimposed on  $A$  without altering the net lift,  $L_0$  and net volume,  $V_0$ . If this distribution  $l^0 + t^0 + s^0$  were not orthogonal to  $A$ , then  $C$  could be adjusted to give a negative interference drag with  $A$  greater than the drag of  $C(l^0 + t^0 + s^0)$  by itself. Hence the distribution  $A$  could be improved and therefore would not be an optimum. It is also true that any possible improvement of  $A$  must be obtainable by superposition of a loading of the type  $C(l^0 + t^0 + s^0)$  on  $A$ . So for  $A$  to be an optimum it is both necessary and sufficient that  $A$  be orthogonal to any loading  $l^0 + t^0 + s^0$ .

However,  $l_1^1 + t_1^0 + s_1^0$  and  $l_2^0 + t_2^1 + s_2^0$  are each orthogonal to any  $l^0 + t^0 + s^0$  since each one is an optimal distribution in its own restricted class. Therefore because of the linearity of the interference terms  $L_0(l_1^1 + t_1^0 + s_1^0) + V_0(l_2^0 + t_2^1 + s_2^0)$  is orthogonal to any  $l^0 + t^0 + s^0$  and  $A(x,y,z)$  is the optimum distribution having lift =  $L_0$  and volume =  $V_0$ .

The Drag of the Optimum Distribution Providing Lift and Volume in a Region Having a Horizontal Plane of Symmetry

The drag of the optimum distribution  $A(x,y,z)$  must next be determined. If  $l_1^1 + t_1^0 + s_1^0$  is orthogonal to  $l_2^0 + t_2^1 + s_2^0$  then the drag of  $A(x,y,z)$  is just the sum of the drags of  $L_0(l_1^1 + t_1^0 + s_1^0)$  and of  $V_0(l_2^0 + t_2^1 + s_2^0)$ . We know that  $(l_2^0 + t_2^1 + s_2^0) \perp (t_1^0 + s_1^0)$  so the question arises is  $(l_2^0 + t_2^1 + s_2^0)$  also  $\perp l_1^1$ ? (Here the symbol " $\perp$ " indicates orthogonality.)

In order to answer this question it is convenient to represent  $l_1^1(x,y,z)$  by a concentrated lift of one unit  $l_{18}^1$  plus a distribution containing zero net lift  $l_1^0(x,y,z)$ . The concentrated unit of lift can be placed anywhere in the space and then  $l_1^0(x,y,z)$  is simply the difference between  $l_1^1(x,y,z)$  and  $l_{18}^1$ . Similarly it is convenient to replace  $t_2^1$  by  $t_{28}^1 + t_2^0(x,y,z)$ . The optimum distribution is then

$$A(x,y,z) = L_0(l_{18}^1 + l_1^0 + t_1^0 + s_1^0) + V_0(t_{28}^1 + l_2^0 + t_2^0 + s_2^0)$$

The distributions in brackets are orthogonal if

$$l_{18}^1 \perp t_{28}^1 + l_2^0 + t_2^0 + s_2^0$$

or if

$$t_{28}^1 \perp l_{18}^1 + l_1^0 + t_1^0 + s_1^0$$

The concentrated unit of lift  $l_{18}^1$  may be located at any point in the space and has the same interference drag with  $(t_{28}^1 + l_2^0 + t_2^0 + s_2^0)$  for all locations. Thus if there is any point in the space where a unit of lift has no interference with  $(t_{28}^1 + l_2^0 + t_2^0 + s_2^0)$  the orthogonality of the two components of  $A(x,y,z)$  is assured. (This does not depend on the connectivity or the convexity of the space.)

For example, if the boundary of a space has a horizontal plane of symmetry, then there are optimum distributions in the space having symmetry properties. (The proof is similar to that given in Ch. VIII for a lift distribution.) If some portion of the plane of symmetry is contained inside the space then the concentrated unit of lift can be located in this plane and orthogonality demonstrated.

B. THE NON-INTERFERENCE OF SOURCES WITH OPTIMUM DISTRIBUTIONS OF LIFTING ELEMENTS IN A SPHERICAL SPACE

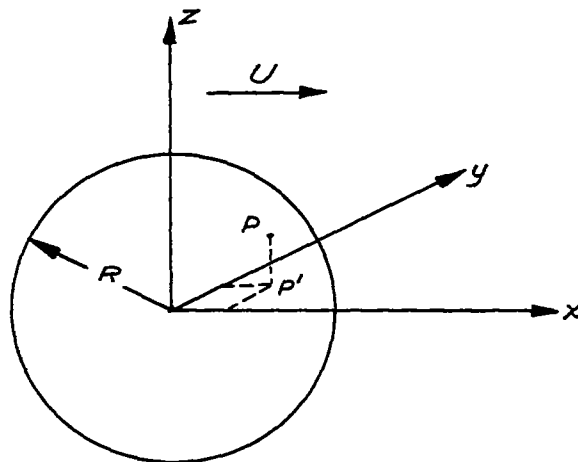
In general there is interference between non-planar distributions of sources and lifting elements, as shown by Hayes<sup>(1)</sup>. This means that in general the optimum distribution of singularities which provides one unit of lift may contain volume elements or sources as well as lifting elements. However for certain spaces it can be proved that there is no interference between a source and the optimum distribution of lifting elements alone. So for these spaces the optimum way of providing lift requires no sources.

Following is a proof that a single source placed at any point within a sphere has no interference drag with the optimum distributions of lifting elements alone in the sphere.

An optimum distribution of the total lift, L, within a sphere of radius "R" (center at the origin) is given by (see Appendix VI-1)

$$l_{opt} = \frac{L}{\pi^2 R^2 \sqrt{R^2 - r^2}}$$

where r = Spherical radius to any point. Let a source located at an arbitrary point, P, within the sphere be denoted by S, and let P' be the projection of P on the horizontal (x-y) plane. The potential of S is identical with that caused by some lifting element distribution,  $l^1$ , on the line between P and P' plus a source S' at P'. (See Ch. III Section B. The shells which have sources and sinks on the top and bottom faces respectively are arranged to form a vertical column of infinitesimal cross section.) The distribution  $l^1$  has zero net lift.



The interference between  $l_{opt}$  and  $S$  is equal to the interference between  $l_{opt}$  and  $S'$  plus the interference between  $l_{opt}$  and  $l^1$ . The first component is zero because of the symmetry of  $l_{opt}$  about the x-y plane, (see the discussions of interference in Ch. IV). If the second component were not zero it would be possible to obtain a distribution of lifting elements alone with lower drag than  $l_{opt}$ . Since  $l_{opt}$  has the minimum drag by definition, the second interference component is also zero. This completes the proof for a particular  $l_{opt}$ .

This proof can be extended to the entire family of optimum lift distributions in the sphere as follows. As previously mentioned, all of the optimum distributions produce identical effects far out on the Mach cone and far behind the wing system. Interference drag terms can be computed from these distant effects alone. Hence a source has the same interference drag with each of the optimum distributions, and this is zero for all cases since it has been proved zero for one case.

This proves that source distributions in a spherical volume cannot reduce the drag attained with any of the optimum distributions of lifting elements alone in that volume.

Similar methods may be applied to ellipsoids having one principal axis vertical, to double Mach cones, and to many other volumes. It is sufficient that the volume have a horizontal plane of symmetry, and that the vertical lines connecting all points in the volume with this plane are entirely contained within the volume.

### C. THE NON-INTERFERENCE OF SIDEFORCE ELEMENTS WITH OPTIMUM DISTRIBUTIONS OF LIFTING ELEMENTS IN A SPHERICAL SPACE

As shown by Hayes<sup>(1)</sup> there is, in general, interference between non-planar distributions of lifting elements, sideforce elements and sources. It has been proven in Ch. IX-B that there is no interference between a source and the optimum distribution of lifting elements alone in a spherical space. It remains to show a similar result for the interference of a sideforce element with the same optimum lift distributions. The proof will be carried out in a manner similar to that of the previous proof.

Consider an optimum distribution of total lift  $L$  in a sphere of radius  $R$ ; the lift distribution is given by

$$l_{opt} = \frac{L}{\pi^2 R^2 \sqrt{R^2 - r^2}}$$

where  $r$  is the radius to any point from the center of the spherical space. Let  $S$  be a sideforce element at a point  $P$  within the sphere, and let  $P'$  be the projection of  $P$  on the  $xy$  plane.

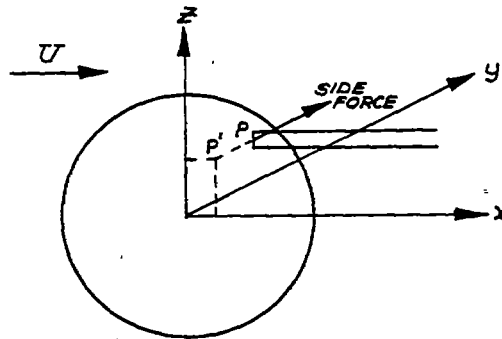


Fig. 9c-1

As part of the proof it is necessary to show how a sideforce element can be transferred from one point to another along a line parallel to the  $y$  axis. The procedure is shown in Fig. 9c-2. First a vortex ring of infinitesimal height and finite width,  $d$ , is superimposed on the original sideforce element; the strength and placement of the former is

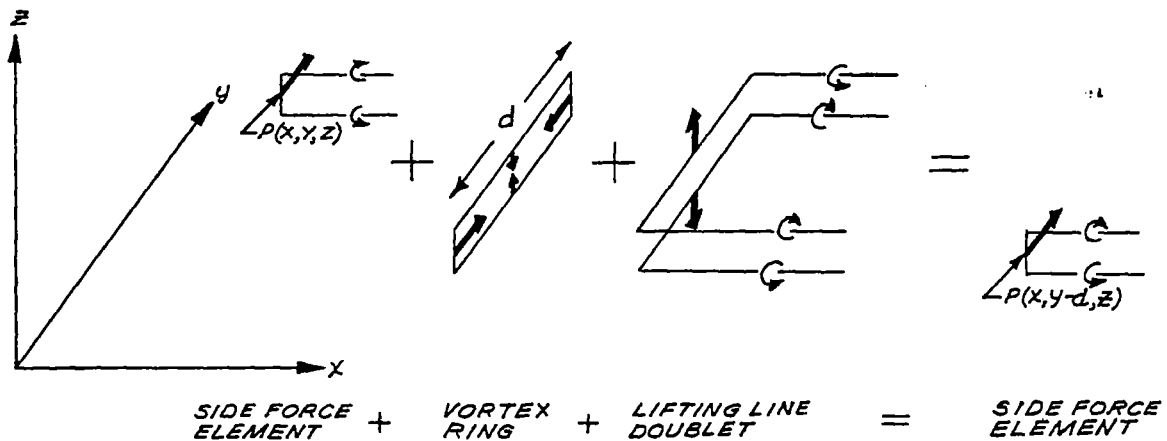


Fig. 9c-2

to be such that the sideforce at  $P(x, y, z)$  is just canceled. The potential for the vortex ring can be found by integrating the potentials for constant-strength infinitesimal vortex rings (Ch. IIIA) distributed along

the line  $x, z = \text{Constants}$ . The second step is to superimpose on the vortex ring a finite width lifting line "doublet." This latter singularity is formed by taking the limit as two equal and opposite strength finite width lifting elements are brought together keeping the product of lifting element strength and distance apart constant. The potential of the original sideforce element at  $P(x, y, z)$  plus the two added elements,  $\phi_S(x, y, z) + \phi_V + \phi_D$ , is identical to that for a sideforce element at  $P(x, y-d, z)$ .

Thus the potential of a sideforce element "S" inside the spherical space is the same as that for a finite vortex ring "V," plus a lifting line doublet "D," plus a sideforce element "S'" in the vertical plane of symmetry (at  $P'$  in Fig. 9c-1). The interference drag between the optimum lift distribution  $l_{opt}$  and S is equal to the interference drag between  $l_{opt}$  and S' plus that between  $l_{opt}$  and V plus that between  $l_{opt}$  and D. The last of these drags must be zero since D is a lift distribution having zero net lift; if this were not zero D could be combined with  $l_{opt}$  to form another distribution having less drag than  $l_{opt}$  (Section 4H), in contradiction of original assumptions. Since V can be thought of as built up from distributions of infinitesimal vortex rings, which in turn are made up of source-sink doublets with axes aligned with the stream direction, the interference drag between V and  $l_{opt}$  is zero by the proof given in Ch. IX-B.

The only possible interference drag with  $l_{opt}$  could be that of the sideforce element S' in the vertical plane of symmetry, and this can be shown to be zero because of the symmetry. Consider the interference drag of S' with lifting elements in the rear Mach cone of S' as shown in Fig. 9c-3a. The interference drag will be due to the downwash of S'

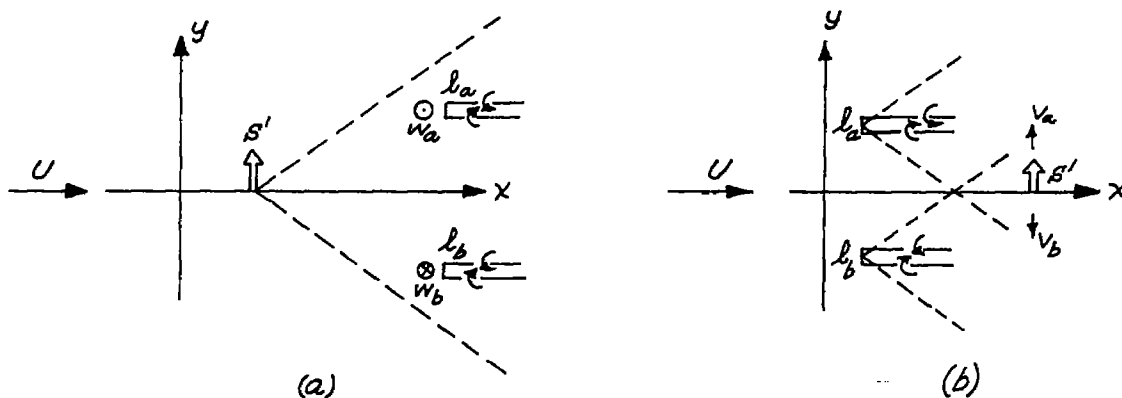


Fig. 9c-3

iY

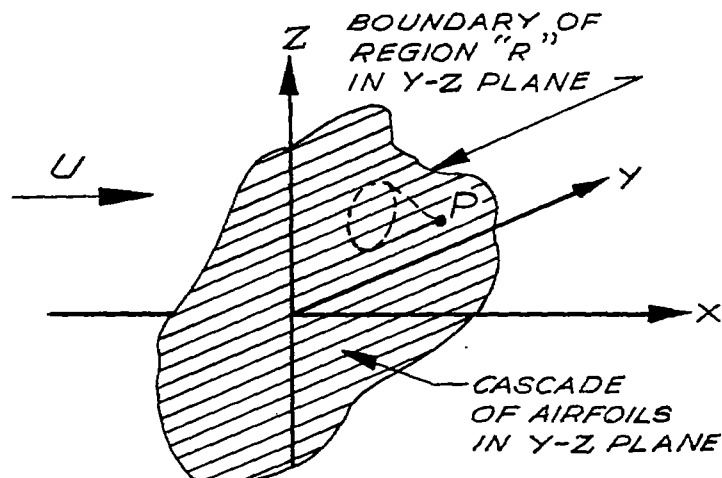
acting on the lifting elements (see Ch. IV-J); for each lift element  $l_b$  which receives a downwash from  $S'$  there is another lift element  $l_a$  of the same strength which receives an upwash of equal magnitude. Hence the interference drag of  $S'$  with each pair of lifting elements in its rear Mach cone is zero. Consider now Fig. 9c-3b representing  $S'$  and a pair of lift elements in its fore Mach cone. The interference drag here is due to sidewash fields from the lift elements acting on  $S'$ . But for every lift element  $l_a$  producing a sidewash  $v_a$  on  $S'$  there is a symmetrically placed  $l_b$  producing a sidewash  $v_b = -v_a$  on  $S'$ . Again the interference drag is zero. Thus there is no interference drag between  $S'$  and  $l_{opt}$  and hence none between  $S$  and  $l_{opt}$  for this particular  $l_{opt}$ . Following the same type of reasoning as is given in Ch. IX-B, this proof can be extended to all optimum distributions within the sphere; this is so because of the uniqueness of the optimum external flow field.

Thus it is proven that sideforce distributions, as well as source distributions, in a spherical space cannot reduce the drag attained with any of the optimum distributions of lifting elements alone in that space.

Similar methods may be applied to other spaces if those spaces have both a horizontal and a vertical plane of symmetry containing the free stream direction and meet certain convexity requirements. The latter can be stated as requirements that straight lines from each point within the space which extend to the planes of symmetry and are perpendicular to them must lie entirely within the space.

#### D. INTERFERENCE PROBLEMS IN CERTAIN SPACES BOUNDED BY MACH ENVELOPES

Let some region "R" be chosen in the y-z plane, which is perpendicular to the flow direction. Consider the space "S" consisting of points such as "P" whose fore or aft Mach cones intersect areas in the



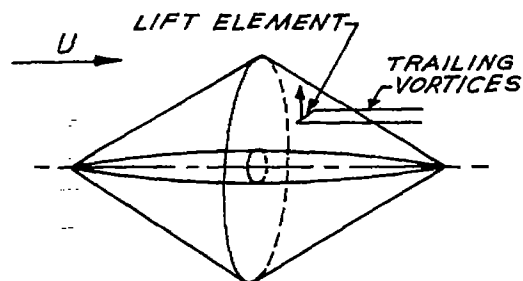
A set of parallel Mach planes cutting this source distribution determines an equivalent lineal source distribution according to the method of Hayes. For convenience, this equivalent lineal source distribution will be denoted

y-z plane which are completely contained in the region "R." An optimum distribution of lift in this space is given by a uniformly loaded cascade of airfoils (of infinitesimal chord and gap) covering the region "R," since this gives constant downwash in the combined flow field.

The resulting flow pattern is two-dimensional within the space "S." It then follows that the sidewash and pressure are zero in this space and sideforce elements or sources introduced in "S" have no interference with the optimum lift distribution.

E. THE INTERFERENCE BETWEEN LIFT AND SIDEFORCE ELEMENTS AND AN OPTIMUM DISTRIBUTION OF VOLUME ELEMENTS

Consider a Sears-Haack body placed on the axis of a double Mach cone, and place a lifting element as shown in the illustration. The interference drag between body and lifting element is composed of two parts, the effect of the body nose on the lifting element and the effect of the lifting element on the tail of the body.



The nose of the body corresponds to a source distribution and produces an upwash velocity at the lifting element. This causes negative drag. The lifting element produces a positive pressure at the tail of the body. This also causes negative drag so the total interference drag is negative. (This argument, of course, applies not only to the Sears-Haack shape but to other shapes also.)

The total drag of the combination is equal to the drag of the Sears-Haack body alone plus the drag of the lifting element alone plus the interference drag. The drag of the lifting element alone is proportional to the square of the lift it carries. However, the interference drag is proportional to the first power of the lift on the element and to the first power of the strength of those sources and sinks in the body which are affected by interference. The lift carried by the element can, therefore, always be made small enough so that the drag of the element alone is less (in absolute magnitude) than the interference drag. Thus, the total drag of the combination can be made less than the drag of the Sears-Haack body alone.

This suggests placing elements of lift and sideforce in a ring about the Sears-Haack body, and so arranged that the force on each element is directed radially outward from the body. This process may be used to construct a central body plus cylindrical shell which has zero drag (see Ch. IX-F).

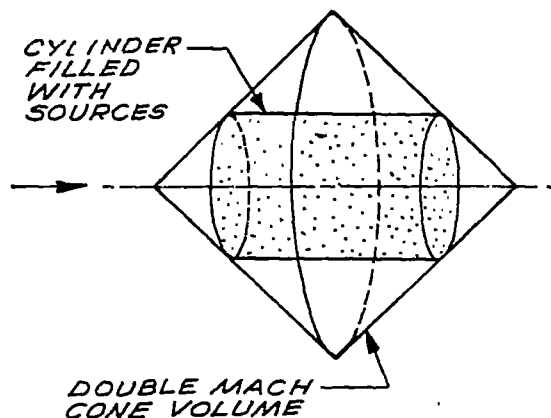
Such a system was investigated first by Ferrari<sup>(21)</sup> and later by Ferri<sup>(20)</sup>, and its two-dimensional analogue is the Busemann biplane.

It, therefore, appears that the optimum distribution in space of volume elements alone yields minimum drag values consistent with the Sears-Haack values. However, the optimum distribution of volume elements plus lifting and sideforce elements should give zero drag for any total volume.

#### F. RING WING AND CENTRAL BODY OF REVOLUTION HAVING ZERO DRAG

The theoretical minimum drag value for a distribution of thickness elements that has no interference with lift or sideforce elements is the drag of a Sears-Haack body. It has been stated in Ch. IX-E that interferences between thickness distributions and distributions of lift or sideforce may provide negative drag contributions which reduce the theoretical minimum wave drag of a system to zero. This Section illustrates, for the double Mach cone volume, a central body of revolution which, together with a certain distribution of radial forces on a cylindrical shell, has zero wave drag. The method employed here to design such a system makes use of certain equivalences between sources and line distributions of elementary vortex shells. (These equivalences are discussed in Ch. III-B.)

Consider a radially symmetric, continuous distribution of sources filling a cylindrical space contained within the double Mach cone volume.



by  $F(x)$ . Because of the radial symmetry of this case,  $F(x)$  is independent of the angle  $\theta$  on the distant control surface. A central body of revolution which is represented by the negative of  $F(x)$  will just cancel the velocities induced at the distant control surface by the original sources. The drag of the combined system is then zero. The remaining step is to relate the original source distribution to a distribution of radial forces around the boundary of the cylindrical space. It can be shown (see Ch. III-B) that a source and a sink of equal strength, lying on the same line parallel to the flow direction, have exactly the same effect at the distant control surface as a line of constant strength elementary vortex shells connecting the source and the sink. If such vortex shells are considered to replace a source distribution whose strength is independent of the radial distance, the forces on adjoining shells inside the cylinder cancel one another, while the forces on the outer sides of the shells next to the boundary of the cylindrical space determine the radial force. A cylindrical shell having this radial load distribution plus a central body of revolution which corresponds to the source distribution  $-F(x)$  constitute a system having zero drag.

As an example, suppose that a cylinder within a double Mach cone volume is considered to contain a source distribution which varies linearly with axial distance but is independent of radial distance. That is, the source strength per unit area inside the cylinder is

$$f = -f_0 \left(1 - \frac{2x}{c}\right)$$

where  $x$  is measured from the leading edge of the cylinder,  $c$  is the cylinder length, and  $f_0$  is the strength of the sources at the rear face of the cylinder. The equivalent linear source strength corresponding to this original distribution is given by

$$\frac{\beta^2}{c^2} F(x) = \left(\frac{\beta R}{c}\right)^2 f_0 \left\{ \left(1 - \frac{2x}{c}\right) \left[ \frac{x}{\beta R} \sqrt{1 - \left(\frac{x}{\beta R}\right)^2} + \cos^{-1} \left(\frac{-x}{\beta R}\right) \right] + \frac{4}{3} \left(\frac{\beta R}{c}\right) \left[1 - \left(\frac{x}{\beta R}\right)^2\right]^{3/2} \right\} \quad -\beta R \leq x \leq +\beta R$$

$$\frac{\beta^2}{c^2} F(x) = \left(\frac{\beta R}{c}\right)^2 f_0 \left[ -\pi \left(1 - \frac{2x}{c}\right) \right] \quad \beta R \leq x \leq c - \beta R$$

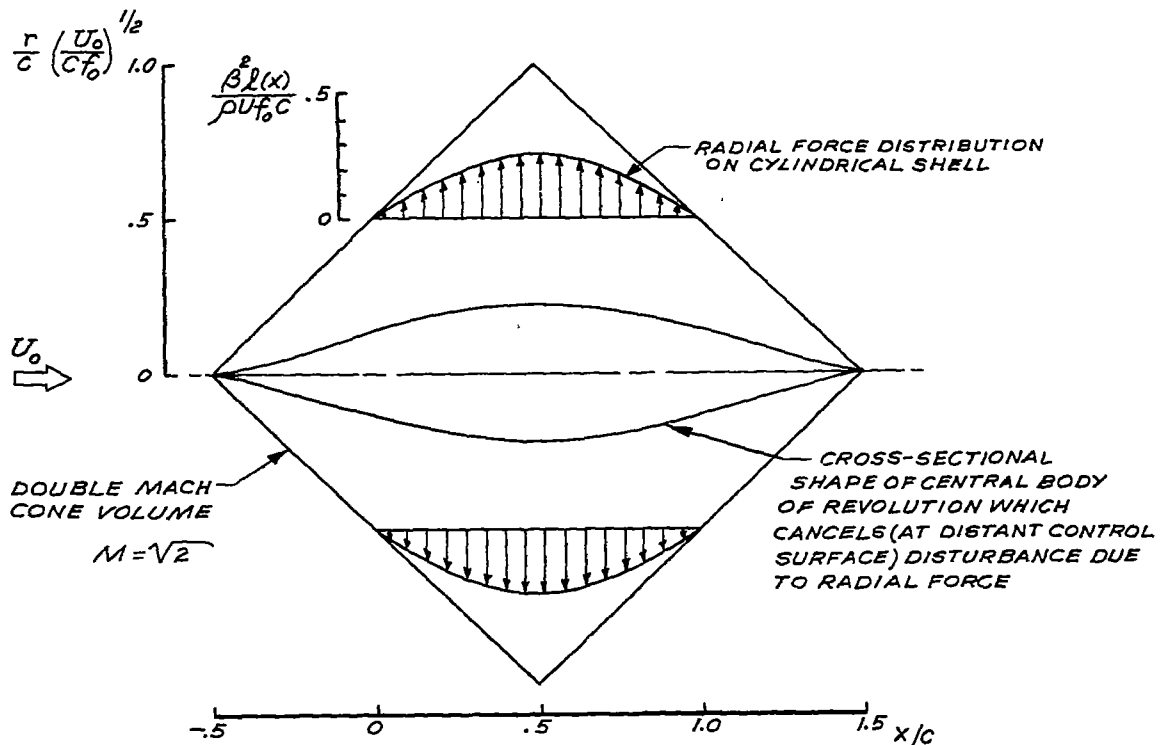
where R is the cylinder radius. Now, if the negative of this source distribution is assumed to represent a body of revolution, then within the accuracy of slender body theory the area distribution of the central body is

$$S(x) = - \frac{1}{U} \int_{-\beta R}^x F(x) dx$$

For illustration, the dimensions of the cylinder are assumed to be such that  $\beta R/c = 1/2$ ; that is, the radius is half the distance between the axis and the apex of the double Mach cone volume. The shape of the central body of revolution which cancels the effect of the original source distribution for this case is shown in the accompanying figure. The distribution of radial force which can replace the original linearly varying source distribution is

$$l(x) = \frac{\rho V}{\beta^2} f_0 \int_0^x \left(1 - \frac{2x}{c}\right) dx = \frac{\rho V f_0 c}{\beta^2} \left(\frac{x}{c}\right) \left(1 - \frac{x}{c}\right)$$

$$l(x) = \frac{\rho V}{\beta^2} f$$



CENTRAL BODY OF REVOLUTION AND RADIAL FORCE DISTRIBUTION HAVING ZERO WAVE DRAG

CHAPTER X. RESULTS AND CONCLUSIONS

It appears that certain idealized spatial distributions of lift and thickness may produce materially less wave drag and vortex drag than comparable planar systems. It is by no means certain that such advantages can be realized in practical aircraft designs, but further investigation of specific configurations is warranted.

One of the interesting features of spatial lift and thickness distributions is that optimum arrangements are generally not unique. This may raise the problem of determining which member of an optimum family has the least surface area or is best adapted for structure.

Another interesting property of spatial distributions is the interference which may arise between lift and thickness distributions. This interference can be used to account for the zero wave drag of a Busemann biplane or of Ferrari's ring wing plus central body. However it is shown that in some cases thickness distributions have no interference with an optimum spatial distribution of lifting elements, and so cannot be used to reduce the drag due to lift in such cases.

A number of other results are obtained in this report and detailed discussions of the basic singularities and Hayes' method of drag evaluation are included. However it is clear that the scope of the field is such that this investigation must be regarded as a preliminary exploration.

CHAPTER XI. REFERENCES

1. Hayes, Wallace D., "Linearized Supersonic Flow," North American Aviation, Inc., Los Angeles, Report No. A.L. 222, June, 1947.
2. Graham, E. W.; Lagerstrom, P. A.; Beane, B. J.; Licher, R. M.; Rodriguez, A. M.; "Reduction of Drag Due to Lift at Supersonic Speeds," WADC Technical Report 54-524, April, 1954.
3. Graham, E. W.; Beane, B. J.; Licher, R. M.; "The Drag of Non-Planar Thickness Distributions in Supersonic Flow," Aeronautical Quarterly, Vol. VI, No. 2, pg. 99, May 1955.
4. Robinson, A., "On Source and Vortex Distributions in the Linearized Theory of Steady Supersonic Flow," Quarterly Journal of Mechanics and Applied Mathematics, Vol. I, 1948.
5. Hadamard, J., "Lectures in Cauchy's Problem in Linear Partial Differential Equations," Yale University, New Haven, 1923.
6. von Kármán, T., "Supersonic Aerodynamics - Principles and Applications," Journal of the Aeronautical Sciences, Vol. 14, No. 7, 1947.
7. von Kármán, T., "The Problem of Resistance in Compressible Fluids," Proc. 5th Volta Congress, R. Accad. D'Italia (Rome), pp. 222 - 277 (1936).
8. Rodriguez, A. M.; Lagerstrom, P. A.; and Graham, E. W.; "Theorems Concerning the Drag Reduction of Wings of Fixed Planform," Journal of the Aeronautical Sciences, Vol. 21, No. 1, pg. 1, January, 1954.
9. Graham, E. W., "A Drag Reduction Method for Wings of Fixed Planform," Journal of the Aeronautical Sciences, Vol. 19, No. 12, pg. 823, December, 1952.
10. Beane, Beverly J., "Examples of Drag Reduction for Delta Wings," Douglas Aircraft Company, Inc. Report SM-14447, January 12, 1953.

11. Walker, K., "Examples of Drag Reduction for Rectangular Wings," Douglas Aircraft Company, Inc. Report SM-14446, January 15, 1953.
12. Munk, Max M., "The Reversal Theorem of Linearized Supersonic Airfoil Theory," Journal of Applied Physics, Vol. 21, No. 2, pp. 159 - 161, February, 1950.
13. Jones, Robert T., "The Minimum Drag of Thin Wings in Frictionless Flow," Journal of the Aeronautical Sciences, Vol. 18, No. 2, pg. 75, February, 1951.
14. Jones, Robert T., "Theoretical Determination of the Minimum Drag of Airfoils at Supersonic Speeds," Journal of the Aeronautical Sciences, Vol. 19, No. 12, December, 1952.
15. Munk, Max M., "The Minimum Induced Drag of Airfoils," NACA T.R. No. 121, 1921.
16. Sears, William R., "On Projectiles of Minimum Wave Drag," Quarterly of Applied Mathematics, Vol. IV, No. 4, January 1947.
17. Haack, W., "Geschossformen Kleinsten Wellenwiderstandes," Bericht 138 der Lilienthal-Gesellschaft für Luftfahrt.
18. Lamb, Sir Horace, "Hydrodynamics," 6th Revised Edition, 1945, Dover Publications, New York.
19. Hildebrand, F. B., "Methods of Applied Mathematics," Prentice-Hall, 1952.
20. Ferri, A., "Application of the Method of Characteristics to Supersonic Rotational Flow," NACA T.R. 841, 1946.
21. Ferrari, C., "Campi di Corrente Ipersonora Attorno a Solidi di Rivoluzione," L'Aerotecnica, Vol. XVII, No. 6, 1937, pp. 507 - 518. Also available as "Supersonic Flow Fields About Bodies of Revolution," Brown University, Graduate Division of Applied Mathematics, Translation No. A9-T-29, 1948.
22. Bleviss, Z. O., "Some Integrated Volume Properties in Linearized Flow and Their Connection With Drag Reduction at Supersonic Speeds," Douglas Aircraft Company, Inc. Report SM-19469, February 1956.